

# PONTE SULLO STRETTO DI MESSINA



## PROGETTO DEFINITIVO

### EUROLINK S.C.p.A.

IMPREGILO S.p.A. (MANDATARIA)  
 SOCIETÀ ITALIANA PER CONDOTTE D'ACQUA S.p.A. (MANDANTE)  
 COOPERATIVA MURATORI E CEMENTISTI - C.M.C. DI RAVENNA SOC. COOP. A.R.L. (MANDANTE)  
 SACYR S.A.U. (MANDANTE)  
 ISHIKAWAJIMA - HARIMA HEAVY INDUSTRIES CO. LTD (MANDANTE)  
 A.C.I. S.C.P.A. - CONSORZIO STABILE (MANDANTE)

<p>IL PROGETTISTA Ing E.M.Veje <b>COWI</b>   Dott. Ing. E. Pagani Ordine Ingegneri Milano n° 15408</p>	<p>IL CONTRAENTE GENERALE  Project Manager (Ing. P.P. Marcheselli)</p>	<p>STRETTO DI MESSINA Direttore Generale e RUP Validazione (Ing. G. Fiammenghi)</p>	<p>STRETTO DI MESSINA Amministratore Delegato (Dott. P. Ciucci)</p>
-----------------------------------------------------------------------------------------------------------------------------------------------------------------------------------------------------------------------	------------------------------------------------------------------------------------	-------------------------------------------------------------------------------------------------	-----------------------------------------------------------------------------

<p><i>Unità Funzionale</i>      OPERA D'ATTRAVERSAMENTO <i>Tipo di sistema</i>        SOVRASTRUTTURE <i>Raggruppamento di opere/attività</i>      Impalcato <i>Opera - tratto d'opera - parte d'opera</i>      Impalcato <i>Titolo del documento</i>      Specialist Technical Design Report, Annex</p>	<p><b>PS0075_F0</b></p>
-------------------------------------------------------------------------------------------------------------------------------------------------------------------------------------------------------------------------------------------------------------------------------------------------------------------------	-------------------------

CODICE	<table border="1" style="width: 100%; text-align: center;"> <tr> <td>C</td><td>G</td><td>1</td><td>0</td><td>0</td><td>0</td><td>P</td><td>R</td><td>X</td><td>D</td><td>P</td><td>S</td><td>V</td><td>I</td><td>3</td><td>I</td><td>M</td><td>0</td><td>0</td><td>0</td><td>0</td><td>0</td><td>0</td><td>0</td><td>1</td><td>F0</td> </tr> </table>	C	G	1	0	0	0	P	R	X	D	P	S	V	I	3	I	M	0	0	0	0	0	0	0	1	F0
C	G	1	0	0	0	P	R	X	D	P	S	V	I	3	I	M	0	0	0	0	0	0	0	1	F0		

REV	DATA	DESCRIZIONE	REDATTO	VERIFICATO	APPROVATO
F0	20/06/2011	EMISSIONEREVISIONE PER NOTIFICA SDM PROT. 0184 DEL 18/02/2011	HPO,AMOL,JESO	HPO	HPO/LSJ



		<b>Ponte sullo Stretto di Messina</b> <b>PROGETTO DEFINITIVO</b>		
Specialist Technical Design Report, Annex		<i>Codice documento</i> PS0075_F0-ok.doc	<i>Rev</i> F0	<i>Data</i> 20/06/2011

## INDICE

INDICE .....	3
1 Executive Summary .....	7
1.1 Introduction .....	7
1.2 Scope .....	7
1.3 Materials .....	8
1.4 Structural Analysis .....	8
1.5 Verification of Longitudinal Steel .....	8
1.5.1 Longitudinal Girders .....	9
1.5.2 Cross Girder .....	12
1.6 Verification of Longitudinal Steel with Transverse Stresses .....	14
1.7 Verification - Transverse Steel .....	15
1.8 Verification using Local FE-Models .....	16
1.8.1 Local FE-model of Suspended Deck .....	17
1.8.2 Roadway and Railway Local FE-Models .....	19
1.8.3 Hanger Anchorage Local FE-Model .....	20
1.9 Fatigue .....	21
2 Introduction .....	22
2.1 Scope of Works .....	22
2.2 Bridge Elevation, Plan and Cross Section of Suspended Deck .....	23
2.3 Design Specifications .....	24
2.3.1 Design Codes .....	24
2.3.2 Material Specifications .....	25
2.3.3 Drawings .....	25
2.3.4 Reports for Suspended Deck .....	28
2.4 Nomenclature .....	29
3 Design Changes .....	29
3.1 Roadway Girder .....	29
3.2 Railway Girder .....	32
3.3 Cross Girder .....	33
3.3.1 Intersections to Roadway and Railway Girders .....	35
4 Limit States .....	37

		<b>Ponte sullo Stretto di Messina</b> <b>PROGETTO DEFINITIVO</b>		
Specialist Technical Design Report, Annex		<i>Codice documento</i> PS0075_F0-ok.doc	<i>Rev</i> F0	<i>Data</i> 20/06/2011

5	Materials .....	37
5.1	Structural Steel .....	37
5.2	High Strength Bolts.....	37
5.3	Welding Consumables.....	37
6	Articulation .....	38
6.1	Overall Static System .....	38
6.2	Interconnection of the Suspended Deck Elements.....	38
7	Global Structural FE-Analyses.....	38
7.1	IBDAS Global Beam Model .....	39
7.2	Second Order Effects and Imperfections.....	39
8	Verification - Longitudinal Steel .....	39
8.1	Verification - Roadway Girder.....	41
8.2	Verification - Railway Girder .....	45
8.3	Verification - Cross Girder .....	59
8.4	Verification - Transverse Stresses.....	65
9	Verification - Transverse Steel.....	68
9.1	Method.....	68
10	Verification using Local FE-Models .....	70
10.1	Introduction.....	70
10.2	Local FE-model of Suspended Deck .....	74
10.3	Local FE-Models of Roadway and Railway Girder .....	84
10.4	Local FE-Model of Hanger Anchorage .....	91
11	Verification - Fatigue Assessments .....	93
11.1	Non man generated loads .....	93
11.2	Fatigue Load Models .....	94
11.2.1	Fatigue Loads for Rail Traffic .....	95
11.2.2	Fatigue Loads for Road Traffic.....	96
11.2.3	Verification of Roadway Girder Deck Plate - Local Effects.....	97
11.3	Stress Concentration Factor (SCF) .....	100
11.3.1	Points investigated .....	100
11.3.2	Stress range determination and SCF results .....	102
11.3.3	Determination of the strengthening thickness – ROBOT model.....	109
11.3.4	Conclusions.....	113

		<b>Ponte sullo Stretto di Messina</b> <b>PROGETTO DEFINITIVO</b>		
Specialist Technical Design Report, Annex	<i>Codice documento</i> PS0075_F0-ok.doc	<i>Rev</i> F0	<i>Data</i> 20/06/2011	

11.4	Fatigue Detail Categories .....	115
11.4.1	Roadway and railway bottom plate details .....	115
11.4.2	Roadway deck details .....	115
11.4.3	Railway deck details .....	118
11.4.4	Cross girder details .....	120
11.4.5	Weld Improvement .....	121
11.4.6	Verification of Cross Girder .....	122
11.4.7	Verification of Railway Girder .....	122
11.4.8	Verification of Roadway Girder .....	123
11.4.9	Verification of Hanger Anchorage .....	124
11.4.10	Articulation system: X-Structure .....	126
12	Special Design Investigations .....	127
12.1	Hanger Replacement .....	127
12.2	Hanger Rupture .....	129



		<b>Ponte sullo Stretto di Messina</b> <b>PROGETTO DEFINITIVO</b>		
Specialist Technical Design Report, Annex		<i>Codice documento</i> PS0075_F0-ok.doc	<i>Rev</i> F0	<i>Data</i> 20/06/2011

# 1 Executive Summary

## 1.1 Introduction

This report describes the design of the following structural elements for the suspended deck:

- Roadway girders: comprising steel sections stiffened by longitudinal trough stiffeners and transverse diaphragms. Individual box girders connected to supporting cross girders. The box girders are completed by aerodynamic fairings.
- Railway girder: comprising steel sections stiffened by longitudinal stiffeners and transverse diaphragms; in particular, longitudinal structural members are arranged under each track. The railway girder sections are connected to the supporting cross girders.
- Cross girders: arranged at 30 m centres, and supported by the hangers, they support the railway and roadway girders; formed as a closed box section of variable height.

The design is based on that shown in the Tender Design. Calculations are based on the global IBDAS model version 3.3.

## 1.2 Scope

This report describes the design of structural steel elements of the suspended deck, from the terminal structures of Sicilia (stationing 88.49) to the terminal structure of Calabria (stationing 3,723.99). The suspended deck is 60 m wide and entirely made of steel. As mentioned above it is formed by three independent longitudinal box girders, two for the roadway and the central one for the railway. The boxes are connected by cross girders at 30 metres spacing.

Design details for the non-structural components for the suspended deck, such as maintenance/access systems and mechanical/electrical installations are provided elsewhere.

In general the Progetto Definitivo of the suspended deck is based on the Tender Design. The Progetto Definitivo specifies the most important design aspects and other technical topics considered of importance and/or special solutions to the design demands. For some part of the suspended deck structures it has been found advantageous to introduce changes to the design, which are described in this report.

		<b>Ponte sullo Stretto di Messina</b> <b>PROGETTO DEFINITIVO</b>		
Specialist Technical Design Report, Annex		<i>Codice documento</i> PS0075_F0-ok.doc	<i>Rev</i> F0	<i>Data</i> 20/06/2011

The Specialist Technical Design Report focuses on summarising the structural design, including the identification of load combinations governing the design of the structural components and the results of the component verifications.

### 1.3 Materials

The structural plate components are fabricated from grade S355 ML, S420 ML and S460 ML structural steel. The steel fabricator has confirmed that the mechanical properties will not vary with material thickness for thicknesses less than 100 mm, as is typical for steel products.

### 1.4 Structural Analysis

The Messina Strait Bridge was modelled and analysed in the COWI proprietary analysis program IBDAS (Integrated Bridge Design and Analysis System). The suspended deck design described in this report is based on model 3.3.

The global model analysis was supplemented by the more detailed local analysis of selected components by local FE-models:

- Bridge section, comprising a cross girder and longitudinal girders to each side;
- Diaphragms;
- Hanger Anchorage;

### 1.5 Verification of Longitudinal Steel

To verify the longitudinal steel of the suspended deck (roadway girder, railway girder and cross girder), a spreadsheet (ADVERS) has been developed based on the Eurocodes. The overall verification is done based on the derived section forces obtained from the global IBDAS FE-model. The verification of selected sections regarding stress and buckling analyses has been performed in accordance with the project specific Design Basis and the Eurocodes (EC).

The spreadsheet is designed for a closed steel box with any type of outer geometry and location of longitudinal stiffeners. The spreadsheet calculates gross and effective section properties for a given set of parameters including the section geometry, plate thicknesses, stiffener types and spacing, diaphragm spacing and length of the moment diagram.

		<b>Ponte sullo Stretto di Messina</b> <b>PROGETTO DEFINITIVO</b>		
Specialist Technical Design Report, Annex		<i>Codice documento</i> PS0075_F0-ok.doc	<i>Rev</i> F0	<i>Data</i> 20/06/2011

The effective section properties are calculated using the "reduced width" method taking into account the effect of shear lag and plate buckling. The column type buckling behaviour is calculated taking local bending from traffic loading into account.

The general ULS load combinations used for verification for the longitudinal steel are static load, dynamic wind and seismic (time history). In general the governing load case for the verification of the longitudinal steel is dynamic wind. However for a few railway girders in the side span, the seismic load combination is governing.

The utilisation ratios (UR) presented in section 1.5 are the von Mises stresses in relation to the design yielding stresses and the utilisation ratios for global plate buckling, with respect to interaction between plate and column buckling according to EN 1993-1-5 sec. 4.5. The critical stress  $\sigma_{Ed, Cr}$  is determined for each plate by considering the plate and stiffeners as an equivalent orthotropic plate according to EN 1993-1-5:2006 Annex A1.

### 1.5.1 Longitudinal Girders

The design of the roadway and railway girders are described together with the changes made since the tender design. Furthermore the method for verifying the roadway and railway girder design with regards to ULS combinations and fatigue loading have been explained.

#### Design changes

Compared with the cross sections in the tender design, the direction of the road traffic has been inverted together with a 2.0 % outward slope of the deck plate. The two L-stiffeners underneath the edge plate has been changed to flat stiffeners to comply with manufacturing optimisation. The first deck trough under the crash barrier at the emergency lane is exchanged by two flat stiffeners and the trough underneath inspection corridor is also exchanged by two flat stiffeners to comply with demands for high fatigue detail categories. Tab plates for the bottom trough stiffeners are removed and replaced by a direct attachment of the troughs to the diaphragm. To fulfil the fatigue demands at the trough joints, the troughs underneath the deck plate are increased locally at a width of 7.3 m. Termination of stiffeners and diaphragms have in general been improved by adding end plates with a radius of min 150 mm. Thereby the fatigue detail category can be improved fulfilling the fatigue demands.

		<b>Ponte sullo Stretto di Messina</b> <b>PROGETTO DEFINITIVO</b>		
Specialist Technical Design Report, Annex		<i>Codice documento</i> PS0075_F0-ok.doc	<i>Rev</i> F0	<i>Data</i> 20/06/2011

Since tender design, changes have been made to the overall shape of the railway girder. The angle of the inclined web has been changed from 44 deg to 63 deg. Angle profiles stiffening the deck plate, web plates and inclined web plates in the tender design, have been replaced with flat stiffeners to comply with manufacturing optimisation. The troughs underneath the deck plate are furthermore exchanged by flat stiffeners to comply with demands for high fatigue detail categories. The extra steel within the flat stiffeners is almost balanced out by reducing the deck plate thickness from 16 mm to 15 mm. To comply with the fatigue demands the bottom flange is increased locally from 10 mm to 15 mm at the erection joints (every 60 m). Due to stress concentrations the bottom plate is furthermore reinforced locally in all spans at the 4 centre diaphragms and at the cross girders in the vicinity of the towers.

#### **Verification method**

The capacity of the stiffeners is verified using ADVERS and the local stress distribution is verified in a local FE-model. All stress verifications have been carried out with consideration of the global and local section properties for the effective cross section properties.

A local FE-model has been developed to verify the T-profiles under the track for train positions critical for the fatigue verification. Furthermore the T-profiles are verified for torsional buckling and plate buckling in ADVERS.

For the roadway deck a FE-model, similar to the one for the railway, has been developed to take in account the local wheel load effects in specific details, depending on the characteristic geometry.

Utilisation ratios for the governing ULS load combination are shown in Figure 1-1 and Figure 1-2 for the roadway girder and railway girder, respectively.

The utilisation ratios presented in the following figures are von Mises stresses in relation to the design yielding stresses. Furthermore utilisation ratios for global plate buckling are shown, with respect to interaction between plate and column buckling according to EN 1993-1-5 sec. 4.5.

		<b>Ponte sullo Stretto di Messina</b> PROGETTO DEFINITIVO	
Specialist Technical Design Report, Annex	Codice documento PS0075_F0-ok.doc	Rev F0	Data 20/06/2011

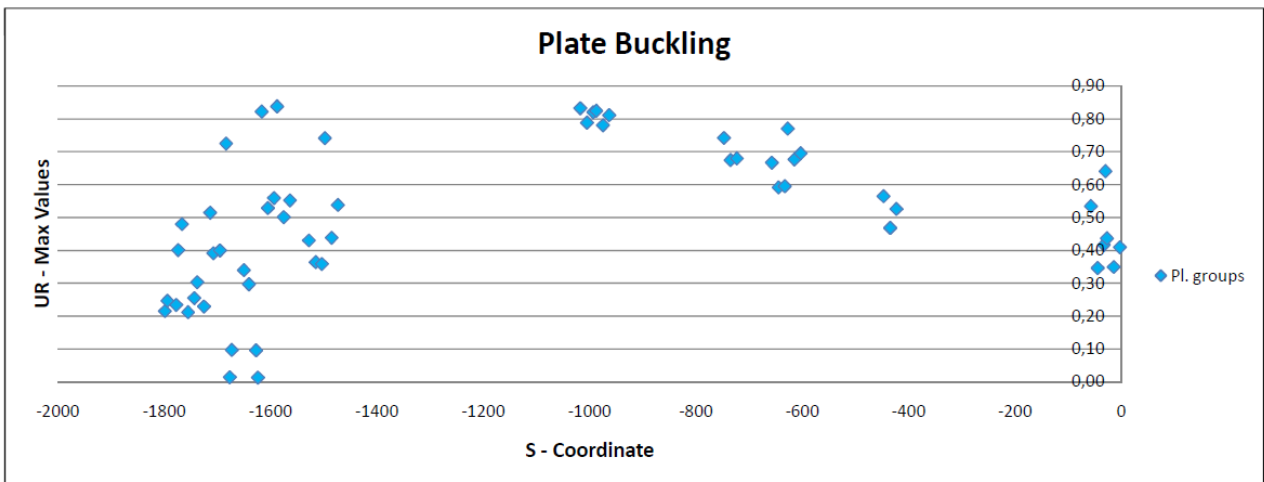
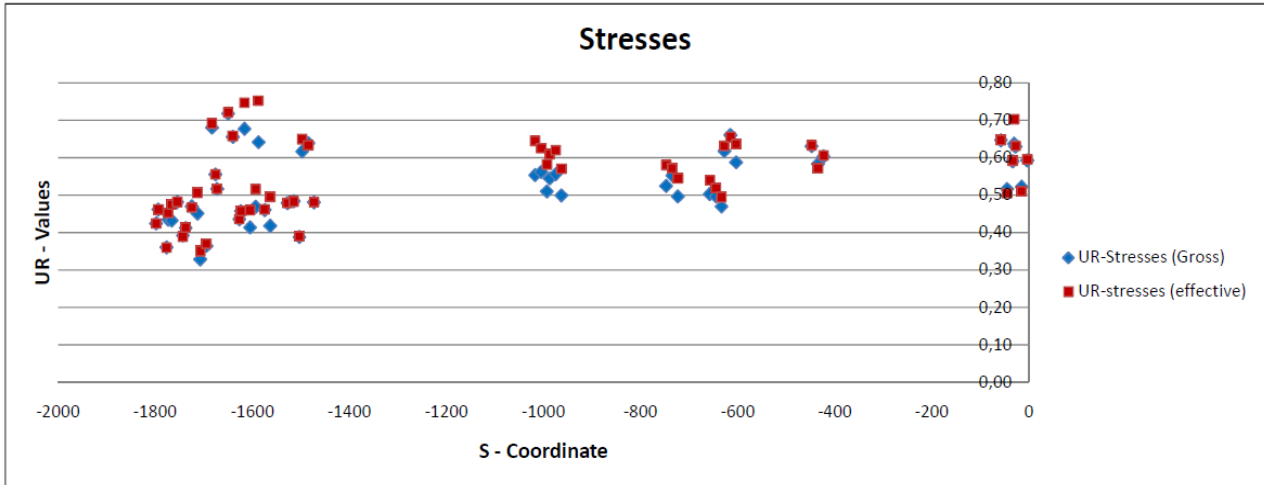


Figure 1-1 Roadway girder - utilisation ratios for ULS load combination dynamic wind, stresses and plate buckling

		<b>Ponte sullo Stretto di Messina</b> <b>PROGETTO DEFINITIVO</b>		
Specialist Technical Design Report, Annex		<i>Codice documento</i> PS0075_F0-ok.doc	<i>Rev</i> F0	<i>Data</i> 20/06/2011

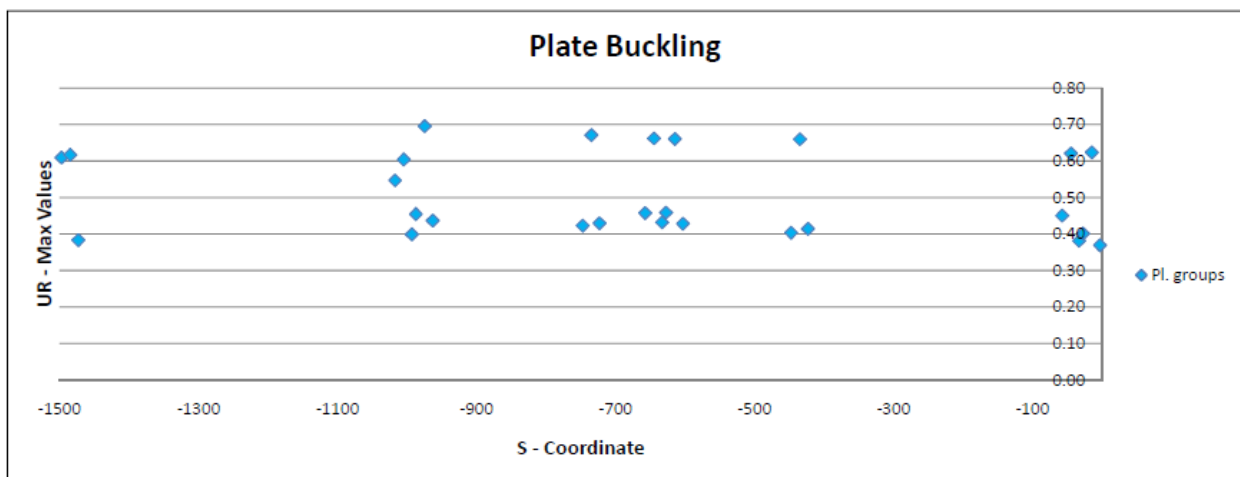
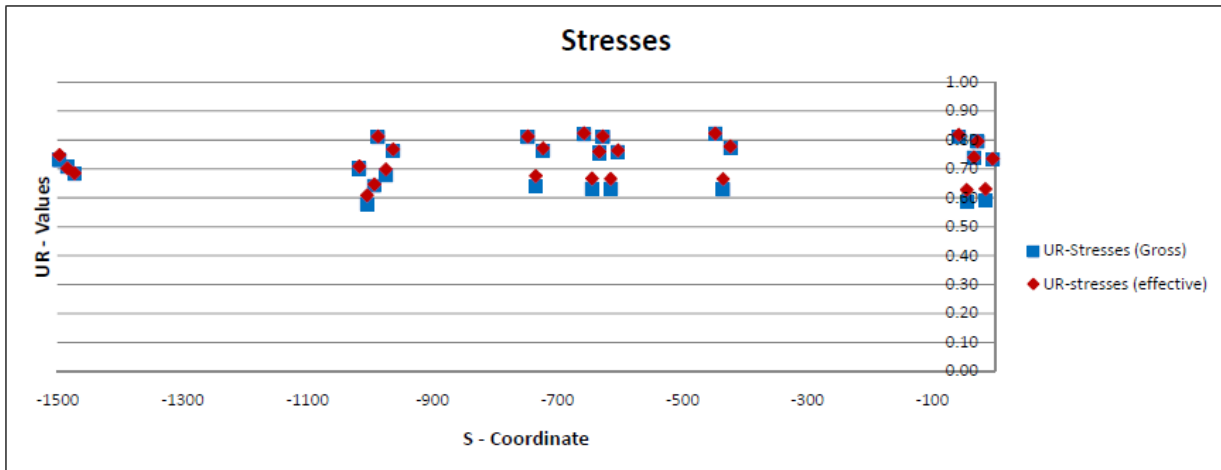


Figure 1-2 Railway Girder - utilisation ratios for stresses and plate buckling in type CF1 & CF2 for ULS load combination dynamic wind

The longitudinal girders have also been verified for seismic loading using a time history analysis. The utilisation ratios are below 1.0 for all cross sections.

### 1.5.2 Cross Girder

In the following the overall design of the cross girder is described together with the changes made since the tender design.

		<b>Ponte sullo Stretto di Messina</b> <b>PROGETTO DEFINITIVO</b>		
Specialist Technical Design Report, Annex		<i>Codice documento</i> PS0075_F0-ok.doc	<i>Rev</i> F0	<i>Data</i> 20/06/2011

## Design changes

Since the tender design, the direction of the road traffic has been inverted. This change led to a continuous 2.0 % outward slope of the top plate throughout the entire length of all cross girders. T-stiffeners at the webs and bottom plate have been replaced with flat stiffeners to comply better with manufacturing optimisation.

The centre 4.4 m of the bottom plate has been increased in thickness by 8 mm, while the two neighbouring plates (2 x 4.05 m) have been increased by 3 mm. The top plate in the vicinity of the railway girder is also increased in thickness by 3-4 mm. All changes have been done to comply with the fatigue demands.

Changes have also been made to the cross girder T7 at the terminal structure. The high demand of torsional capacity due to the adjoining spans led to widen the cross section from 1700 mm to 2700 mm.

The tender design solution presented the diaphragms next to the railway girder with the spacing of 2.5 m. This configuration had been reinforced by an extra transverse stiffener thereby halves the buckling length of the plate.

The arrangements of stiffeners in the cross girder is such that all the stiffeners of roadway and railway decks pass through the interior of the cross girder. This is done to give more favourable interconnection to the road and railway girder sections and to improve the fatigue strength. In addition this arrangement ensures a high driving comfort when passing the cross girder due to the uniform deck stiffness. In the remaining part of the cross girder, longitudinal T-stiffeners are applied to the deck plate in longitudinal direction of the cross girder itself.

The web and bottom troughs at the roadway girder are interrupted at the cross girder web, but extra short trough sections are introduced at both sides of the web being welded to the web by double sided full penetrations welds. Thereby cut outs are avoided in the web towards the hanger anchorage and the demand for a high fatigue detail category has been kept.

The geometry of the hanger anchorage has in general been altered to optimise the design by having a load distribution from the main anchor plate directly into the cross girder web.

		<b>Ponte sullo Stretto di Messina</b> <b>PROGETTO DEFINITIVO</b>		
Specialist Technical Design Report, Annex		<i>Codice documento</i> PS0075_F0-ok.doc	<i>Rev</i> F0	<i>Data</i> 20/06/2011

### Verification method

The longitudinal steel of the cross girders have been verified by using ADVERS based on the derived sectional forces from the IBDAS FE-model. The design is made in accordance with the project specific Design Basis and with background in the Eurocodes (EC).

The utilisation ratios are presented for the relevant cross girders with a more dense distribution around the tower locations where the highest utilisation ratios were expected. In total 31 cross girders have been verified along the whole bridge length including both ends in order to consider possible variation of the most critical stresses. The governing ULS load combination has been found to be the dynamic wind with its highest utilisation ratios for cross girders T1 and T3 in the section next to the railway girder. Utilisation ratios are given in Figure 1-3.

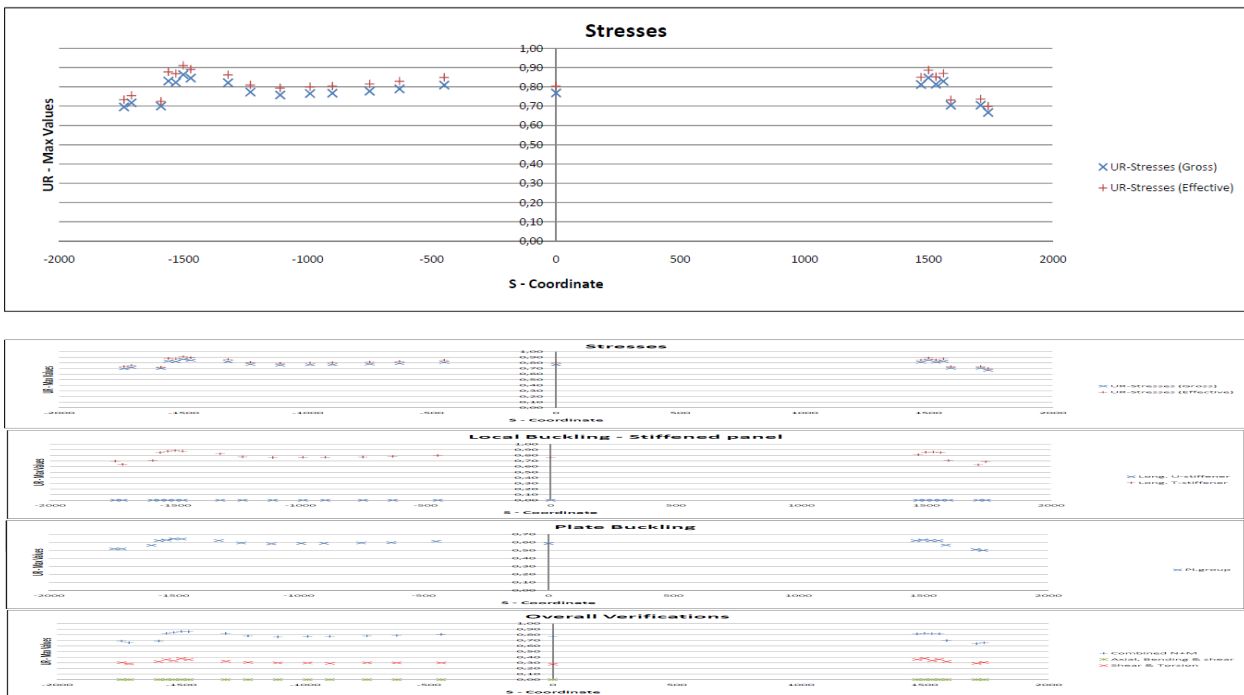


Figure 1-3 Utilisation ratios for cross girders T1 and T3, section 2 ULS dynamic wind load combination

### 1.6 Verification of Longitudinal Steel with Transverse Stresses

Since the "effective width" method as used in ADVERS is not directly applicable in a case where there is uniform transverse stresses accompanying the longitudinal stresses the "reduced stress

		<b>Ponte sullo Stretto di Messina</b> PROGETTO DEFINITIVO		
Specialist Technical Design Report, Annex		<i>Codice documento</i> PS0075_F0-ok.doc	<i>Rev</i> F0	<i>Data</i> 20/06/2011

method" is used. This type of stress analysis is based on gross section properties and subsequent plate buckling checks. From an elastic buckling program critical stresses have been calculated for plate panels subjected to compressive stresses in two directions. These stresses have been used and correspond to the stress limits needed for verification according to the reduced stress method as described in EN 1993-1-5:2005 section 10. This method has been used to determine the utilisation ratios of the considered plates. In addition to this verification also the critical buckling mode has been calculated to identify the critical areas of the plate panel, as illustrated in Figure 1-4.

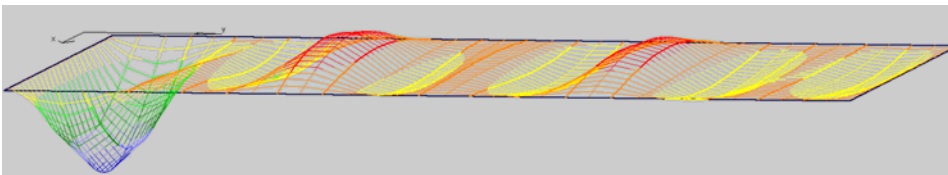


Figure 1-4 Illustration of critical buckling mode for determining critical stresses

## 1.7 Verification - Transverse Steel

The spreadsheet ADVERS does not consider verification of the transverse diaphragm steel. A spreadsheet has been developed in combination with a calculation program for elastic buckling of plates for verification of the different sub-panels of the diaphragms.

The diaphragm is divided into sub-panels by distributed vertical stiffeners. It is verified that these stiffeners have sufficient capacity to support the diaphragm panels sufficiently. Each sub-panel of the diaphragm is subjected to the stress distribution from both global and local traffic loading at its specific location for verification of the stability. Critical stress conditions have been calculated for the panel from the local FE-models of the bridge. These stresses have been applied to the panels using an elastic buckling programme in order to calculate a critical stress ratio factor  $\phi_{cr}$ . The critical stress ratio factor is similar to and has been used as  $\alpha_{cr}$  in the reduced stress method of EN 1993-1-5:2006, section 10 in order to verify the considered panels.

		<b>Ponte sullo Stretto di Messina</b> <b>PROGETTO DEFINITIVO</b>		
Specialist Technical Design Report, Annex		<i>Codice documento</i> PS0075_F0-ok.doc	<i>Rev</i> F0	<i>Data</i> 20/06/2011

## 1.8 Verification using Local FE-Models

The local FE-models are performed in the computer programme Robot Structural Analyses, an integrated graphic program used for modelling, analysing and designing various types of structures. The general purpose of the local models has been to verify the proposed element solution and to document that the stress flow is acceptable with respect to ULS load combinations. Boundary conditions are determined from the global IBDAS bridge model and loading have been applied on the model in accordance with the global IBDAS bridge model.

In total four different models have been made:

- Bridge deck local FE-model describing the cross girder and the longitudinal railway and roadway girders determining the stress level in the plate elements with special regards to stresses in the cross girder outer plates, diaphragms and at the intersection between girders.
- Roadway local FE-model describing the stress level in the diaphragm of the roadway girder with regards to the stress concentration at the troughs, cope holes, diaphragm stiffeners and openings and further more to determine von Mises stresses in skin plates including local loading effect from local wheel loads. The local longitudinal stresses are a result of the roadway troughs spanning between transverse diaphragms. Since the troughs are continuous, both hogging and sagging moments must be considered in determining local stresses. Therefore, in calculating stresses in the top plate and top plate stiffeners, both minimum and maximum stresses are considered.
- Railway local FE-model describing the stress level in the diaphragm of the railway girder with regards to the stress concentration at the troughs, diaphragm stiffeners and openings and further more to determine von Mises stresses in skin plates and top plate stiffeners including local loading effect from local wheel loads. In calculating stresses in the top plate and top plate stiffeners, both minimum and maximum stresses are considered.
- Hanger anchorage local FE-model describing the stress level in the plates related to the hanger anchorages. The general purpose of the local models is to verify the proposed element solutions and to document that the stress flow is acceptable with respect to ULS load combination.

		<b>Ponte sullo Stretto di Messina</b> <b>PROGETTO DEFINITIVO</b>		
Specialist Technical Design Report, Annex	<i>Codice documento</i> PS0075_F0-ok.doc	<i>Rev</i> F0	<i>Data</i> 20/06/2011	

The purpose of the local FE-models is to verify the local design and verify that the stress level is acceptable for applied ULS load combinations. As shown in the following chapters this criteria is fulfilled with some local areas where stresses are within an acceptable yielding range. In these cases it has been verified that yielding areas and peak stresses are acceptable.

Furthermore a semi-local IBDAS FE-model has been developed within the global analysis model enabling a more detailed modeling with shell elements and diaphragms to be used for selected parts. Only a local part of the main span is modeled with shell elements whereas the rest of the suspended deck is modeled with beam elements.

A detailed description of the model can be found in the report “Semi-local IBDAS Model, Suspended Deck”.

As a verification of the local FE-models, axial stress values in the stress plots from the local FE-models is compared with the results from the semi-local IBDAS model.

### 1.8.1 Local FE-model of Suspended Deck

In the cross girder webs access openings are carried out every 120m and since the FE-model represents a typical cross girder, access openings at these locations are therefore not modelled. A documentation of the longitudinal stresses ( $s_{XX}$ ) for the load combination maximising the bending moment in the cross girder is shown in the following. In Figure 1-5 the ROBOT bridge deck local FE-model is shown followed by the semi-local IBDAS model in Figure 1-6.

		<b>Ponte sullo Stretto di Messina</b> <b>PROGETTO DEFINITIVO</b>		
Specialist Technical Design Report, Annex		Codice documento PS0075_F0-ok.doc	Rev F0	Data 20/06/2011

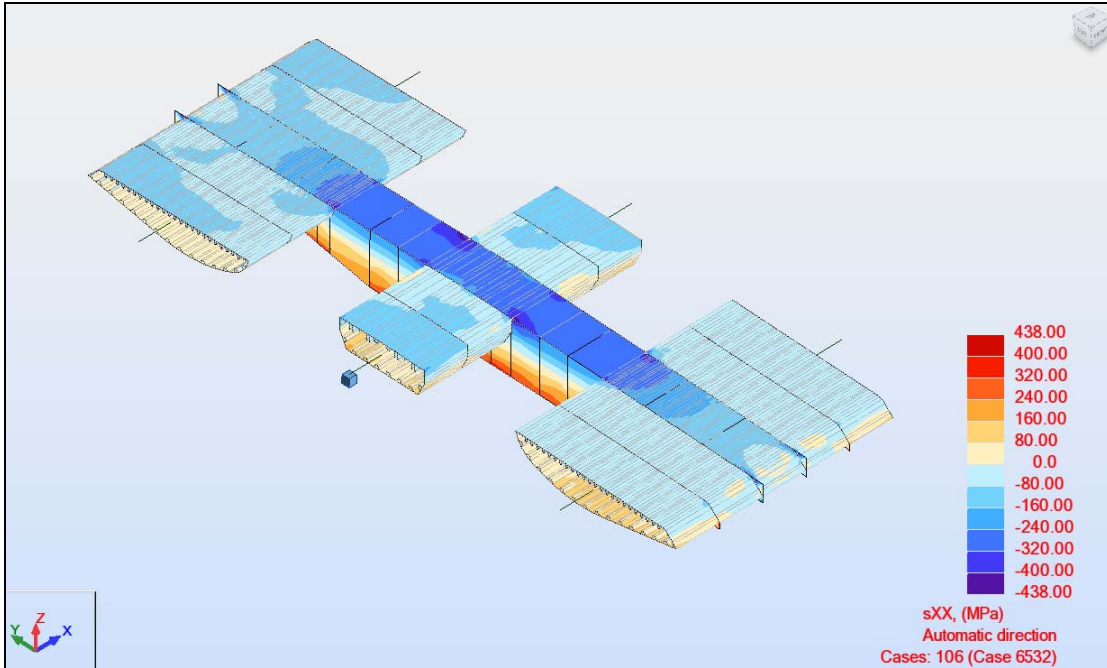


Figure 1-5 Stresses in longitudinal direction of cross girder (sXX) – ROBOT local FE-model

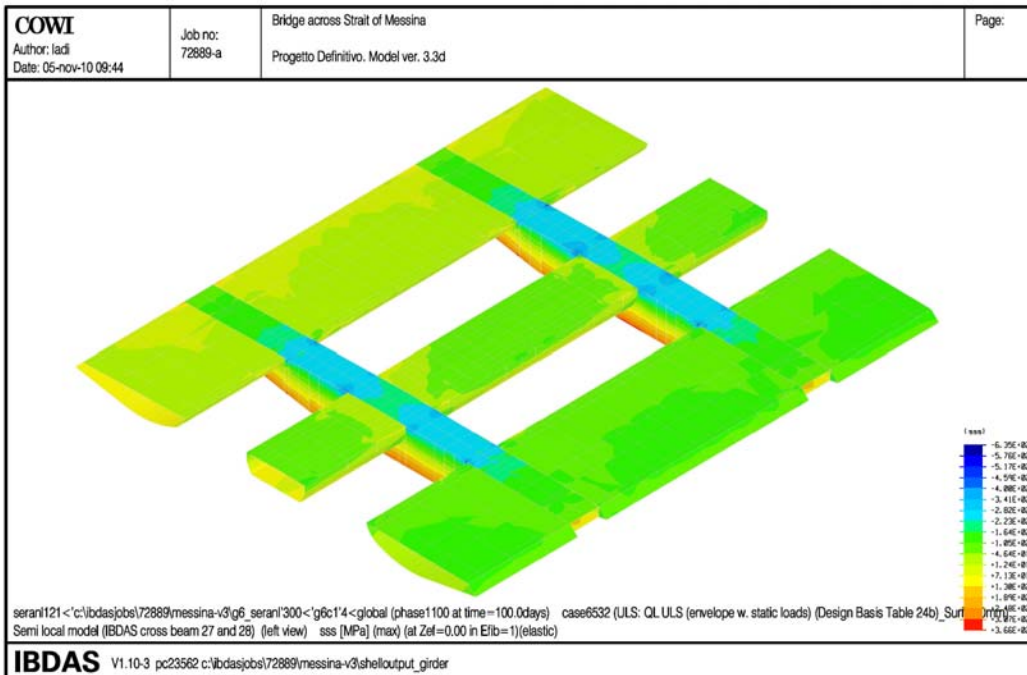


Figure 1-6 Stresses in longitudinal direction of girders sXX – semi-local IBDAS model

		<b>Ponte sullo Stretto di Messina</b> <b>PROGETTO DEFINITIVO</b>		
Specialist Technical Design Report, Annex		<i>Codice documento</i> PS0075_F0-ok.doc	<i>Rev</i> F0	<i>Data</i> 20/06/2011

### 1.8.2 Roadway and Railway Local FE-Models

The transverse steel comprises diaphragms spaced 3.75 m. Local FE-models of the roadway and railway girder have been created for verification of the diaphragms. A stress plot from the local FE-model of the roadway girder diaphragm is shown in Figure 1-7 for the load case with traffic load fixated for maximum  $M_y$ .

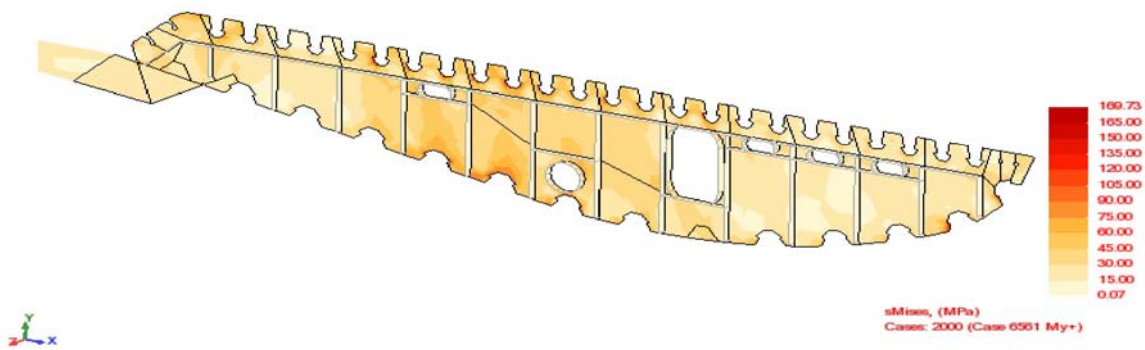


Figure 1-7 von Mises stresses – diaphragm, case 2000 ( $M_y$ )

A stress plot from the local FE-model of the railway girder diaphragm is shown in Figure 1-8 for the load case with dead load and traffic load fixated for maximum  $M_y$ . It is seen that the overall stress level is acceptable for steel S355.

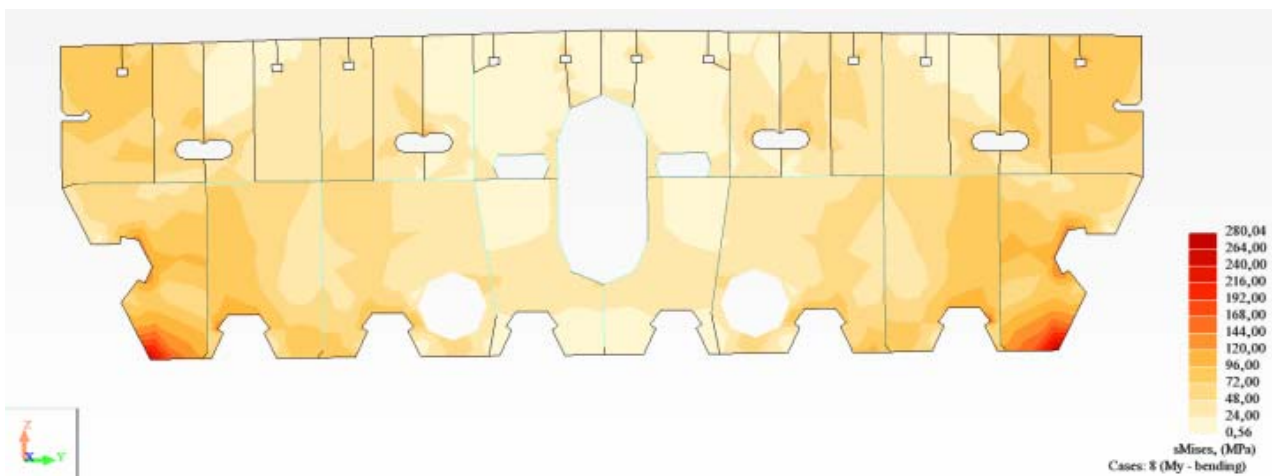


Figure 1-8 von Mises stresses – diaphragm, case 12 ( $M_y$ )

		<b>Ponte sullo Stretto di Messina</b> PROGETTO DEFINITIVO		
Specialist Technical Design Report, Annex		<i>Codice documento</i> PS0075_F0-ok.doc	<i>Rev</i> F0	<i>Data</i> 20/06/2011

### 1.8.3 Hanger Anchorage Local FE-Model

The verification of the hanger anchorage is done with respect to ULS hanger forces and ULS rotation from IBDAS. Rotations appear due to relative displacements between cables and suspended deck. The overall length of the model is 30 m between mid-spans of the longitudinal roadway girder and a width of 26 m comprising half a cross girder. The relatively large extension of the model will ensure correct boundary conditions and stress distribution for the plates related to the hanger anchorage.

The following hanger anchorage types have been modelled; AP1 with spherical bearings, AP1 without spherical bearings, AP2 and AP3, which represents the hanger anchorages from cross girder number 9 to 111.

The maximum rotations are both represented in cross girder 60 which is exactly in the centre of main span.

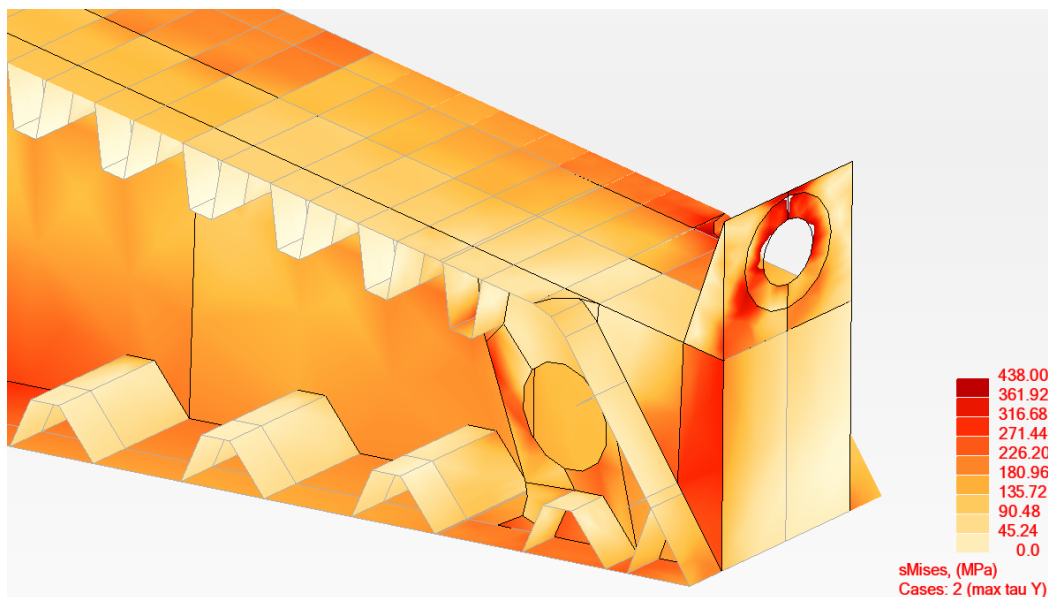


Figure 1-9 von Mises stress plot of AP1 on cross girder 60 with maximum  $\theta_y$  rotation

The Figure 1-9 shows the hanger anchorages at cross girder number 52 to 68, where it has been necessary to add an extra stiffener due to the relatively large hanger rotation in this area.

		<b>Ponte sullo Stretto di Messina</b> <b>PROGETTO DEFINITIVO</b>		
Specialist Technical Design Report, Annex	<i>Codice documento</i> PS0075_F0-ok.doc	<i>Rev</i> F0	<i>Data</i> 20/06/2011	

## 1.9 Fatigue

According to the Design Basis, the railway fatigue load has been based on the standard traffic mix whose composition may be found in EN 1991-2 Table D.1; it includes 67 train transits expected per day per track with a traffic volume of 24.95 million tonnes per year. The roadway fatigue load comprises of 2 million transits per year of heavy roadway vehicles for each direction fulfilling the traffic category 1 defined in EN 1991-2 4.6.1. During the 200 years design life of the bridge the total number of transits for the railway girder hence becomes 4.89 million for each track and 400 million for the roadway girder in each direction (slow lane).

The "unlimited life method" and the "damage accumulation method" (Palmgren-Miners summation of damage) have both been used for the fatigue assessment of the main structural components subjected to direct man generated loads. In addition the wind induced fatigue degradation has been accounted for in the damage accumulation method by a damage of 0.05; this implies the verification to be fulfilled only when the damage from traffic loads is lower then 0.95.

For the fatigue loads the following assumptions have been made:

- Railway traffic: 67 trains per day giving a total of 4.89 million in 200 years per track
- Roadway traffic: 2 million heavy vehicles per year, i.e. 400 million in the 200 year design life
- Speed of trains: maximum speed of trains
- Dynamic factors have been calculated in accordance with Eurocode EN 1991-2 Annex D "Basis for the fatigue assessment of railway structures"
- The likelihood of two train meets at any given point on the bridge during passing is 12%

According to the "Safe Life" assessment method in EN1993-1-9 section 3 and the recommendation included in the RFI44/F the following partial factors have been used:  $\gamma_m = 1.15$  has been applied to local details of the orthotropic roadway deck, while a safety factor of  $\gamma_m = 1.35$  has been applied to all other details.

Furthermore through the FE analysis of the railway box girder it has been found which stress concentration factors are to be applied to the stresses for the fatigue verification, which is based on the IBDAS beam model.

		<b>Ponte sullo Stretto di Messina</b> <b>PROGETTO DEFINITIVO</b>		
Specialist Technical Design Report, Annex		<i>Codice documento</i> PS0075_F0-ok.doc	<i>Rev</i> F0	<i>Data</i> 20/06/2011

## 2 Introduction

### 2.1 Scope of Works

This section of the report describes the design of structural steel elements of the suspended deck, from the terminal structures of Sicilia (stationing 88.49) to the terminal structure of Calabria (stationing 3,723.99). The suspended deck is 60 m wide and entirely made of steel. It is formed by three independent longitudinal box girders, two for the roadway and the central one for the railway. The boxes are connected by cross girders at 30 metres spacing.

Design details for the non-structural components for the suspended deck, such as maintenance/access systems and mechanical/electrical installations are provided elsewhere.

In general the Progetto Definitivo of the suspended deck is based on the Tender Design. The Progetto Definitivo specifies the most important design aspects and other technical topics considered of importance and/or special solutions to the design demands. For some part of the suspended deck structures it has been found advantageous to introduce changes to the design, which will be described in this report.

		<b>Ponte sullo Stretto di Messina</b> <b>PROGETTO DEFINITIVO</b>					
Specialist Technical Design Report, Annex		Codice documento PS0075_F0-ok.doc	<table border="1" style="width: 100%;"> <tr> <td style="width: 50%;">Rev</td> <td style="width: 50%;">Data</td> </tr> <tr> <td>F0</td> <td>20/06/2011</td> </tr> </table>	Rev	Data	F0	20/06/2011
Rev	Data						
F0	20/06/2011						

## 2.2 Bridge Elevation, Plan and Cross Section of Suspended Deck

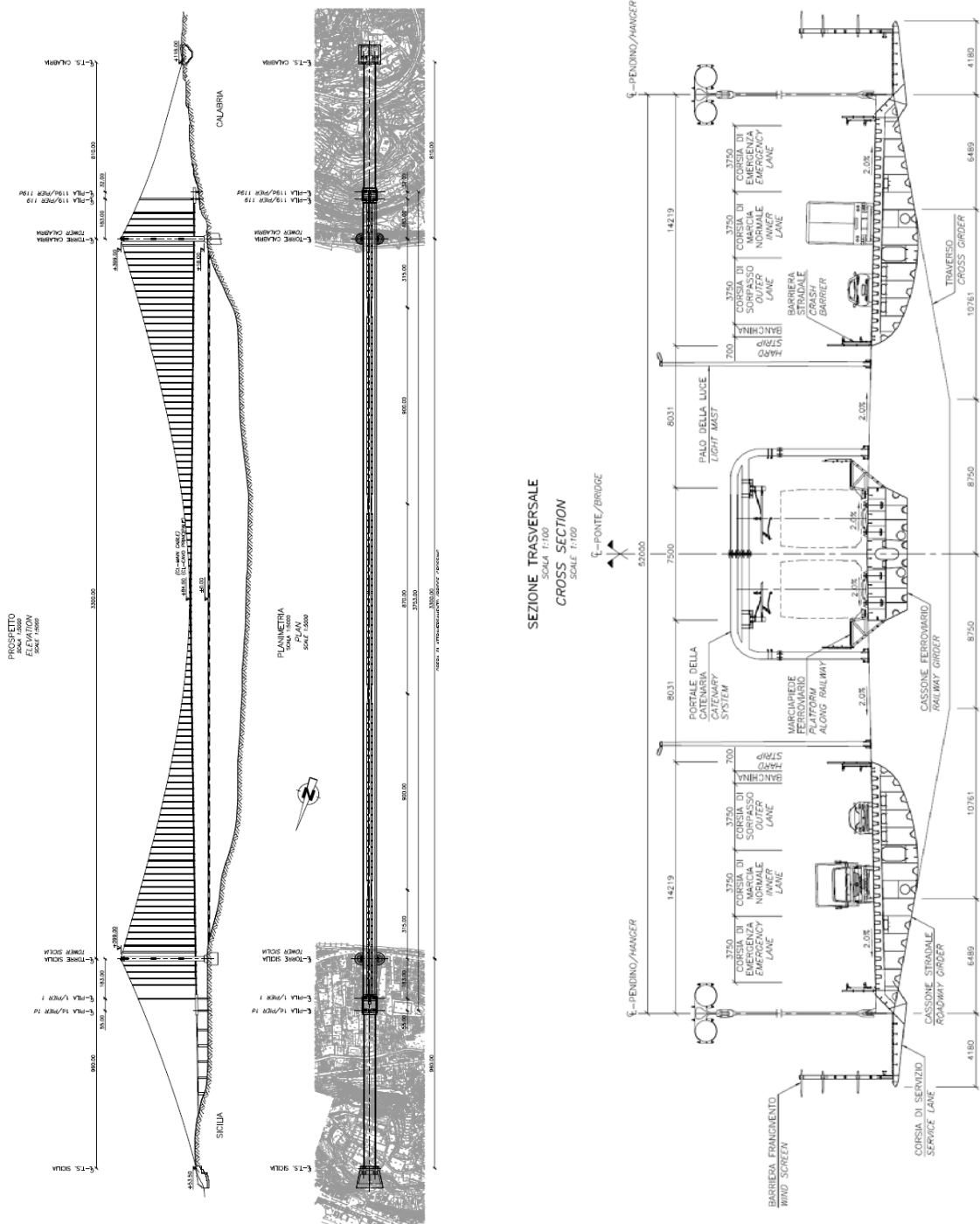


Figure 2-1 Bridge elevation, plan and cross section of suspended deck

		<b>Ponte sullo Stretto di Messina</b> <b>PROGETTO DEFINITIVO</b>		
Specialist Technical Design Report, Annex		<i>Codice documento</i> PS0075_F0-ok.doc	<i>Rev</i> F0	<i>Data</i> 20/06/2011

## 2.3 Design Specifications

GCG.F.04.01 “Engineering – Definitive and Detailed Design: Basis of Design and Expected Performance Levels,” Stretto di Messina, 2004 October 27.

GCG.F.05.03 “Design Development – Requirements and Guidelines,” Stretto di Messina, 2004 October 22.

GCG.G.03.02 “Structural Steel Works and Protective Coatings,” Stretto di Messina, 2004 July 30.

CG.10.00-P-RG-D-P-GE-00-00-00-00-02-A “Design Basis, Structural, Annex.”

### 2.3.1 Design Codes

“Norme tecniche per le costruzioni,” 2008 (NTC08).

EN 1991 Eurocode 1: Actions on Structures – Part 2: Traffic loads on bridges

EN 1993 Eurocode 3: Design of Steel Structures – Part 1-1: General rules and rules for buildings

EN 1993 Eurocode 3: Design of Steel Structures – Part 1-5: Plated structural elements

EN 1993 Eurocode 3: Design of Steel Structures – Part 1-8: Design of joints

EN 1993 Eurocode 3: Design of Steel Structures – Part 1-9: Fatigue

EN 1993 Eurocode 3: Design of Steel Structures – Part 1-10: Selection of steel for fracture toughness and through thickness properties

EN 1993 Eurocode 3: Design of Steel Structures – Part 2: Steel Bridges

Rete Ferroviaria Italia - Istruzione No. 44F “Verifiche a fatica dei ponti ferroviari”

Recommendations for Fatigue Design of Welded Joints and Components, International Institute of Welding (IIW), doc. XIII-2151-07/XV-1254-07, May 2007

Recommendations on Post Weld Fatigue Life Improvement of Steel and Aluminium Structures, International Institute of Welding (IIW), doc. XIII-2200r7-07, 06 July 2010

European Convention for Constructional Steelwork (ECCS), Eurocode, Design Manual, 1-9CL\_Pics-v40, September 2010

		<b>Ponte sullo Stretto di Messina</b> <b>PROGETTO DEFINITIVO</b>		
Specialist Technical Design Report, Annex		<i>Codice documento</i> PS0075_F0-ok.doc	<i>Rev</i> F0	<i>Data</i> 20/06/2011

### 2.3.2 Material Specifications

EN 10025-1:2004 Hot-rolled products of structural steels – Part 1: General delivery conditions.

EN 10025-2:2004 Hot-rolled products of structural steels – Part 2: Technical delivery conditions for non-alloy structural steels.

EN 10025-3:2004 Hot-rolled products of structural steels – Part 3: Technical delivery conditions for normalised / normalised weldable fine grain structural steels.

EN 10025-4:2004 Hot-rolled products of structural steels – Part 4: Technical delivery conditions for thermomechanical rolled weldable fine grain structural steels.

EN 10164:2004 Steel products with improved deformation properties perpendicular to the surface of the product – Technical delivery conditions.

EN ISO 898-1:2009 Mechanical properties of fasteners made of carbon steel and alloy steel – Part 1: Bolts, screws and studs.

EN ISO 3506-1:2009 Mechanical properties of corrosion-resistance stainless-steel fasteners – Part 1: Bolts, screws and studs

EN ISO 3506-2:2009 Mechanical properties of corrosion-resistance stainless-steel fasteners – Part 2: Nuts

EN 20898-2:1994 Mechanical properties of fasteners – Part 2: Nuts with special proof load values – coarse thread (ISO 898-2:1992).

UNI EN 14399:2005-3 High-strength structural bolting assemblies for preloading - Part 3: System HR - Hexagon bolt and nut assemblies

EN ISO 14555:1998 Welding-Arc stud welding of metallic materials. May 1995.

EN ISO 13918:1998 Welding-Studs for arc stud welding-January 1997.

### 2.3.3 Drawings

The suspended deck design drawings accompanying this report are listed in Table 2-1.

		<b>Ponte sullo Stretto di Messina</b> <b>PROGETTO DEFINITIVO</b>		
Specialist Technical Design Report, Annex		<i>Codice documento</i> PS0075_F0-ok.doc	<i>Rev</i> F0	<i>Data</i> 20/06/2011

**Table 2-1** *Suspended deck drawings accompanying this report*

Drawing Title	Drawing Number
Overview, Elevation	CG.10.00-P-AX-D-P-SV-I3-00-00-00-00-01_0
Overview Plan, Sicilia	CG.10.00-P-PX-D-P-SV-I3-00-00-00-00-01_0
Overview Plan, Calabria	CG.10.00-P-PX-D-P-SV-I3-00-00-00-00-04_0
Main Span, Plan and Section	CG.10.00-P-PX-D-P-SV-I3-00-00-00-00-02_0
Tower Location, Plan	CG.10.00-P-PX-D-P-SV-I3-00-00-00-00-03_0
Tower Location, Sections	CG.10.00-P-WX-D-P-SV-I3-00-00-00-00-01_0
Side Span, Plan and Section	CG.10.00-P-LX-D-P-SV-I3-00-00-00-00-01_0
Bridge End Sicilia, Plan and Section	CG.10.00-P-LX-D-P-SV-I3-00-00-00-00-02_0
Bridge End Sicilia, Sections	CG.10.00-P-WX-D-P-SV-I3-00-00-00-00-02_0
Bridge End Calabria, Plan and Section	CG.10.00-P-LX-D-P-SV-I3-00-00-00-00-03_0
Bridge End Calabria, Sections	CG.10.00-P-WX-D-P-SV-I3-00-00-00-00-03_0
Roadway - Main and Side Span - Section	CG.10.00-P-WX-D-P-SV-I3-CS-00-00-00-01_0
Roadway - Main and Side Span - Diaphragms	CG.10.00-P-AX-D-P-SV-I3-CS-00-D0-00-01_0
Roadway - Main and Side Span - Details 1	CG.10.00-P-BX-D-P-SV-I3-CS-00-00-00-01_0
Roadway - Main and Side Span - Details 2	CG.10.00-P-BX-D-P-SV-I3-CS-00-00-00-02_0
Roadway - Tower Location - Section and Elevation	CG.10.00-P-AX-D-P-SV-I3-CS-00-00-00-01_0
Roadway - Tower Location - Diaphragms	CG.10.00-P-AX-D-P-SV-I3-CS-00-0D-00-02_0
Roadway - Tower Location - Details	CG.10.00-P-BX-D-P-SV-I3-CS-00-00-00-03_0
Roadway - Bridge End - Section	CG.10.00-P-LX-D-P-SV-I3-CS-00-00-00-01_0
Roadway - Bridge End - Diaphragms	CG.10.00-P-AX-D-P-SV-I3-CS-00-D0-00-03_0
Railway - Main Span - Section	CG.10.00-P-WX-D-P-SV-I3-CF-00-00-00-01_0
Railway - Main Span - Diaphragms	CG.10.00-P-AX-D-P-SV-I3-CF-00-D0-00-01_0
Railway - Main Span - Details 1	CG.10.00-P-BX-D-P-SV-I3-CF-00-00-00-01_0
Railway - Main Span - Details 2	CG.10.00-P-BX-D-P-SV-I3-CF-00-00-00-02_0
Railway - Tower Location - Section	CG.10.00-P-WX-D-P-SV-I3-CF-00-00-00-02_0
Railway - Tower Location - Diaphragms	CG.10.00-P-AX-D-P-SV-I3-CF-00-D0-00-02_0
Railway - Tower Location - Details	CG.10.00-P-BX-D-P-SV-I3-CF-00-00-00-03_0

Railway - Side Span - Section	CG.10.00-P-WX-D-P-SV-I3-CF-00-00-00-03_0
Railway - Side Span - Diaphragms	CG.10.00-P-AX-D-P-SV-I3-CF-00-D0-00-03_0
Railway - Bridge End - Section	CG.10.00-P-WX-D-P-SV-I3-CF-00-00-00-04_0
Railway - Bridge End - Diaphragms	CG.10.00-P-AX-D-P-SV-I3-CF-00-D0-00-04_0
Railway - Bridge End - Elevation	CG.10.00-P-AX-D-P-SV-I3-CF-00-00-00-01_0
Railway - Bridge End - Intersection	CG.10.00-P-AX-D-P-SV-I3-CF-00-00-00-02_0
Cross Girder - Main Span - Section 1	CG.10.00-P-WX-D-P-SV-I3-TP-00-00-00-01_0
Cross Girder - Main Span - Section 2	CG.10.00-P-WX-D-P-SV-I3-TP-00-00-00-02_0
Cross Girder - Main Span - Diaphragms 1	CG.10.00-P-AX-D-P-SV-I3-TP-00-D0-00-01_0
Cross Girder - Main Span - Diaphragms 2	CG.10.00-P-AX-D-P-SV-I3-TP-00-D0-00-06_0
Cross Girder - Main Span - Details 1	CG.10.00-P-BX-D-P-SV-I3-TP-00-00-00-01_0
Cross Girder - Main Span - Details 2	CG.10.00-P-BX-D-P-SV-I3-TP-00-00-00-02_0
Cross Girder - Tower Location - Section 1	CG.10.00-P-WX-D-P-SV-I3-TP-00-00-00-03_0
Cross Girder - Tower Location - Section 2	CG.10.00-P-WX-D-P-SV-I3-TP-00-00-00-07_0
Cross Girder - Tower Location - Sections 3	CG.10.00-P-WX-D-P-SV-I3-TP-00-00-00-04_0
Cross Girder - Tower Location - Diaphragms 1	CG.10.00-P-AX-D-P-SV-I3-TP-00-D0-00-02_0
Cross Girder - Tower Location - Diaphragms 2	CG.10.00-P-AX-D-P-SV-I3-TP-00-D0-00-03_0
Cross Girder - Tower Location - Diaphragms 3	CG.10.00-P-AX-D-P-SV-I3-TP-00-D0-00-07_0
Cross Girder - Tower Location - Diaphragms 4	CG.10.00-P-AX-D-P-SV-I3-TP-00-D0-00-08_0
Cross Girder - Side Span - Section 1	CG.10.00-P-WX-D-P-SV-I3-TP-00-00-00-05_0
Cross Girder - Side Span - Section 2	CG.10.00-P-WX-D-P-SV-I3-TP-00-00-00-08_0
Cross Girder - Side Span - Diaphragms 1	CG.10.00-P-AX-D-P-SV-I3-TP-00-D0-00-04_0
Cross Girder - Side Span - Diaphragms 2	CG.10.00-P-AX-D-P-SV-I3-TP-00-D0-00-09_0
Cross Girder - Bridge End - Section 1	CG.10.00-P-WX-D-P-SV-I3-TP-00-00-00-06_0
Cross Girder - Bridge End - Section 2	CG.10.00-P-WX-D-P-SV-I3-TP-00-00-00-09_0
Cross Girder - Bridge End - Diaphragms	CG.10.00-P-AX-D-P-SV-I3-TP-00-D0-00-05_0
Cross Girder - Hanger Anchorage 1	CG.10.00-P-AX-D-P-SV-I3-TP-00-00-00-03_0
Cross Girder - Hanger Anchorage 2	CG.10.00-P-AX-D-P-SV-I3-TP-00-00-00-04_0
Cross Girder - Hanger Anchorage 3	CG.10.00-P-AX-D-P-SV-I3-TP-00-00-00-05_0

		<b>Ponte sullo Stretto di Messina</b> <b>PROGETTO DEFINITIVO</b>		
Specialist Technical Design Report, Annex		<i>Codice documento</i> PS0075_F0-ok.doc	<i>Rev</i> F0	<i>Data</i> 20/06/2011

Cross Girder - Hanger Anchorage 4	CG.10.00-P-AX-D-P-SV-I3-TP-00-00-00-06_0
Cross Over - Plan and sections	CG.10.00-P-WX-D-P-SV-I3-00-00-00-00-04_0
Cross Over – Details 1	CG.10.00-P-BX-D-P-SV-I3-00-00-00-00-01_0
Cross Over – Details 2	CG.10.00-P-BX-D-P-SV-I3-00-00-00-00-02_0
Cross Over – Consoles	CG.10.00-P-AX-D-P-SV-I3-00-00-00-00-06_0
Portal for Road Signs - Consoles	CG.10.00-P-AX-D-P-SV-I3-00-00-00-00-07_0
Base Plates	CG.10.00-P-AX-D-P-SV-I3-00-00-00-00-05_0
Accesses 1	CG.10.00-P-AX-D-P-SV-I3-00-00-00-00-02_0
Accesses 2	CG.10.00-P-AX-D-P-SV-I3-00-00-00-00-03_0
Accesses 3	CG.10.00-P-AX-D-P-SV-I3-00-00-00-00-04_0
Dehumidification - General Layout	CG.10.00-P-PX-D-P-SV-I3-00-00-00-00-05_0
Dehumidification - Cross Girder Layout 1	CG.10.00-P-AX-D-P-SV-I3-00-00-00-00-08_0
Dehumidification - Cross Girder Layout 2	CG.10.00-P-AX-D-P-SV-I3-00-00-00-00-09_0
Dehumidification - Cross Girder Layout 3	CG.10.00-P-AX-D-P-SV-I3-00-00-00-00-10_0
Cable Trays and Transits - Cross Girder Layout	CG.10.00-P-AX-D-P-SV-I3-00-00-00-00-11_0
Cable Trays and Transits - Roadway Girder Layout	CG.10.00-P-AX-D-P-SV-I3-00-00-00-00-12_0
Cable Trays and Transits - Details	CG.10.00-P-BX-D-P-SV-I3-00-00-00-00-03_0

### 2.3.4 Reports for Suspended Deck

The suspended deck design reports listed in Table 2-2 provide all the information regarding the suspended deck design principles and verifications.

*Table 2-2 Suspended deck design reports*

Report Title	Report Number
Specialist Technical Design Report, Suspended Deck	CG.10.00-P-RX-D-P-SV-I3-IM-00-00-00-01_0
General Design Principles for Suspended Deck	CG.10.00-P-RG-D-P-SV-I3-IM-00-00-00-01_0
Design Report - Roadway, Railway and Cross Girders	CG.10.00-P-CL-D-P-SV-I3-00-00-00-00-01_0
Design Report - Support Structures	CG.10.00-P-CL-D-P-SV-I3-00-00-00-00-02_0

		<b>Ponte sullo Stretto di Messina</b> <b>PROGETTO DEFINITIVO</b>		
Specialist Technical Design Report, Annex		<i>Codice documento</i> PS0075_F0-ok.doc	<i>Rev</i> F0	<i>Data</i> 20/06/2011

Design Report - Local FE-models of Suspended Deck	CG.10.00-P-CL-D-P-SV-I3-00-00-00-00-03_0
Design Report - Fatigue Assessment of Suspended Deck	CG.10.00-P-CL-D-P-SV-I3-00-00-00-00-04_0
Design Report - Special Design Investigations	CG.10.00-P-CL-D-P-SV-I3-00-00-00-00-05_0

## 2.4 Nomenclature

The section provides descriptions of terms commonly used throughout the report to refer to various suspended deck components:

*Roadway girder* - orthotropic steel box for roadway traffic connected by the cross girders.

*Railway girder* - orthotropic steel box for railway traffic connected by the cross girders.

*Cross girder* – the transverse beams connecting the railway girder and roadway girders every 30m.

*Longitudinal Stiffeners* – the longitudinal plate elements used to stiffen the vertical suspended deck plate, bottom plates and webs as well as the deck and bottom plate and webs of the cross girders.

*Transverse Diaphragms* – diaphragms implemented at both the roadway, railway and cross girders.

*Hanger Anchorage* – the connection of the hanger cables to the cross girders.

*Railway Fastening System* – the connection of the railway tracks to the railway girder.

*T-beam* – Longitudinal T-beams underneath the four rails carrying the local train loads.

*Drop-in span* – the 60 m road girder span at the towers.

## 3 Design Changes

### 3.1 Roadway Girder

1. Compared with the cross section in the tender design the primary modification is the 2.0 % outward inclination of the top plate which previously had an inward slope. As a consequence of this change the gully for drainage of the pavement is moved to the outer edge of the deck

		<b>Ponte sullo Stretto di Messina</b> <b>PROGETTO DEFINITIVO</b>		
Specialist Technical Design Report, Annex		<i>Codice documento</i> PS0075_F0-ok.doc	<i>Rev</i> F0	<i>Data</i> 20/06/2011

plate, the position of the crash barriers are adjusted slightly due to the longitudinal water channel is placed at the outer edge of the deck plate.

2. Besides the primarily modification on the cross section, the direction of the road traffic has been inverted, which has an impact on the deck plate thickness for lane configuration.
3. Due to optimisation of the overall cross section, simplification of the hanger anchorage and connection details to the service lane the overall width of the roadway girder has been reduced. The outer edge plate of the roadway girder has become more inclined to ease the connection to the hanger anchorages, and the radius forming the connection between roadway deck plate and edge plate has been modified to give better room for the longitudinal water channel. The theoretical horizontal width of the roadway girder now becomes 14.227 m.
4. The two L-stiffeners underneath the edge plate have been changed to flat stiffeners to comply with manufacturing optimisation. The first deck trough under the crash barrier at the emergency lane is replaced by two flat stiffeners and the trough underneath the inspection corridor is also replaced by two flat stiffeners to comply with demands for high fatigue detail categories. To fulfil the fatigue demands, the tooth plate supporting the troughs at the diaphragms is increased from 10 mm to 15 mm in the slow and fast lane together with a modified shape of the cut outs.
5. The verifications are made under the assumption that the pavement thickness of 12 mm might change to 40 mm, whereas the thickness of 12 mm is used for stress concentration verification of the orthotropic deck and the thickness of 40 mm will be used for the global dead load.
6. Preparations carried out for 3 additional cross-overs for later implementation.
7. Safety factors for fatigue strength have been increased giving thicker plates. The roadway deck plate in the two traffic lanes is increased from 16 mm to 17 mm, and the troughs underneath are in general increased from 7 mm to 9 mm.
8. To fulfil the fatigue demands at the trough joints, the troughs underneath the deck plate are increased locally at a width of 7.3m. The thickness is increased from 9 mm to 10 mm and 14 mm at the cross girder joints from 9 mm to 11 mm and 13 mm at the erection joints.
9. To fulfil the fatigue demands at the joints in the bottom plate, the thickness is in general increased locally from 8 mm to 13 mm at the cross girder joints and at the erection joints (every 60m).

		<b>Ponte sullo Stretto di Messina</b> <b>PROGETTO DEFINITIVO</b>		
Specialist Technical Design Report, Annex		<i>Codice documento</i> PS0075_F0-ok.doc	<i>Rev</i> F0	<i>Data</i> 20/06/2011

10. Tab plates for the bottom trough stiffeners are removed and replaced by a direct attachment of the troughs to the diaphragm. Cope holes are maintained at the flange of the trough stiffener.
11. The base plates for roadway crash barrier have been changed from welded to bolted solution to comply with demands for high fatigue detail categories.
12. To comply with the fatigue demands, the fixation of the gullies is changed from welded to bolted solution with two joint sealants.
13. The number of drainage pipes inside the roadway girder has been reduced from 3 to 1 pipe and the holes in the roadway diaphragms for cables have been relocated.
14. Manhole inside the roadway girder has been changed in size to 1300x800 mm due to shear forces in the diaphragm.
15. Termination of stiffeners and diaphragms have in general been improved by adding endplates with a radius of min 150 mm. Thereby the detail fatigue category can be improved fulfilling the fatigue demands.
16. To comply with the fatigue demands, weld improvement has furthermore been introduced in general by ground smoothing of all the 6 bottom flange/diaphragm joints between the cross girders.

The above mentioned modifications have changed the overall geometry of the cross section as shown in Figure 3-1.

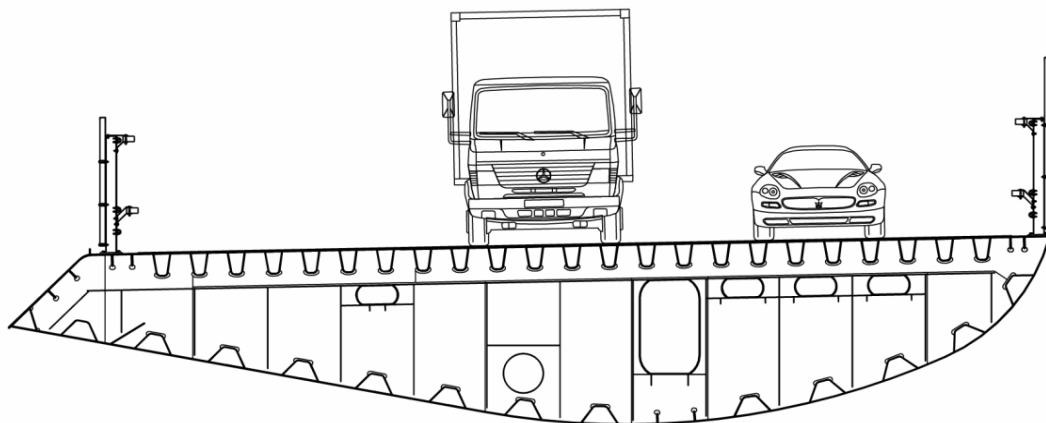


Figure 3-1 Modified cross section for roadway girder (service lane not shown)

		<b>Ponte sullo Stretto di Messina</b> <b>PROGETTO DEFINITIVO</b>		
Specialist Technical Design Report, Annex		<i>Codice documento</i> PS0075_F0-ok.doc	<i>Rev</i> F0	<i>Data</i> 20/06/2011

### 3.2 Railway Girder

1. Since tender design, changes have been made to the overall shape of the steel box girder. The angle of the inclined web is changed from 44 deg to 63 deg while the vertical web plate remains unchanged. The thickness of the bottom plate is lowered from 12 mm to 10 mm to keep cross section properties almost unchanged.
2. Angle profiles stiffening the deck plate, inclined bottom plate and web plates in the tender design, are replaced with flat stiffeners to comply with manufacturing optimisation.
3. The troughs underneath the deck plate are furthermore exchanged by flat stiffeners to comply with demands for high fatigue detail categories. The extra steel within the flat stiffeners is almost balanced out by reducing the deck plate thickness from 16 mm to 15 mm.
4. T-beams, flat and trough stiffeners are continuous throughout the diaphragms to eliminate fatigue problems by interruption. The diaphragm at support of T-stiffeners is reinforced locally from 10 mm to 15 mm.
5. Safety factors for fatigue strength have been increased giving demands for thicker plates.
6. The rail fastening system has been modified since the tender design to a full welded solution with additional stiffening per 1250 mm. The L-profiles of the railway track superstructure will furthermore allow for dewatering per 10 m.
7. The distance between the intermediate stiffeners supporting the railway superstructure is changed from 1875 mm to 1250 mm. This implies that the number of stiffeners is doubled.
8. To comply with the fatigue demands the bottom plate is increased locally from 10 mm to 15 mm at the erection joints (every 60m). The bottom plate is furthermore reinforced locally in all spans at the 4 centre diaphragms at the inclined webs. For the spans in vicinity of the towers, a partial increment of the bottom plate is further required throughout the cross girder.
9. Railway crash barriers have been implemented into the platform along the railway and their base plates have been modified from welded to bolted solution to comply with demands for high fatigue detail categories. The same argument applies for fixation of the gullies which is changed from welded to bolted solution with two joint sealants.

		<b>Ponte sullo Stretto di Messina</b> <b>PROGETTO DEFINITIVO</b>		
Specialist Technical Design Report, Annex		<i>Codice documento</i> PS0075_F0-ok.doc	<i>Rev</i> F0	<i>Data</i> 20/06/2011

10. Termination of stiffeners and diaphragms have in general been improved by adding end plates with a radius of min 150 mm. Thereby the fatigue detail category can be improved fulfilling the fatigue demands.
11. Changes have been made to the diaphragm where the stiffener and weld layout have been modified. Holes in the railway diaphragms for cables have been relocated and the high voltage cables have been removed from the railway girder. The number of drainage pipes inside the railway girder has furthermore been reduced from four to two pipes.
12. To comply with the fatigue demands, weld improvement has furthermore been introduced in general by ground smoothing of the two centre diaphragm joints. These two diaphragms plus two additional are fully welded by K-welds.

The above mentioned modifications have changed the overall geometry of the cross section as shown in Figure 3-2.

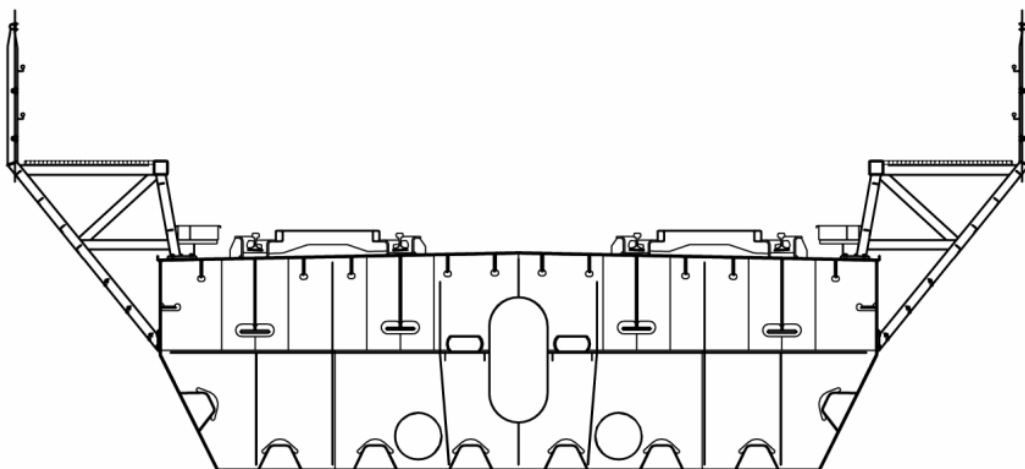


Figure 3-2 Modified cross section for railway girder inclusive walkway along railway

### 3.3 Cross Girder

1. Since the tender design, the direction of the road traffic has been inverted. This change led to a continuous 2.0 % outward slope of the top plate throughout the entire length of all cross girders, see Figure 3-3 (type T1-T3 shown).

		<b>Ponte sullo Stretto di Messina</b> <b>PROGETTO DEFINITIVO</b>		
Specialist Technical Design Report, Annex		<i>Codice documento</i> PS0075_F0-ok.doc	<i>Rev</i> F0	<i>Data</i> 20/06/2011

2. The tender design solution presented the diaphragms next to the railway girder with the spacing of 2.5 m. This configuration had been reinforced by an extra transverse stiffener thereby halves the buckling length of the plate as shown in Figure 3-3.

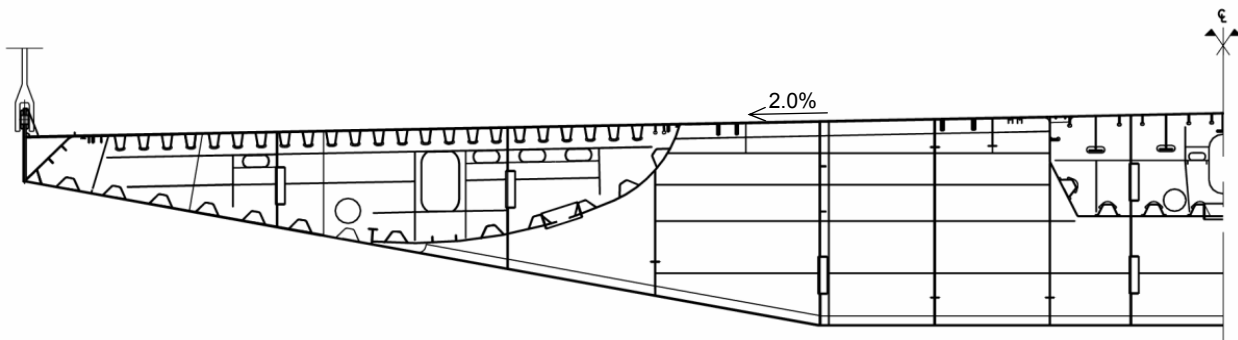


Figure 3-3 Continuous outwards slope of cross girder

3. T-stiffeners at the webs and bottom plate have been replaced with flat stiffeners to comply better with manufacturing optimisation, see Figure 3-3. T- and flat stiffeners are preferred as stiffeners in the cross girders as they are easier to implement in the complicated geometry than ordinary trough profiles.
4. The centre 4.4 m of the bottom plate has been increased in thickness by 8 mm, while the two neighbouring plates (2 x 4.05 m) have been increased by 3 mm. The top plate in the vicinity of the railway girder is also increased in thickness by 3-4 mm. All changes have been done to comply with the fatigue demands.
5. The geometry of the hanger anchorage has in general been altered to optimise the design by having a load distribution from the main anchor plate directly into the cross girder web.

		<b>Ponte sullo Stretto di Messina</b> PROGETTO DEFINITIVO	
Specialist Technical Design Report, Annex	<i>Codice documento</i> PS0075_F0-ok.doc	<i>Rev</i> F0	<i>Data</i> 20/06/2011

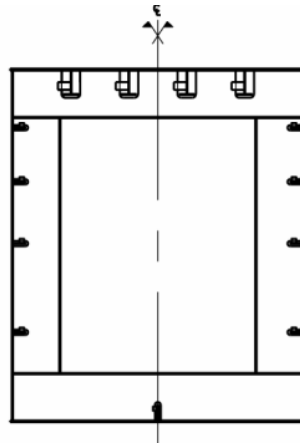


Figure 3-4 Flat stiffeners on cross girder webs and bottom plate

6. To comply with the fatigue demands, weld improvement has furthermore been introduced by ground smoothing all the diaphragms positioned at the horizontal bottom plate. Both the bottom- and top plate and 500 mm of the belonging webs are treated.
7. Termination of stiffeners and diaphragms have in general been improved by adding end plates with a radius of min 150 mm. Thereby the detail fatigue category can be improved fulfilling the fatigue demands.
8. Changes have also been made to the cross girder T7 at the terminal structure. The high demand of torsional capacity due to the adjoining spans led to widen the cross section from 1700 mm to 2700 mm. The width has also been determined to accommodate the expansion joint movement.

### 3.3.1 Intersections to Roadway and Railway Girders

1. The arrangements of stiffeners in the cross girder is such that all the stiffeners of roadway and railway decks pass through the interior of the cross girder. This is done to give more favourable interconnection to the road and railway girder sections and to improve the fatigue strength. In addition this arrangement ensures a high driving comfort when passing the cross girder due to the uniform deck stiffness. In the remaining part of the cross girder, longitudinal T-stiffeners are applied to the deck plate in longitudinal direction of the cross girder itself.
2. The web and bottom troughs at the roadway girder are interrupted at the cross girder web, but extra short trough sections are introduced at both sides of the web being welded to the web by

		<b>Ponte sullo Stretto di Messina</b> <b>PROGETTO DEFINITIVO</b>		
Specialist Technical Design Report, Annex		<i>Codice documento</i> PS0075_F0-ok.doc	<i>Rev</i> F0	<i>Data</i> 20/06/2011

double sided full penetrations welds. Thereby cut outs are avoided in the web towards the hanger anchorage and the demand for a high fatigue detail category has been kept.

3. To fulfil the fatigue demands, the tooth plate supporting the troughs at the web of the roadway girder is increased from 16 mm to 25 mm in the slow and fast lane together with a modified shape of the cut outs.
4. The bottom plate, inclined webs and belonging troughs are passing trough the web of the cross girder, while the vertical web plates are interrupted.

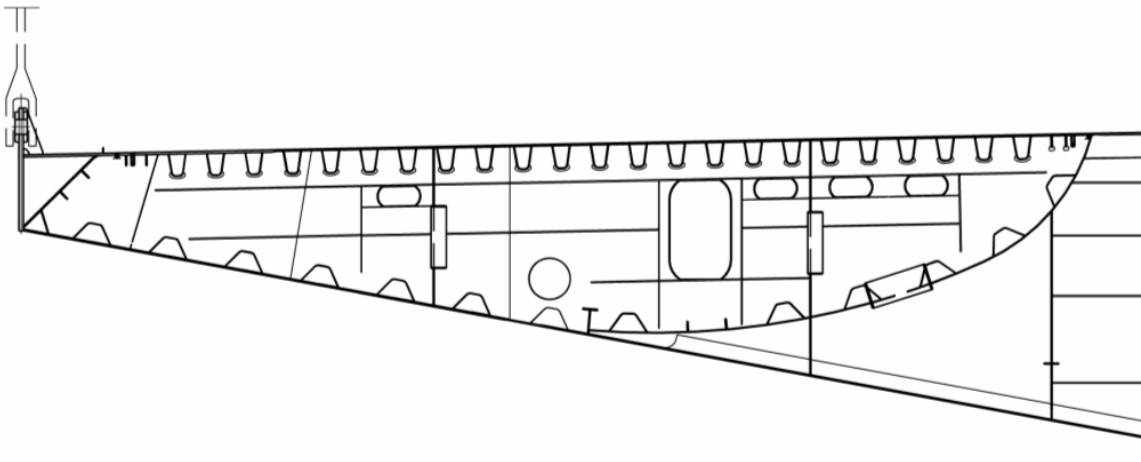


*Figure 3-5 Roadway troughs – cross girder webs intersection detail*

The intersections of the cross girder to roadway and railway girders can be seen in Figure 3-5 and Figure 3-6.

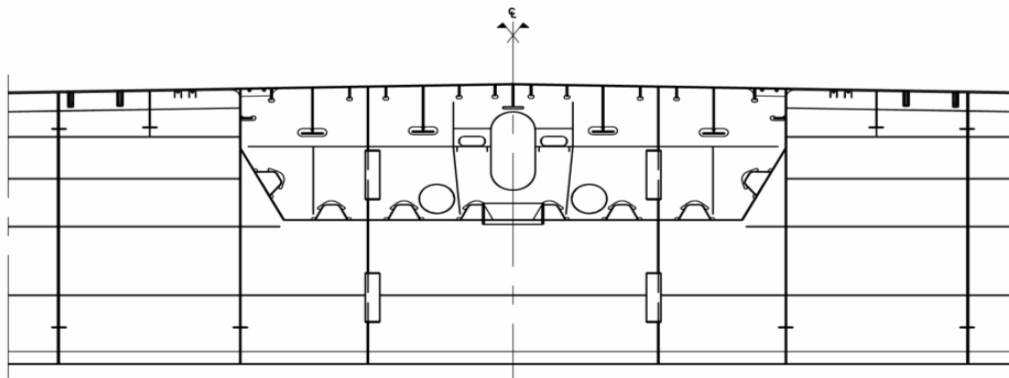


*Figure 3-6 Railway troughs – cross girder web intersection detail*

		<b>Ponte sullo Stretto di Messina</b> <b>PROGETTO DEFINITIVO</b>		
Specialist Technical Design Report, Annex		<i>Codice documento</i> PS0075_F0-ok.doc	<i>Rev</i> F0	<i>Data</i> 20/06/2011

## 4 Limit States

This section describes the limit states and corresponding performance requirements governing the proportioning of the suspended deck components, in accordance with the project design basis GCG.F.04.01 and NTC08.

The suspended deck structural components are verified at Serviceability Limit States (SLS1 and SLS2), Ultimate Limit States and Fatigue Limit States in accordance with the project design basis GCG.F.04.01 and NTC08. Detailed descriptions of the limit states considered in the suspended deck design are provided in CG.10.00-P-RG-D-P-SV-I3-00-00-00-00-01 “General Design Principles for Suspended Deck.”

## 5 Materials

Construction materials used in the suspended deck structural components are summarised in this section. Detailed descriptions of material properties and partial factors considered in the suspended deck design are provided in CG.10.00-P-RG-D-P-SV-I3-00-00-00-00-01 “General Design Principles for Suspended Deck.”

### 5.1 Structural Steel

Suspended deck structural components are fabricated from grade S355ML, S420ML and grade S460 ML structural steels, produced in accordance with EN 10025-4. The steel fabricator has confirmed that the mechanical properties will not vary with material thickness for thicknesses less than 100 mm, as is typical for rolled steel products.

### 5.2 High Strength Bolts

High strength structural bolts of Grade 8.8 or Grade 10.9, produced in accordance with EN ISO 898, are used for all bolted connections. Where appropriate stainless steel bolts in grade A4-70 or A4-80 have been utilised for fastening of ancillary structure at the outside of the suspended deck.

### 5.3 Welding Consumables

Welding consumables shall comply with the requirements of EN 1993-1-8, section 4.2.

		<b>Ponte sullo Stretto di Messina</b> <b>PROGETTO DEFINITIVO</b>		
Specialist Technical Design Report, Annex		<i>Codice documento</i> PS0075_F0-ok.doc	<i>Rev</i> F0	<i>Data</i> 20/06/2011

## 6 Articulation

### 6.1 Overall Static System

The static system for the suspended deck has in general been adopted from the Tender Design:

- The roadway girders are continuous between terminal structures except at two expansion joints placed +/- 30m from each of the towers.
- The railway girder is continuous from one terminal structure to the other. At the terminal structures, bearings are arranged at two locations ensuring both the vertical and horizontal alignment requirements of the railway girder are fulfilled.
- A special structure is installed between the two cross girders in the tower area and consists of two interconnected triangles and a buffer connection to the towers legs. The structure ensures that no transverse bending will be transferred from the main span and through the device to the side span. The X-structure is supported in vertical direction with a pin connection to the railway girder. The X-structure is designed and verified by the articulation group. However the fatigue verification is performed in the document Design Report - Fatigue Assessment of Suspended Deck, CG.10.00-P-CL-D-P-SV-I3-00-00-00-00-03.
- The road and railway box girders are interconnected by closed box cross girders.

### 6.2 Interconnection of the Suspended Deck Elements

The closed steel box cross girders have great torsion rigidity. The interconnection to the longitudinal girders is designed using closed diaphragms, which makes transferring of moments in all 3 directions possible. This applies for the analyses carried out as well as the joint design reflected on the drawings. In this way live loads on the girders are distributed as much as possible to all the deck structures, which minimises adverse deflections.

## 7 Global Structural FE-Analyses

The Messina Strait bridge is modelled and analysed in the COWI developed analysis program IBDAS (Integrated Bridge Design and Analysis System). This section describes the approach to particular aspects of the structural analysis that affect the suspended deck design. The bridge model and structural analysis, in general, are described in the "IBDAS Model, Description."

		<b>Ponte sullo Stretto di Messina</b> <b>PROGETTO DEFINITIVO</b>		
Specialist Technical Design Report, Annex		<i>Codice documento</i> PS0075_F0-ok.doc	<i>Rev</i> F0	<i>Data</i> 20/06/2011

## 7.1 IBDAS Global Beam Model

In the IBDAS global FE-model, the suspended deck structure is generally modelled with beam elements. This model is used for the overall verification of the suspended structure elements. Further a semi-local IBDAS shell FE-model is developed and implemented into the global beam FE-model. Hereby it will be possible to investigate the stress flow within the suspended deck structure in more details with the benefit of getting boundary conditions automatically from the global beam model.

## 7.2 Second Order Effects and Imperfections

All calculations performed with the structural self weight (PP) including self weight of non-structural elements (PN) based on theory of elasticity and second order analysis (geometric non-linear analysis). Additional bending moments due to global 2nd order effects from the design actions of PP and PN are hence directly included in the results from the IBDAS global analysis model.

At present imperfections of the suspended deck elements are anticipated to fulfil the requirements specified in the Eurocodes. Therefore no additional imperfections are considered in the verification of the suspended deck and its elements.

## 8 Verification - Longitudinal Steel

In order to structure and generalise calculations of the longitudinal steel of road-, railway- and cross girders of the Messina Strait Bridge an **Advanced Steel Verification Spreadsheet (ADVERS)** has been developed based on the Eurocodes. The verification of the longitudinal steel girders using ADVERS are based on computerised analyses (IBDAS), member sizing, section verification, stress and buckling checks. The design is made in accordance with the project specific Design Basis and the Eurocodes (EC).

The overall verification of the suspended deck is done based on the derived section forces obtained from the Global IBDAS FE-model.

The general ULS load combinations used for verification for the longitudinal steel are shown in Table 8-1.

		<b>Ponte sullo Stretto di Messina</b> <b>PROGETTO DEFINITIVO</b>		
Specialist Technical Design Report, Annex		<i>Codice documento</i> PS0075_F0-ok.doc	<i>Rev</i> F0	<i>Data</i> 20/06/2011

Table 8-1 Relevant load combinations for verification of longitudinal steel

Load Combination	Description
Static load	Comprising dead load, local traffic load, differential distributed temperature, uniform temperature, static wind (mean wind multiplied by a gust factor), for a model where the longitudinal buffers at the towers are in the fixed mode. In the uniform temperature load case a correction factor accounts for the fixed mode at the towers.
Dynamic wind	Comprising dead load, local traffic load, differential and uniform distributed temperature, dynamic wind where the eight wind directions are combined and applied as envelope values, for a model where the longitudinal buffers at the towers are in the fixed mode.
Seismic (time history)	Dead load, local traffic load, differential and uniform distributed temperature, static wind, for a model where the longitudinal buffers at the towers are in the free mode. These loads are combined with seismic loadings based on time history analysis, where the buffers are working over time.

The utilisation ratios presented in the following chapters are the von Mises stresses in relation to the design yielding stresses. Furthermore utilisation ratios for global plate buckling are shown with respect to interaction between plate and column buckling according to EN 1993-1-5 sec. 4.5. The critical stress  $\sigma_{Ed,Cr}$  is determined for each plate by considering plates and stiffeners as an equivalent orthotropic plate according to EN 1993-1-5:2006 Annex A1.

It should be noted that some components of the suspended deck are subjected to notable seismic damage; these sections are typically located close to the towers and between towers and terminal structures. The vibration periods most influencing the seismic demands on these components will

		<b>Ponte sullo Stretto di Messina</b> PROGETTO DEFINITIVO					
Specialist Technical Design Report, Annex		<i>Codice documento</i> PS0075_F0-ok.doc	<table border="1" style="width: 100%; border-collapse: collapse;"> <thead> <tr> <th style="text-align: left;"><i>Rev</i></th> <th style="text-align: left;"><i>Data</i></th> </tr> </thead> <tbody> <tr> <td>F0</td> <td>20/06/2011</td> </tr> </tbody> </table>	<i>Rev</i>	<i>Data</i>	F0	20/06/2011
<i>Rev</i>	<i>Data</i>						
F0	20/06/2011						

be similar to those influencing the tower response and thus the selected Rayleigh damping coefficients will result in appropriate levels of damping for the relevant suspended deck modes. The most important eigenfrequencies for the seismic load combination has been investigated further for the suspended deck and is found to be in the range of 0.7-2.4 Hz. This gives a damping in the range of 1.7 - 3 %, see Figure 8-1, which is found to be acceptable.

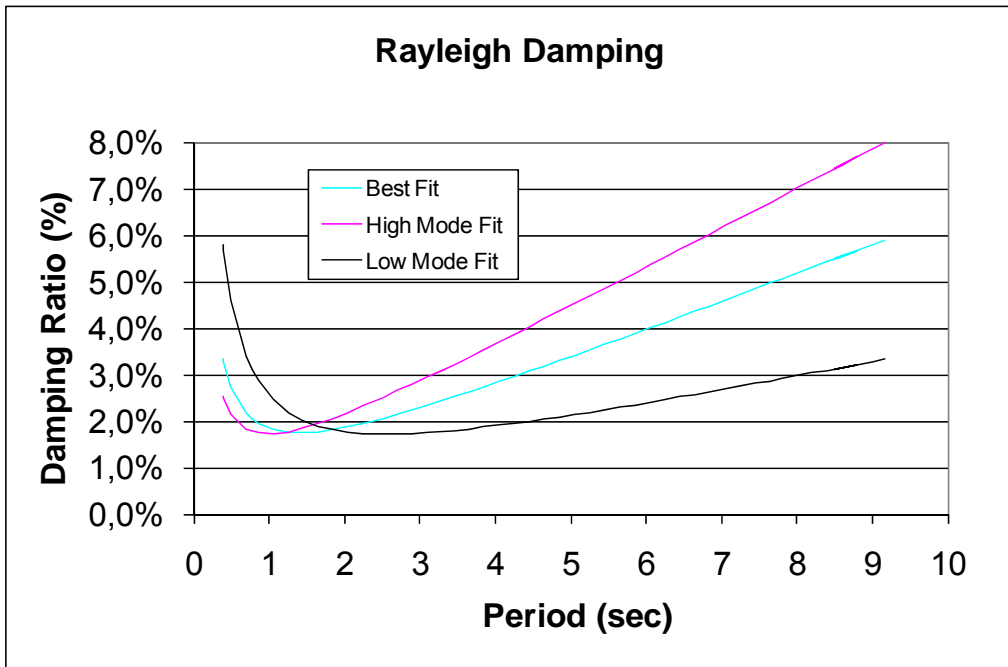


Figure 8-1 Rayleigh damping ratios as used in the global IBDAS model (Best fit)

## 8.1 Verification - Roadway Girder

The longitudinal steel in the two roadway girders are continuous from one terminal structure to the other only interrupted at cross girder T4a and T4b at bearings for the 60 m drop-in span at the towers.

Sectional forces and utilisation ratios are shown in the figures below. The distribution of sectional forces  $N_s$ ,  $M_y$  and  $V_z$  are imported from the IBDAS FE-model. In Figure 8-2 to Figure 8-4 sectional forces are presented for the ULS load combination dynamic wind.

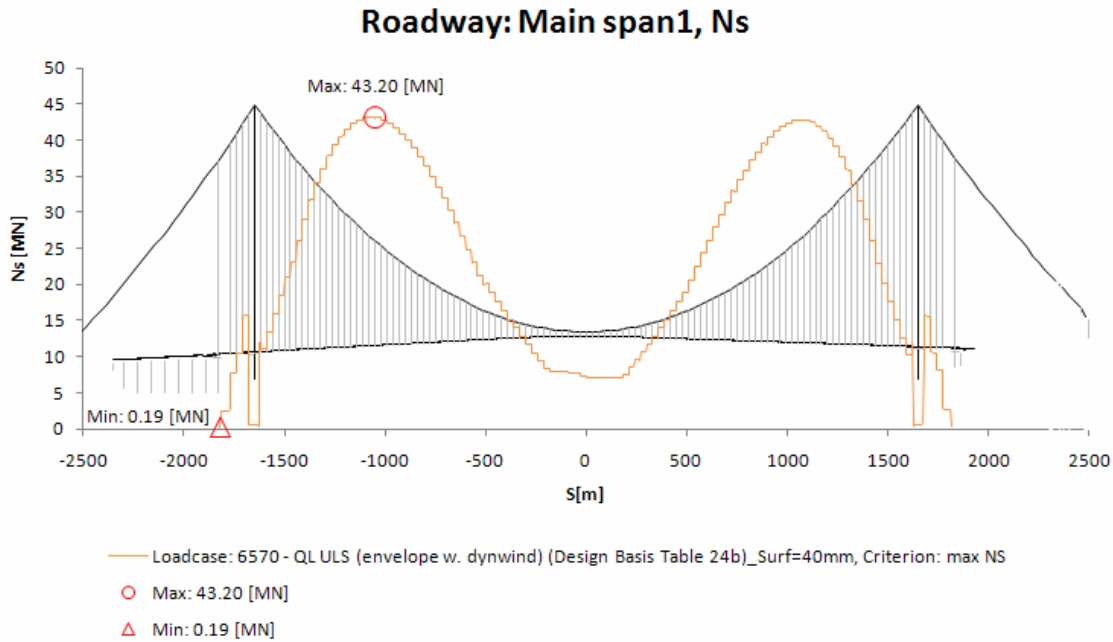


Figure 8-2 Maximal normal force ( $N_{s+}$ ) in roadway girders, ULS dynamic wind load combination

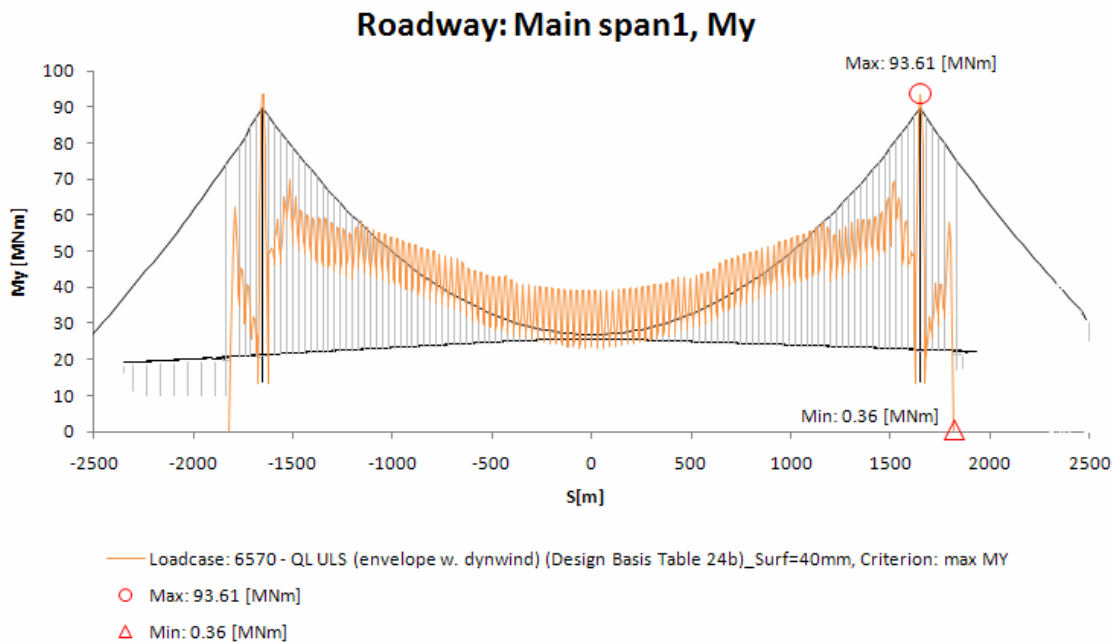


Figure 8-3 Maximal bending moment ( $M_{y+}$ ) in roadway girders, ULS dynamic wind load combination

		<b>Ponte sullo Stretto di Messina</b> PROGETTO DEFINITIVO	
Specialist Technical Design Report, Annex		Codice documento PS0075_F0-ok.doc	Rev Data F0 20/06/2011

### Roadway: Main span1, Vz

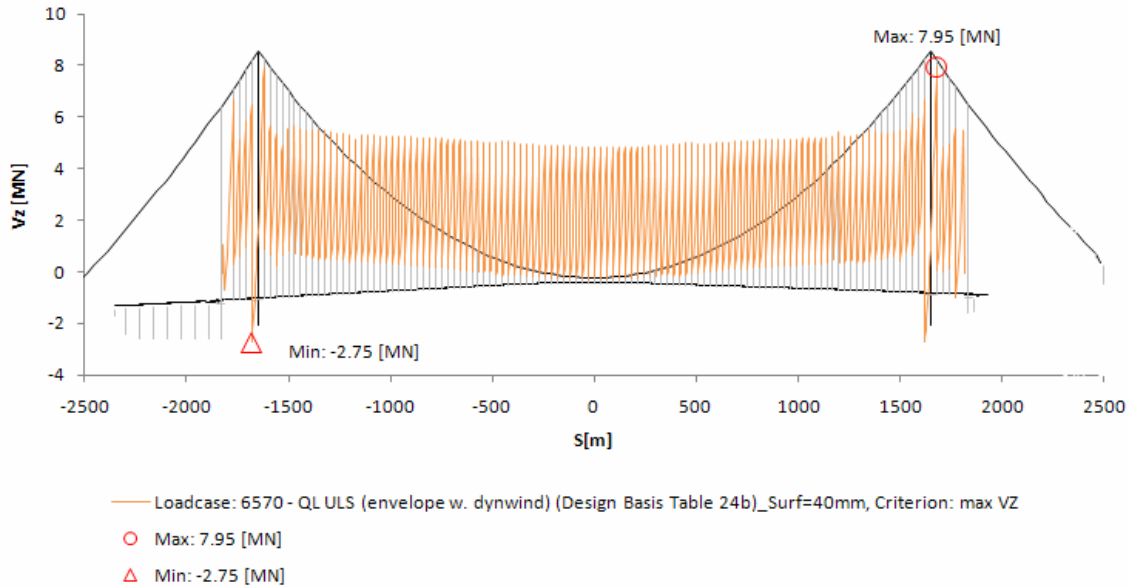


Figure 8-4 Maximal shear force ( $Vz+$ ) in roadway girders, ULS dynamic wind load combination

The utilisation ratios are presented at selected s-coordinates located in the position of governing loads, change in geometry, plate thicknesses and in structural key points like centre of main span, connections to the cross girder and in 60 m drop-in etc. The governing ULS load combination is the dynamic wind and the utilisation ratios for this combination are shown in Figure 8-5.

The figures show the worst utilisation ratio (UR) i.e. demand/capacity for a number of stress points analysed for each cross section. UR's are shown for stresses and buckling of plate panels.

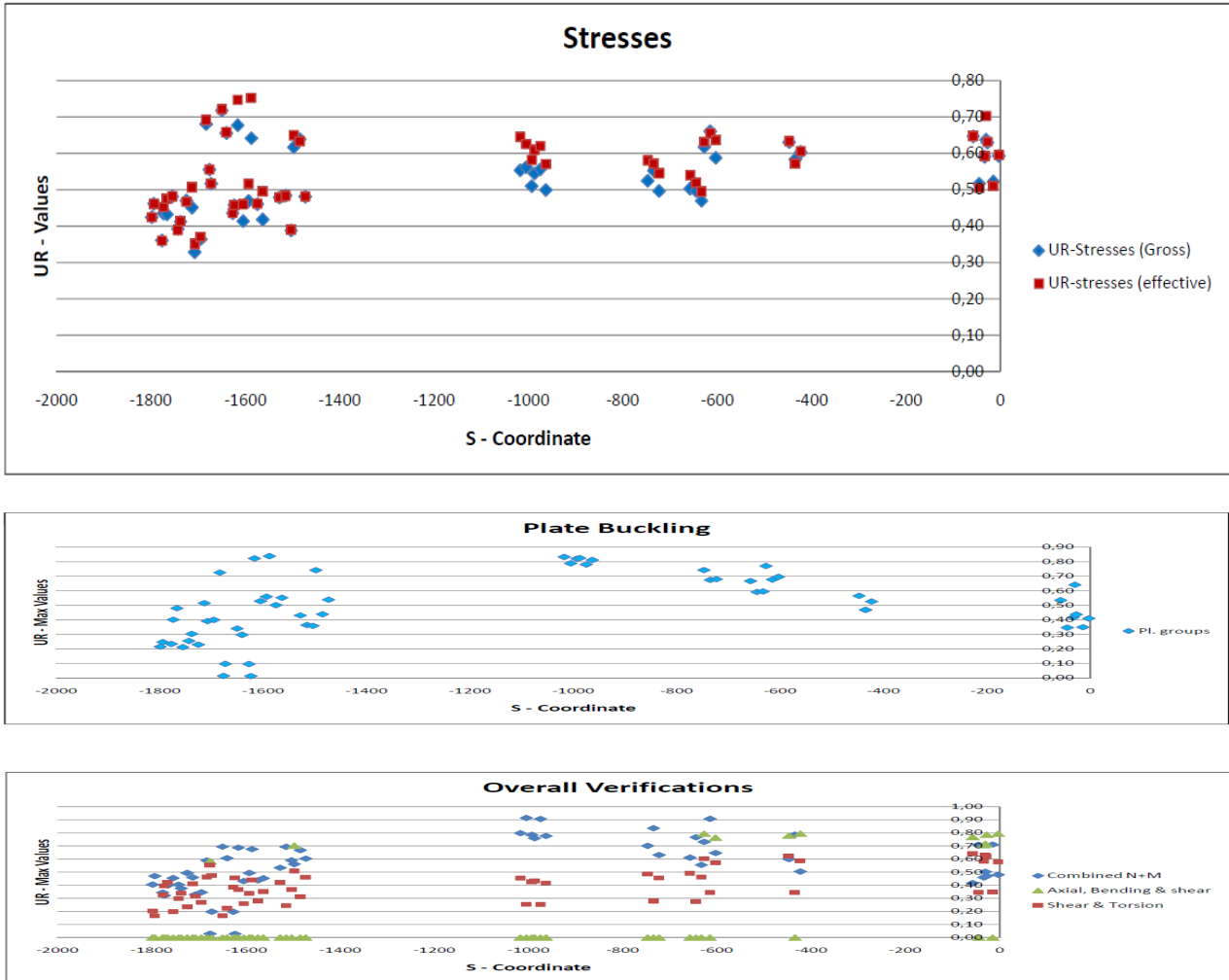


Figure 8-5 Roadway girder - utilisation ratios for ULS load combination dynamic wind, stresses and plate buckling

The roadway girder has also been verified for seismic loading calculated using a time history analysis. The utilisation ratios for ULS load combination seismic time history are shown in Figure 8-6. The selected s-coordinates for the seismic verification have been determined based on a preliminary investigation using a response spectrum analysis.

		<b>Ponte sullo Stretto di Messina</b> <b>PROGETTO DEFINITIVO</b>		
Specialist Technical Design Report, Annex		<i>Codice documento</i> PS0075_F0-ok.doc	<i>Rev</i> F0	<i>Data</i> 20/06/2011

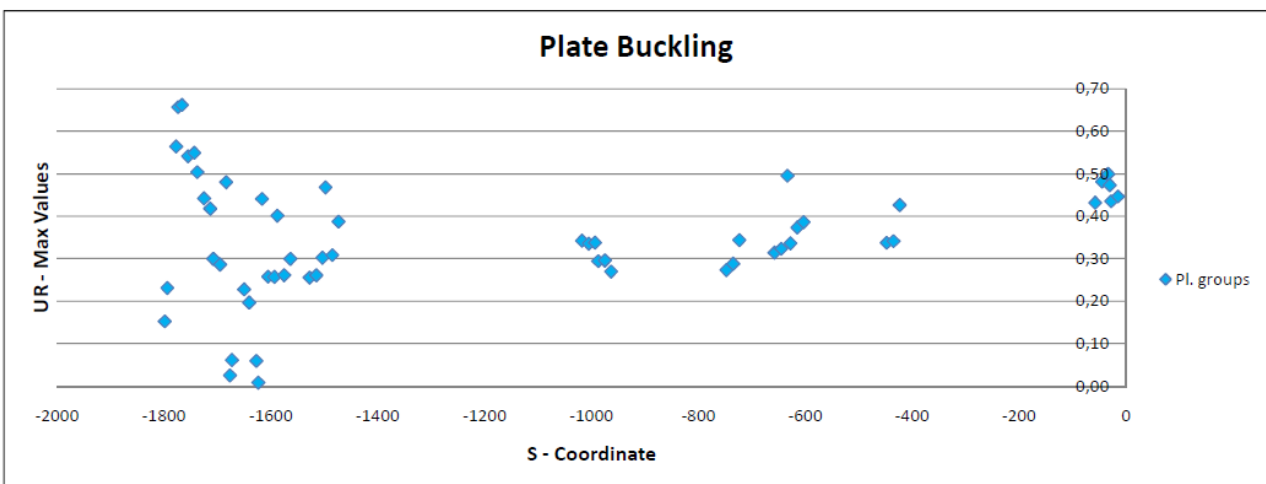
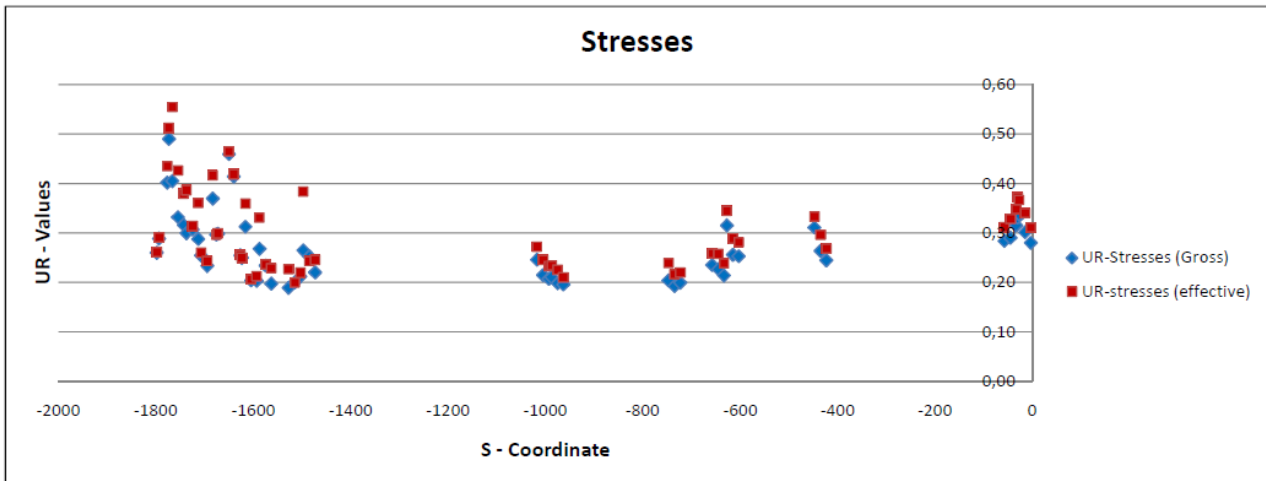


Figure 8-6 Roadway girder - utilisation ratios for ULS load combination seismic (time history), stresses and plate buckling

## 8.2 Verification - Railway Girder

The capacity of the longitudinal steel has been verified using ADVERS. The distribution of sectional forces,  $N_s$ ,  $M_y$  and  $V_z$ , imported from IBDAS are presented in Figure 8-7 to Figure 8-9. The forces are presented for the ULS load combination dynamic wind. The railway girder is continuous from one terminal structure to the other and is therefore subjected to constraining forces in tower span; the tower is located at -1650 m and centreline of main span at 0 m.

### Railway: Main span, Ns

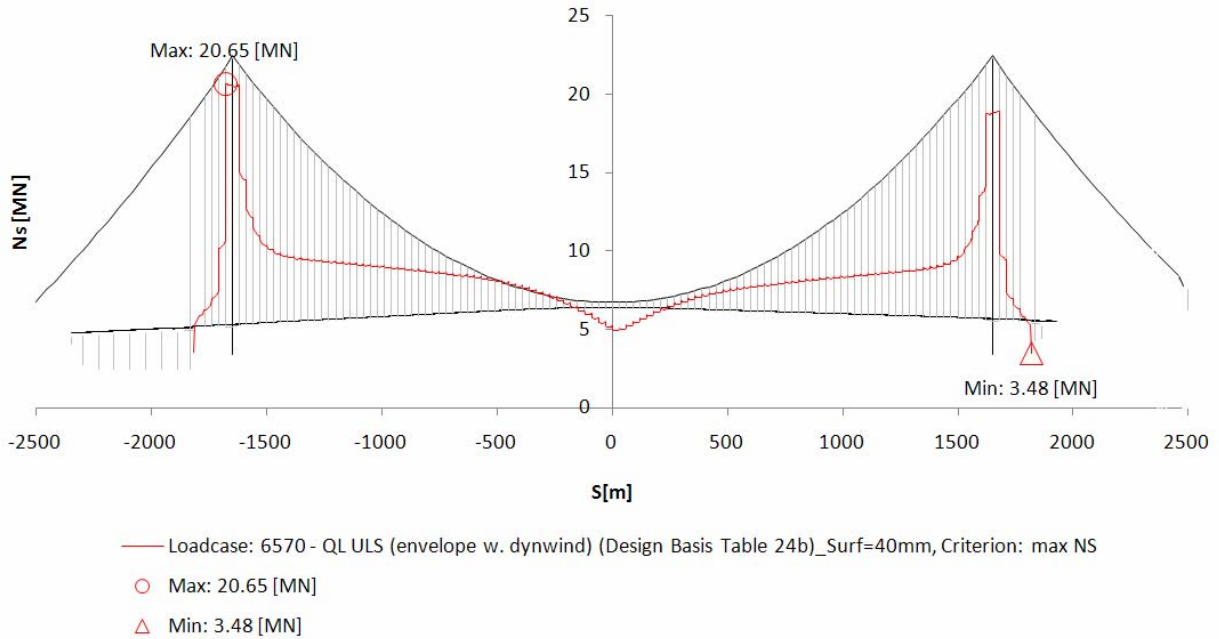


Figure 8-7 Maximal normal force ( $N_s$ ) in railway girder, ULS dynamic wind load combination

### Railway: Main span, My

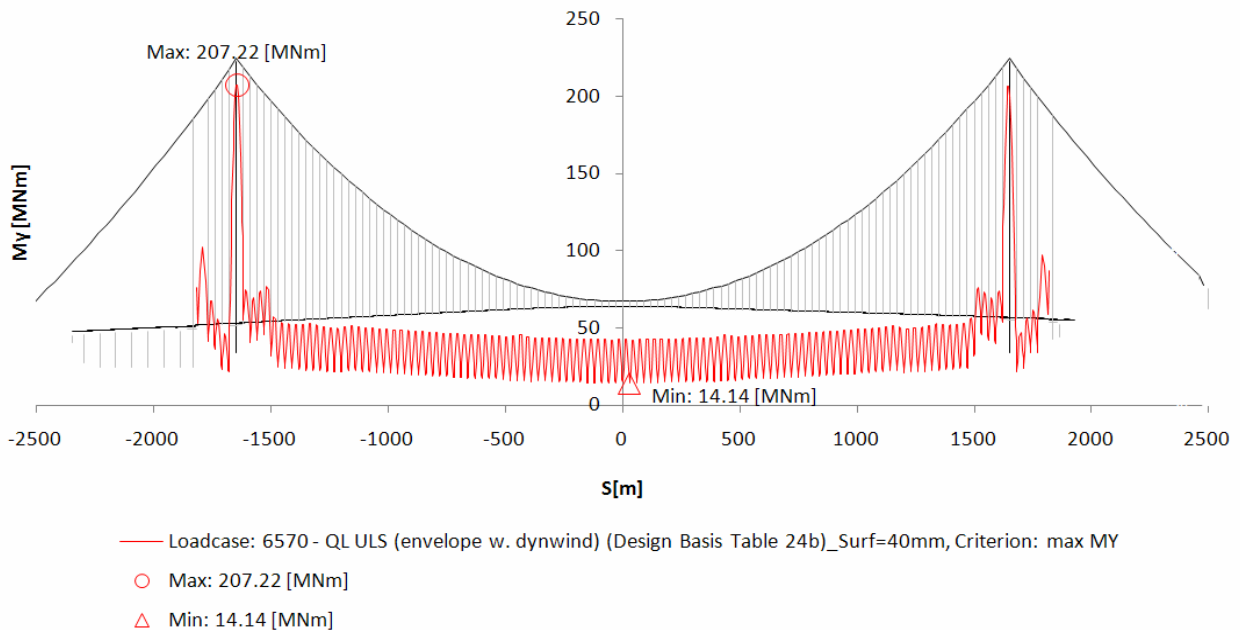
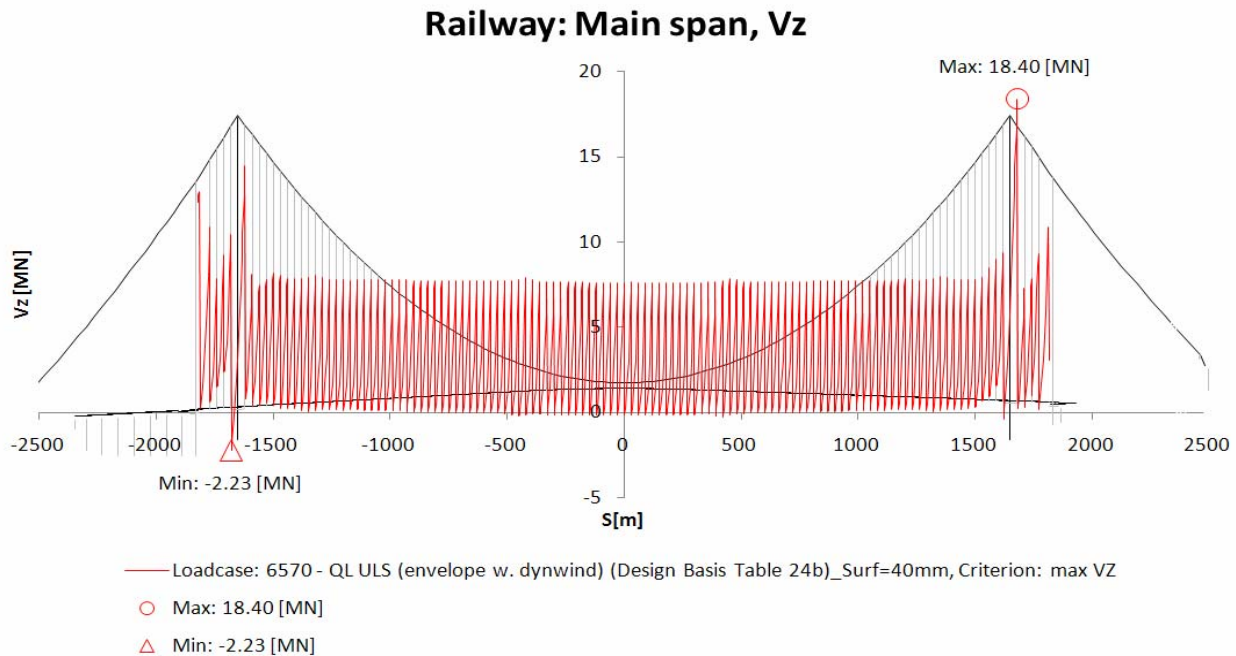


Figure 8-8 Maximal bending moment ( $M_y$ ) in railway girder, ULS dynamic wind load combination

		<b>Ponte sullo Stretto di Messina</b> <b>PROGETTO DEFINITIVO</b>					
Specialist Technical Design Report, Annex		<i>Codice documento</i> PS0075_F0-ok.doc	<table border="1" style="width: 100%; border-collapse: collapse;"> <thead> <tr> <th style="text-align: left;"><i>Rev</i></th> <th style="text-align: left;"><i>Data</i></th> </tr> </thead> <tbody> <tr> <td>F0</td> <td>20/06/2011</td> </tr> </tbody> </table>	<i>Rev</i>	<i>Data</i>	F0	20/06/2011
<i>Rev</i>	<i>Data</i>						
F0	20/06/2011						



**Figure 8-9** Maximal shear force ( $V_{z+}$ ) in railway girder, ULS dynamic wind load combination

The utilisation ratios are presented at selected s-coordinates located in the position of governing loads, changes in geometry, plate thicknesses and in structural key points.

The stiffeners have been checked for both individual and global stability in the general stress condition. Furthermore the stability of interaction between plate and stiffeners has been verified. Finally it has been checked that elastic buckling will not occur in the serviceability limit state, known as plate breathing. All mentioned stress verifications have been carried out with consideration of the global and local section properties for the effective cross section properties in section class 4.

The verification of stresses and global plate buckling are shown in Figure 8-10 to Figure 8-21 for all cross sections based on sectional forces from the governing ULS dynamic wind load case and a seismic load case using time history analysis. The load cases have been verified for selected points. For description of load cases, reference is made to Table 8-1. The utilisation ratios have been taken directly from ADVERS and are all below 1.0.

		<b>Ponte sullo Stretto di Messina</b> <b>PROGETTO DEFINITIVO</b>		
Specialist Technical Design Report, Annex		<i>Codice documento</i> PS0075_F0-ok.doc	<i>Rev</i> F0	<i>Data</i> 20/06/2011

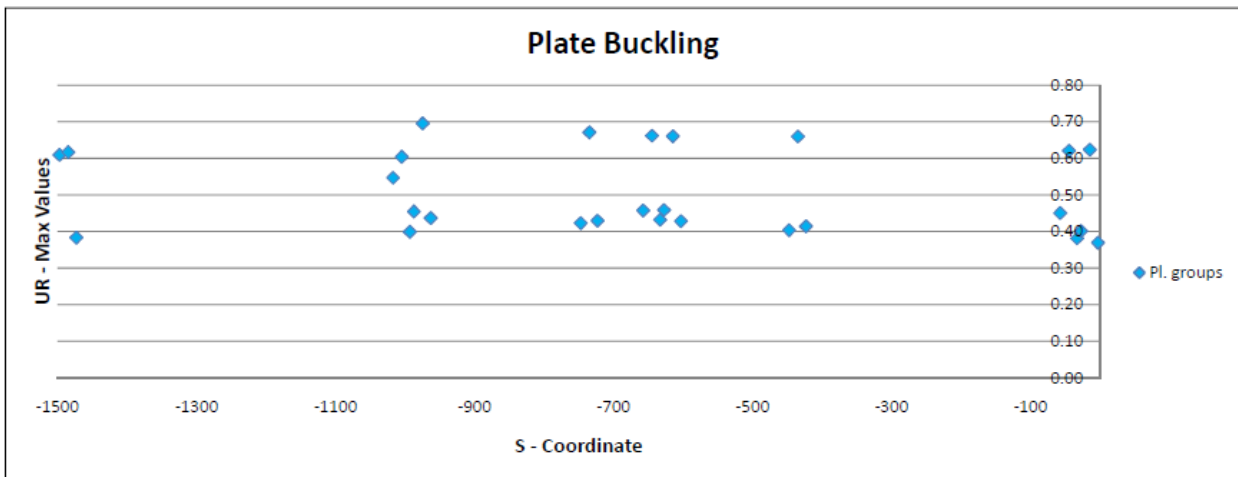
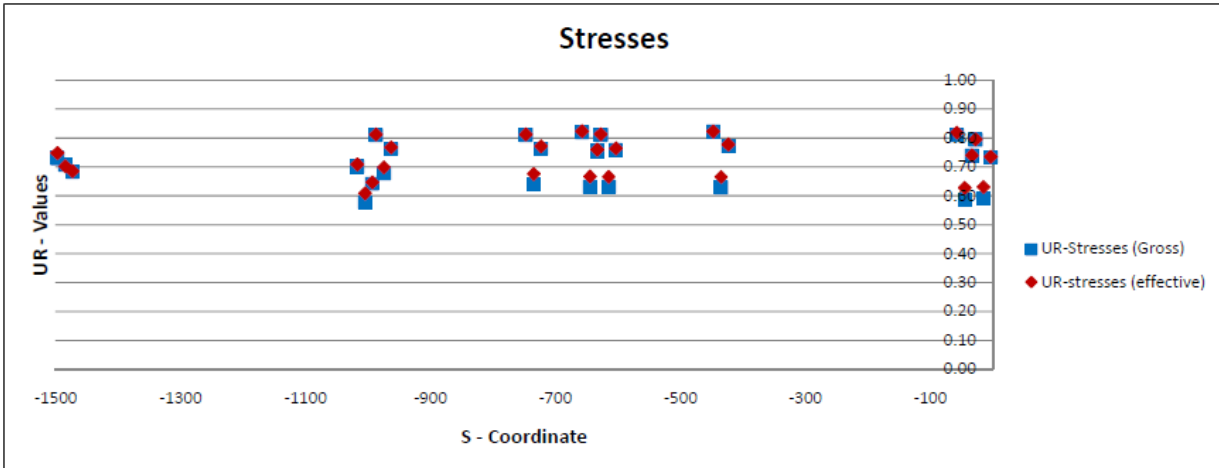


Figure 8-10 Railway Girder - utilisation ratios for stresses and plate buckling in type CF1 & CF2 for ULS load combination dynamic wind

		<b>Ponte sullo Stretto di Messina</b> <b>PROGETTO DEFINITIVO</b>	
Specialist Technical Design Report, Annex	<i>Codice documento</i> PS0075_F0-ok.doc	<i>Rev</i> F0	<i>Data</i> 20/06/2011

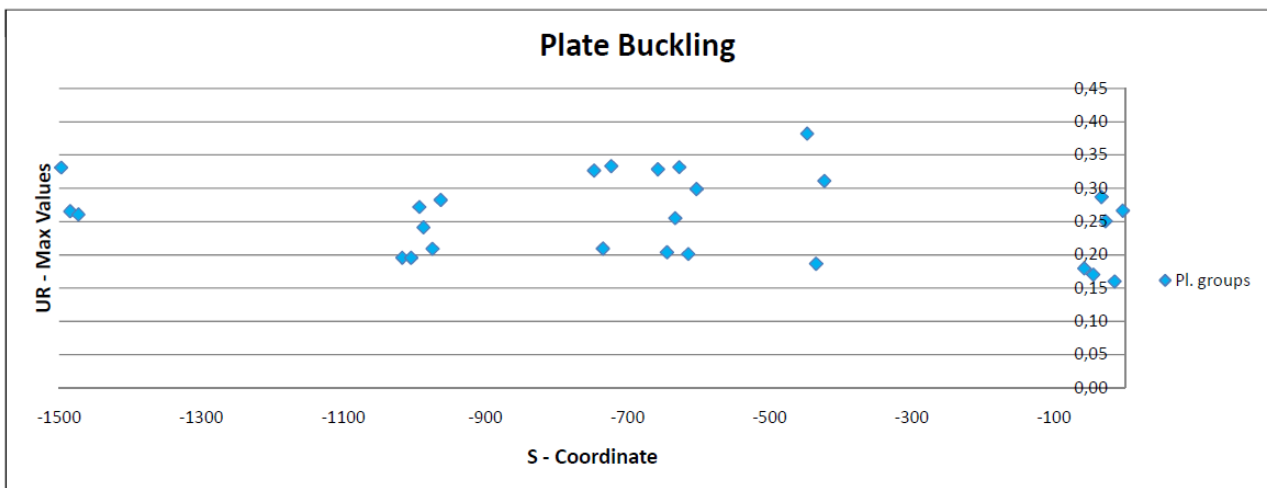
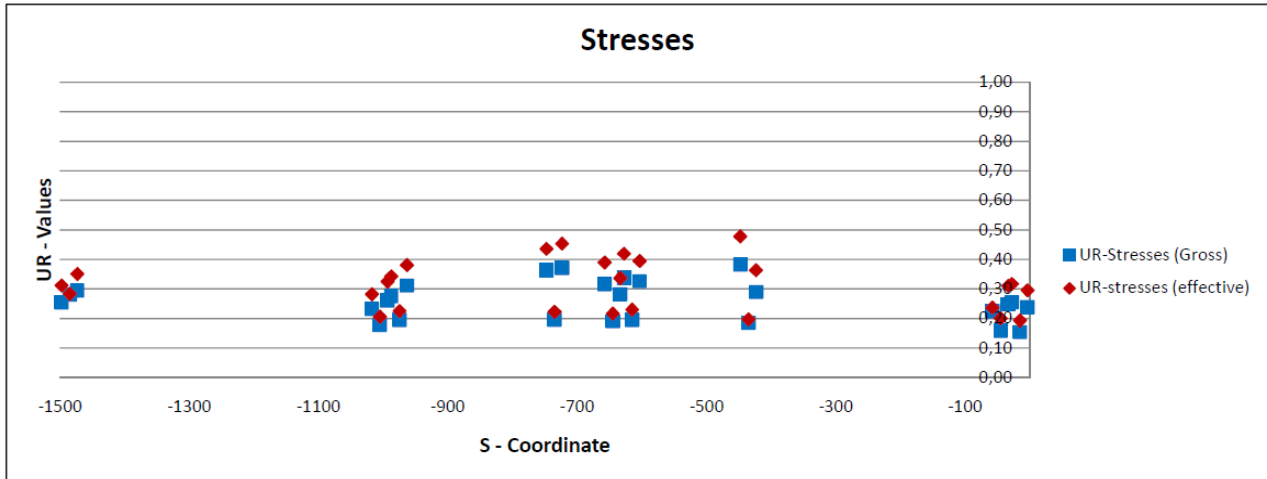


Figure 8-11 Railway girder - utilisation ratios for stresses and plate buckling in type CF1 & CF2 for ULS load combination seismic (time history)

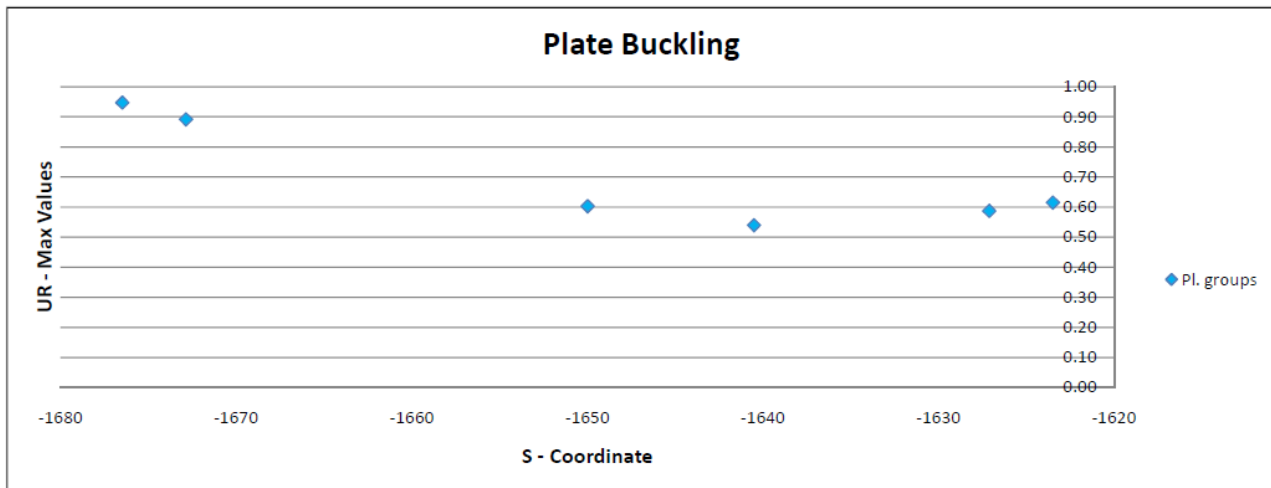
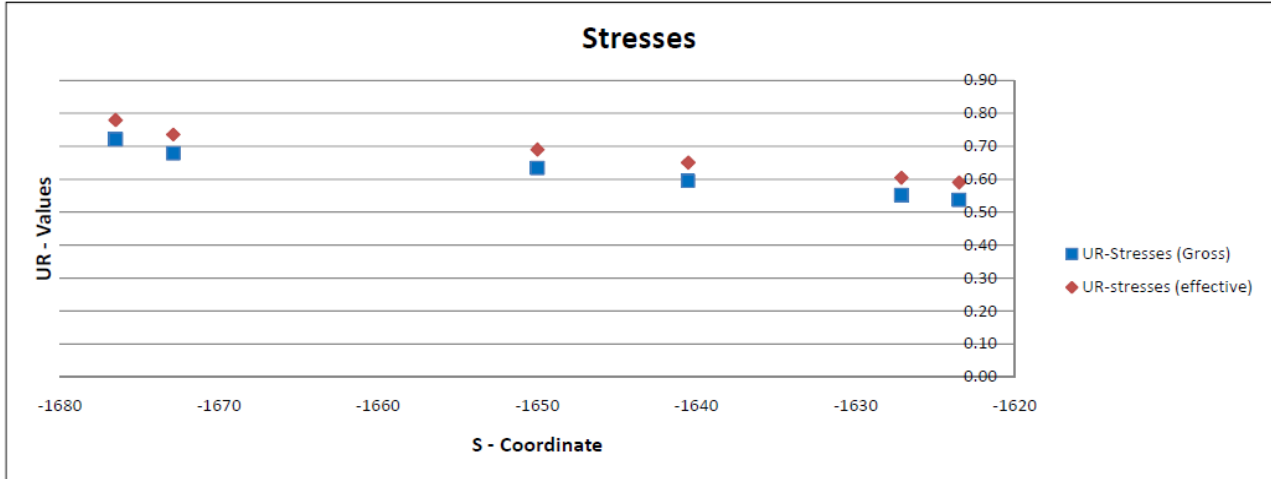


Figure 8-12 Railway girder - utilisation ratios for stresses and plate buckling in type CF4 for ULS load combination dynamic wind

		<b>Ponte sullo Stretto di Messina</b> <b>PROGETTO DEFINITIVO</b>	
Specialist Technical Design Report, Annex	<i>Codice documento</i> PS0075_F0-ok.doc	<i>Rev</i> F0	<i>Data</i> 20/06/2011

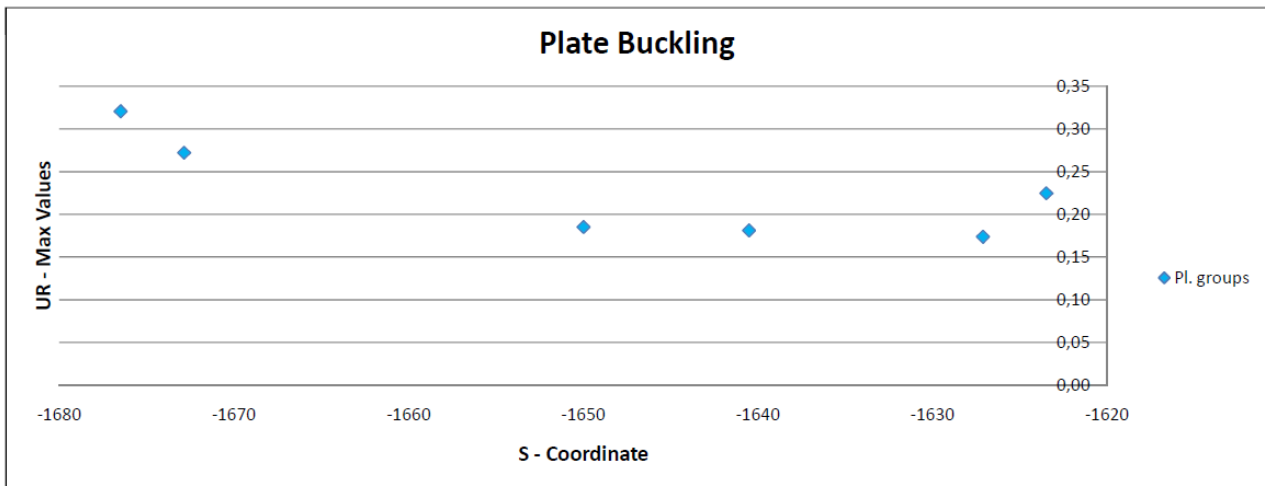
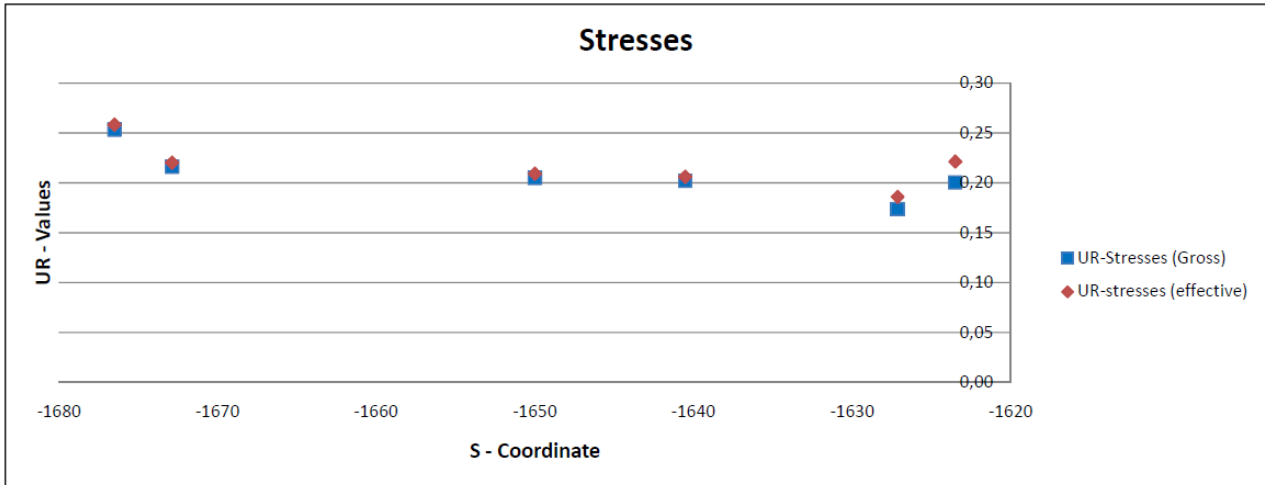
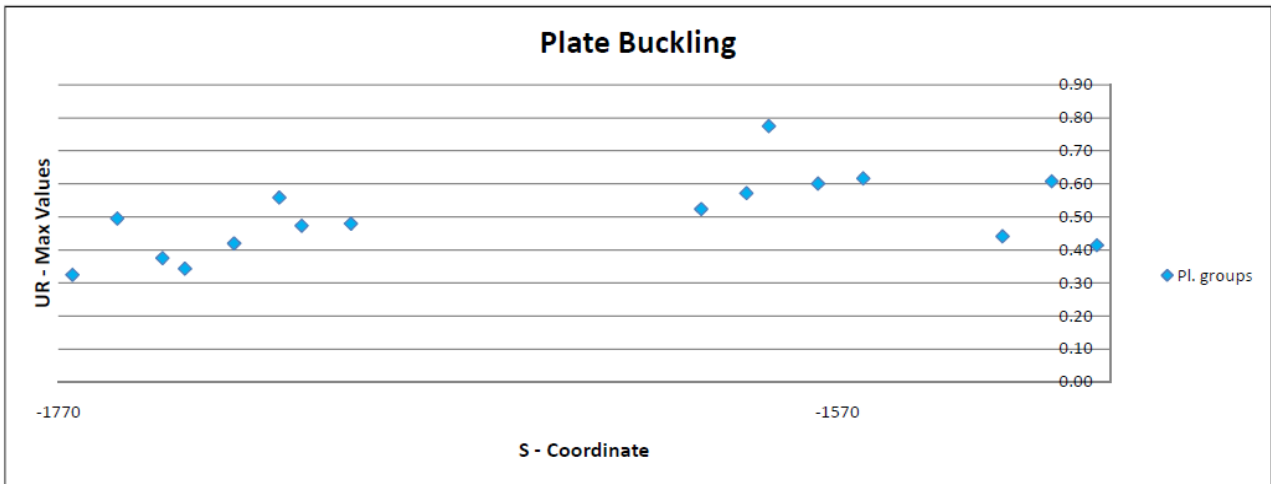
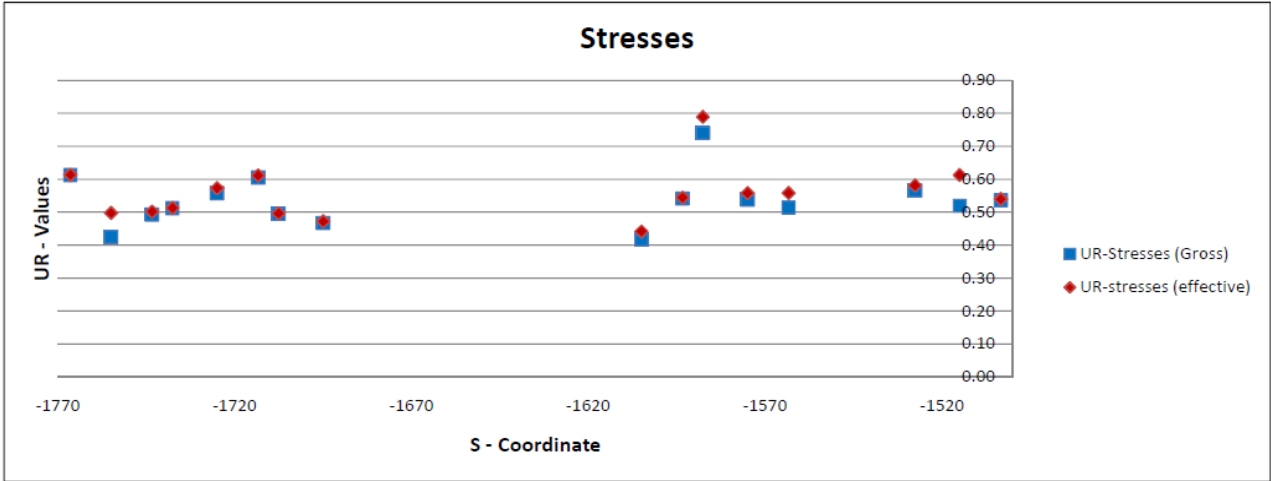


Figure 8-13 Railway girder - utilisation ratios for stresses and plate buckling in type CF4 for ULS load combination seismic (time history)



		<b>Ponte sullo Stretto di Messina</b> <b>PROGETTO DEFINITIVO</b>	
Specialist Technical Design Report, Annex	<i>Codice documento</i> PS0075_F0-ok.doc	<i>Rev</i> F0	<i>Data</i> 20/06/2011

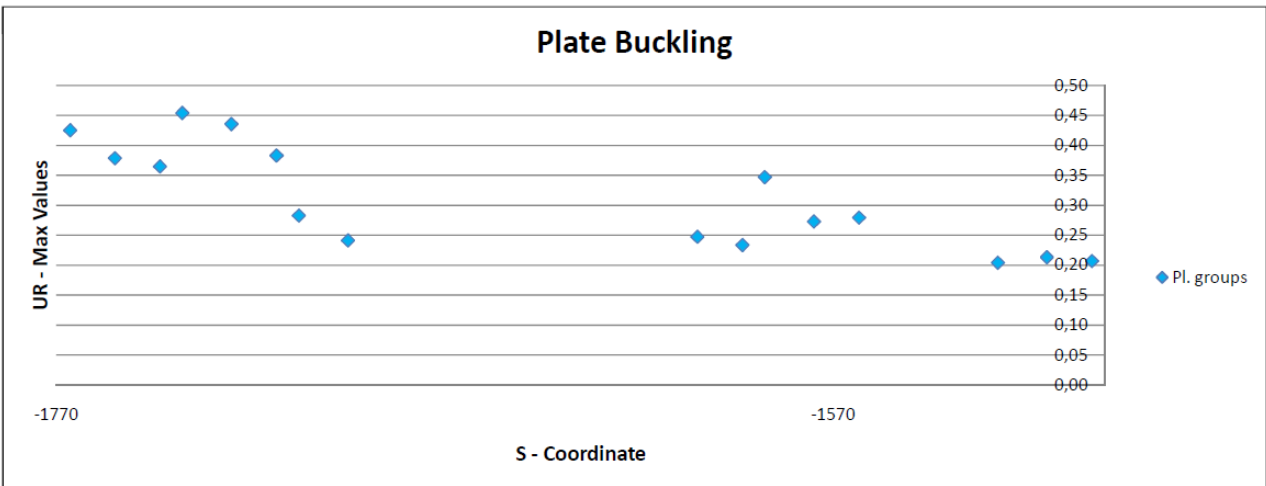
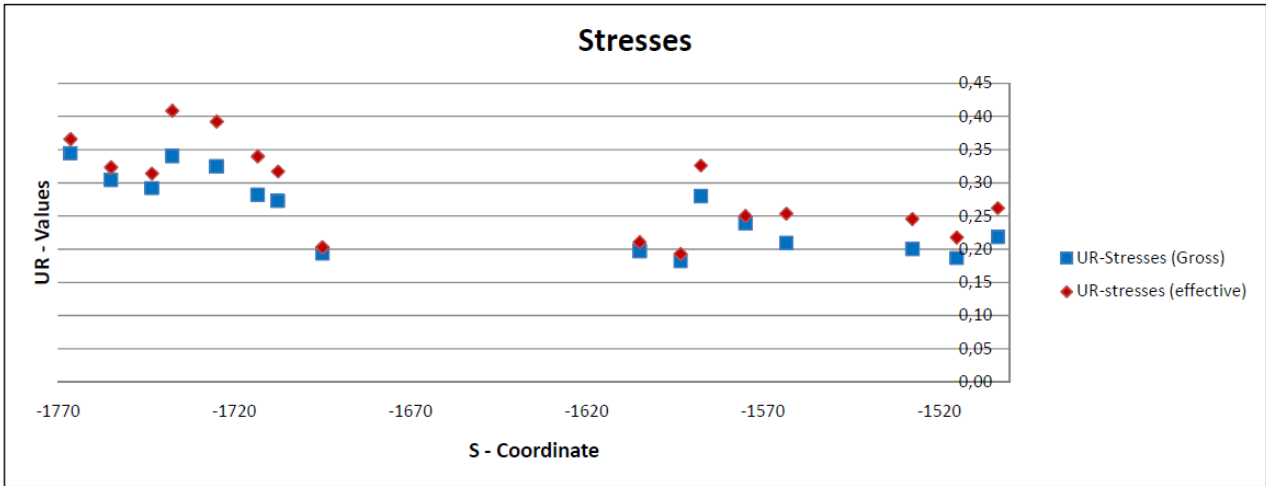


Figure 8-15 Railway girder - utilisation ratios for stresses and plate buckling in type CF3, CF5 & CF6 for ULS load combination seismic (time history)

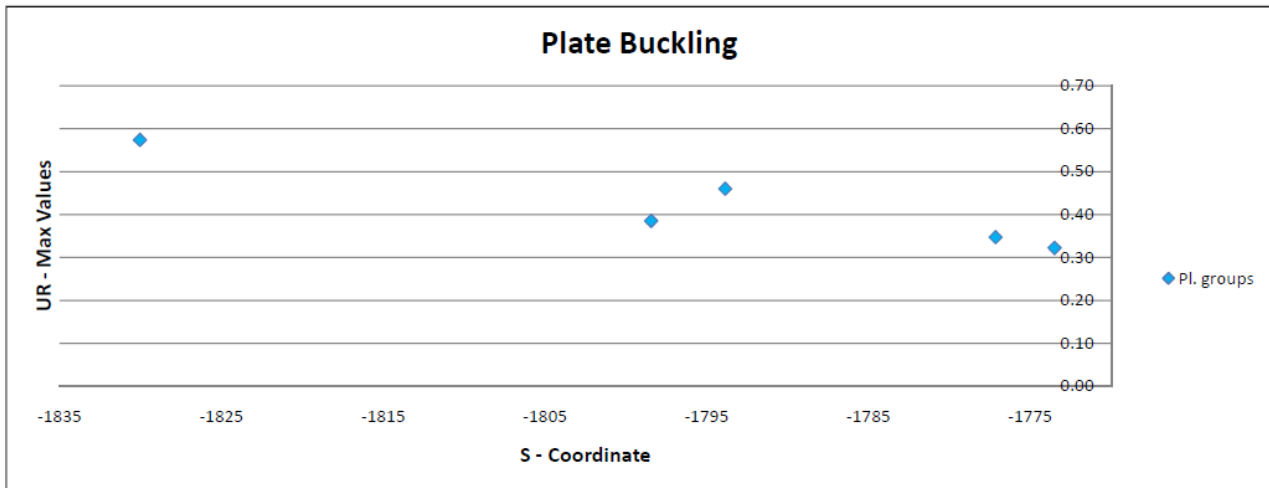
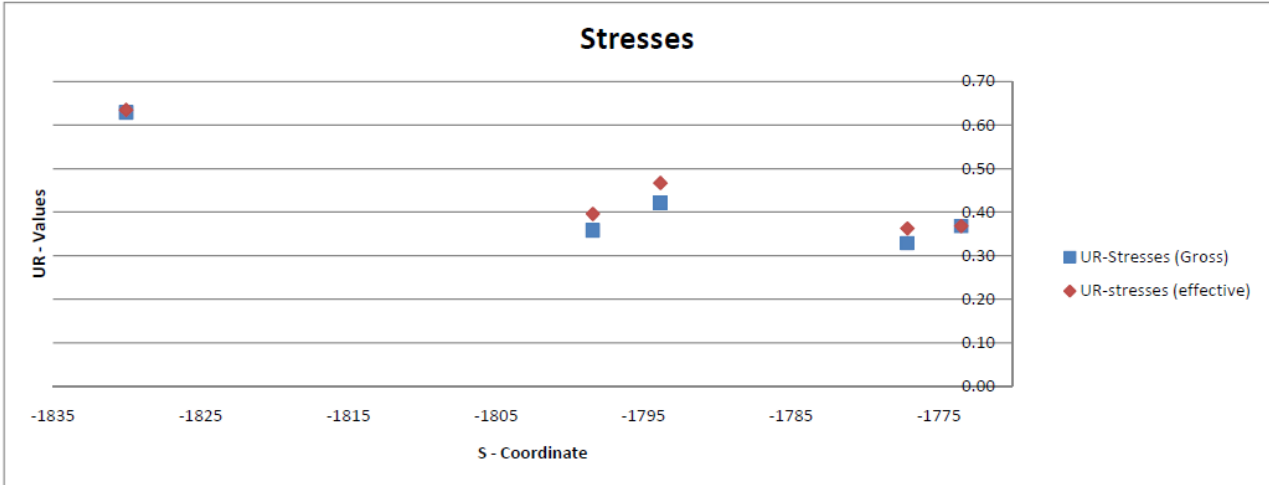


Figure 8-16 Railway girder - utilisation ratios for stresses and plate buckling in type CF7 & CF8 for ULS load combination dynamic wind

		<b>Ponte sullo Stretto di Messina</b> PROGETTO DEFINITIVO		
Specialist Technical Design Report, Annex		Codice documento PS0075_F0-ok.doc	Rev F0	Data 20/06/2011

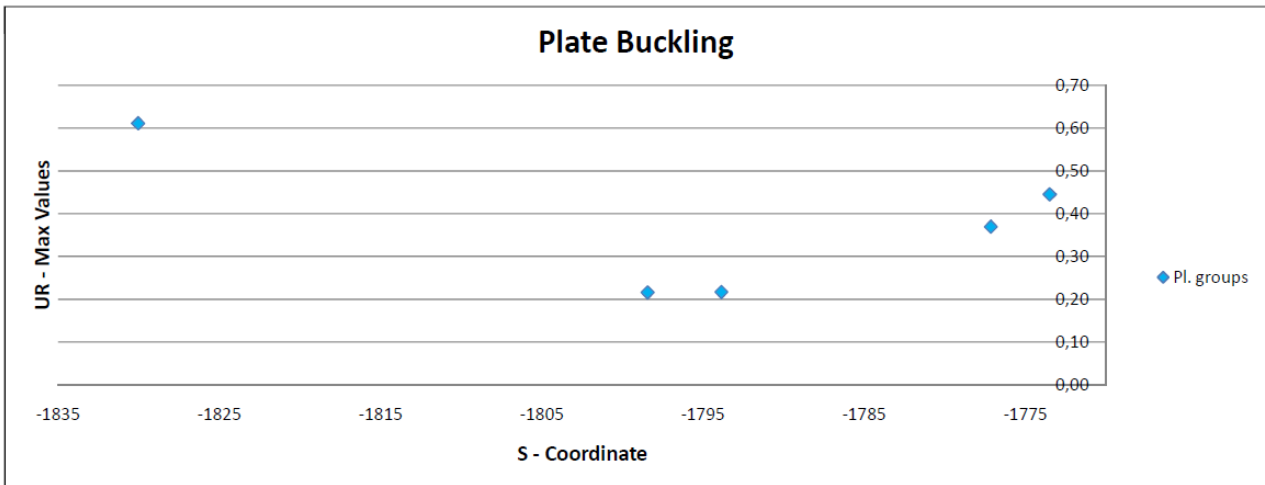
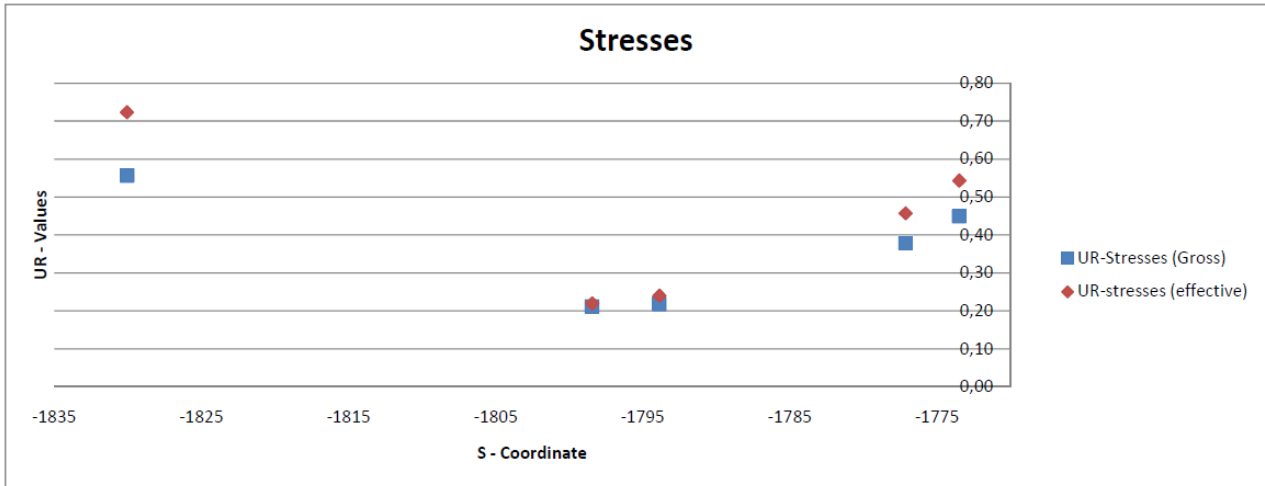


Figure 8-17 Railway girder - utilisation ratios for stresses and plate buckling in type CF7 & CF8 for ULS load combination seismic (time history)

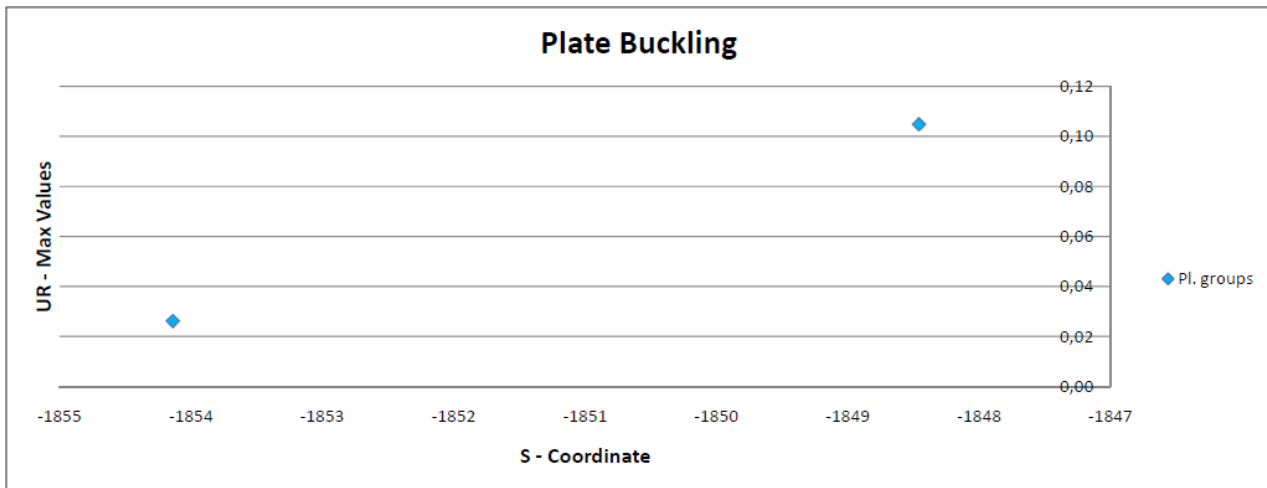
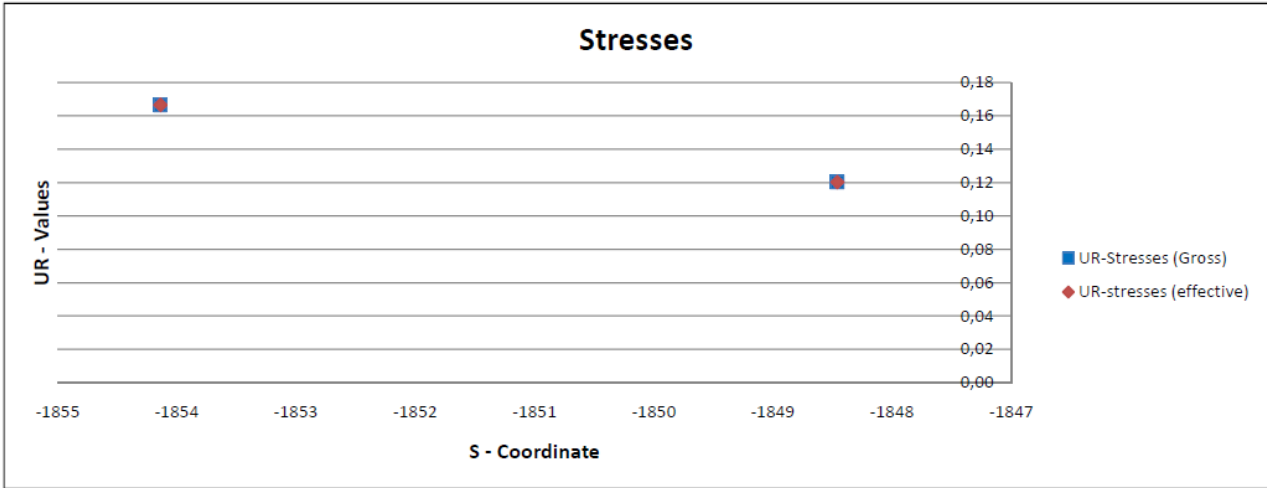


Figure 8-18 Railway girder - utilisation ratios for stresses and plate buckling in type CF9a for ULS load combination dynamic wind

		<b>Ponte sullo Stretto di Messina</b> <b>PROGETTO DEFINITIVO</b>					
Specialist Technical Design Report, Annex		<i>Codice documento</i> PS0075_F0-ok.doc	<table border="1" style="width: 100%; border-collapse: collapse;"> <tr> <td style="width: 50%;"><i>Rev</i></td> <td style="width: 50%;"><i>Data</i></td> </tr> <tr> <td>F0</td> <td>20/06/2011</td> </tr> </table>	<i>Rev</i>	<i>Data</i>	F0	20/06/2011
<i>Rev</i>	<i>Data</i>						
F0	20/06/2011						

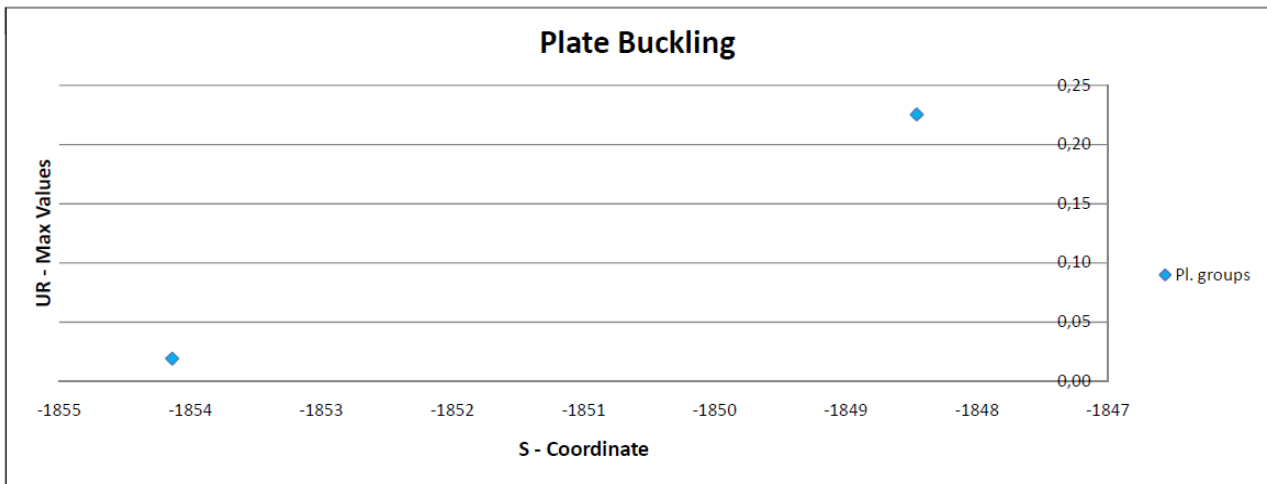
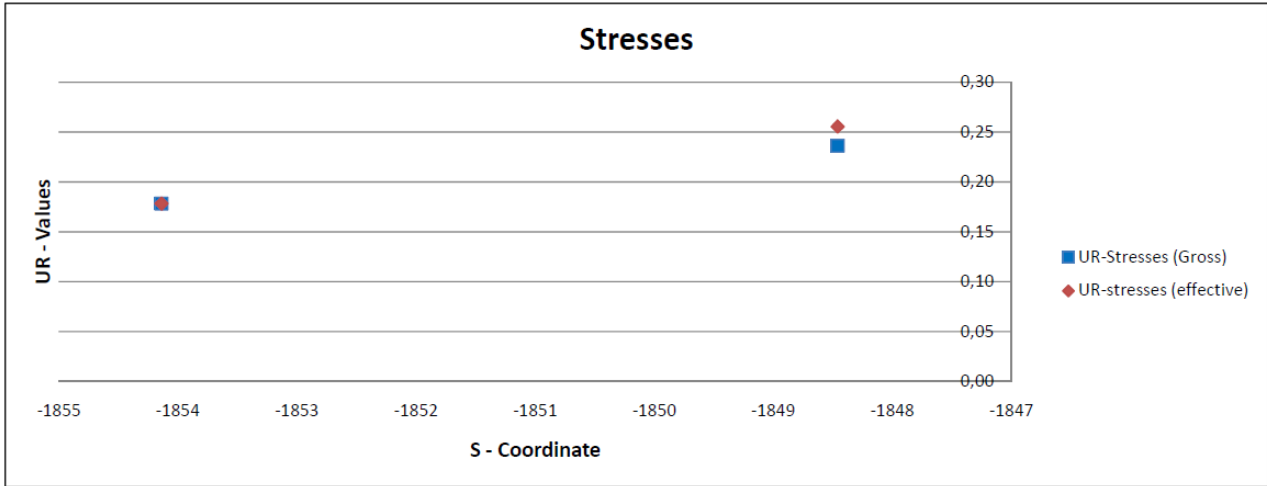


Figure 8-19 Railway girder - utilisation ratios for stresses and plate buckling in type CF9a for ULS load combination seismic (time history)

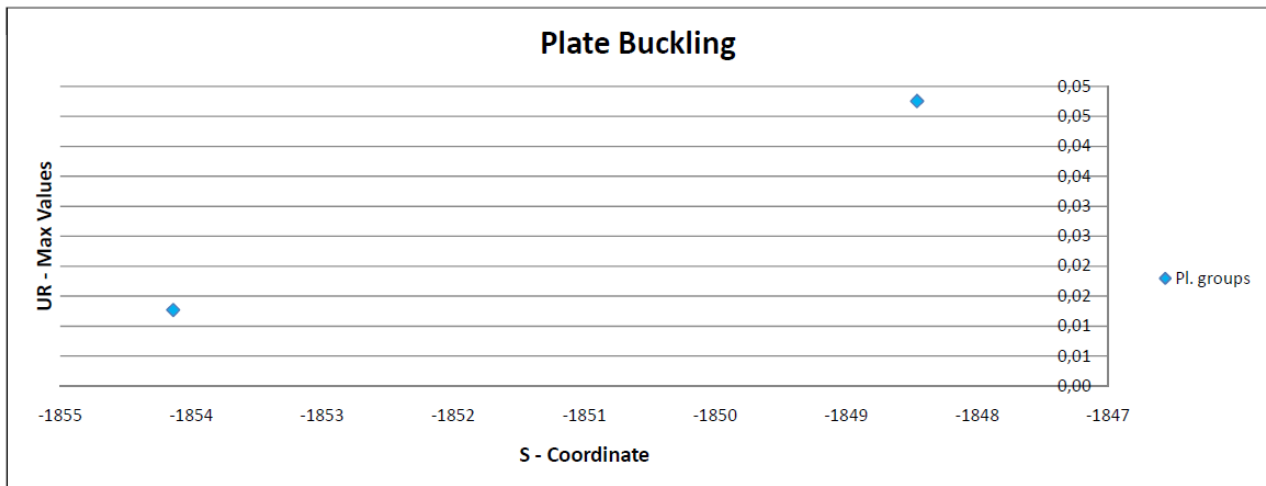
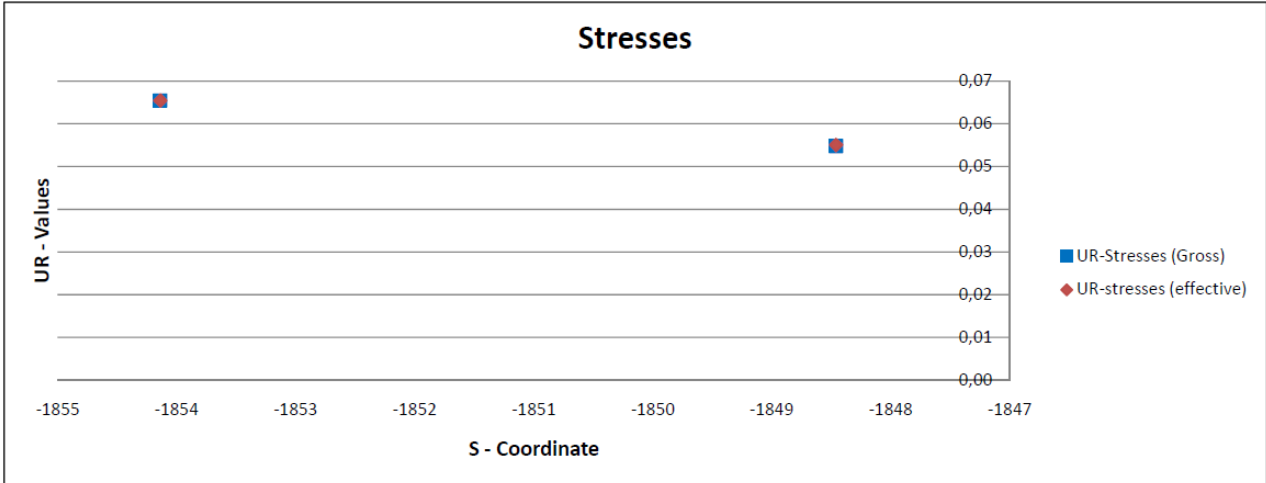


Figure 8-20 Railway girder - utilisation ratios for stresses and plate buckling in type CF9b for ULS load combination dynamic wind

		<b>Ponte sullo Stretto di Messina</b> <b>PROGETTO DEFINITIVO</b>		
Specialist Technical Design Report, Annex		<i>Codice documento</i> PS0075_F0-ok.doc	<i>Rev</i> F0	<i>Data</i> 20/06/2011

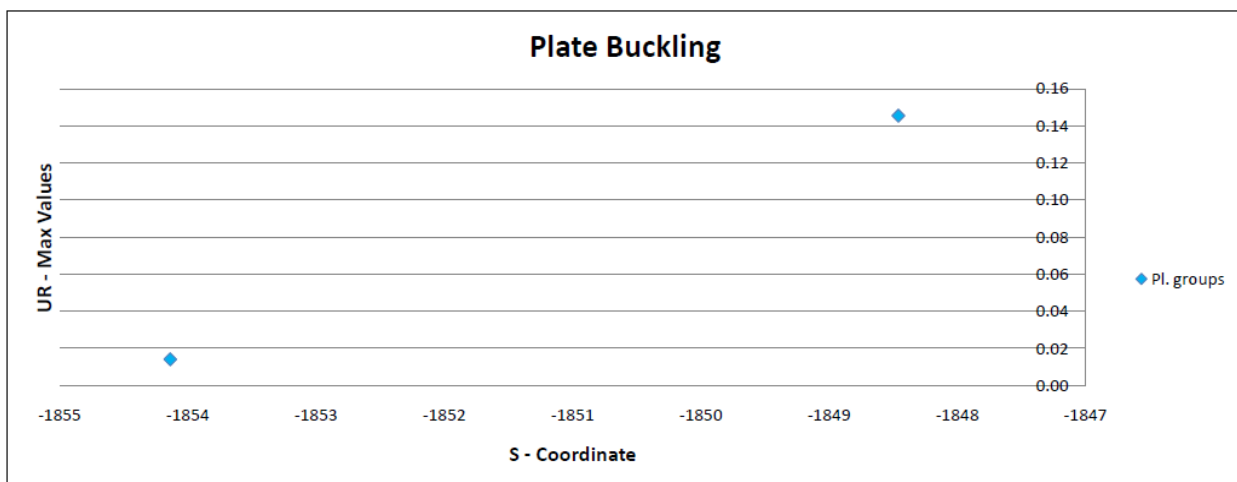
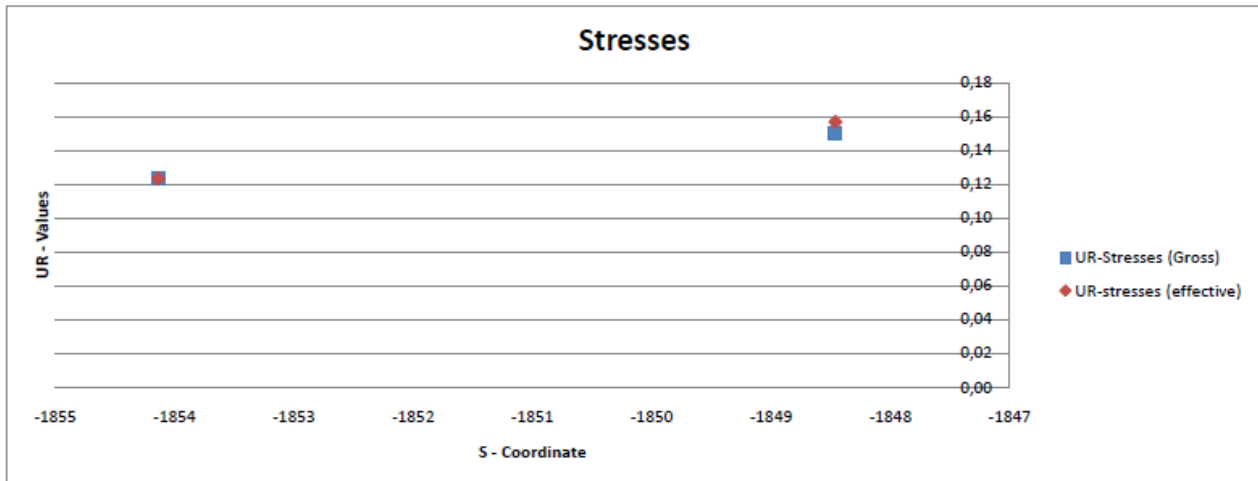


Figure 8-21 Railway girder - utilisation ratios for stresses and plate buckling in type CF9b for ULS load combination seismic (time history)

### 8.3 Verification - Cross Girder

The longitudinal steel of the cross girders spanning between hangers have been verified using ADVERS, determining utilisation ratios for relevant code checks. The utilisation ratios are presented for the relevant cross girders with a more dense distribution around the tower locations where the highest utilisation ratios were expected. All cross girder types have been included and in total 31 cross girders have been verified along the whole bridge length including both ends in order to consider possible variation of the most critical stresses.

		<b>Ponte sullo Stretto di Messina</b> <b>PROGETTO DEFINITIVO</b>		
Specialist Technical Design Report, Annex		<i>Codice documento</i> PS0075_F0-ok.doc	<i>Rev</i> F0	<i>Data</i> 20/06/2011

Each cross girder has been verified in three characteristic sections between the longitudinal girders which can be seen in Figure 8-22.

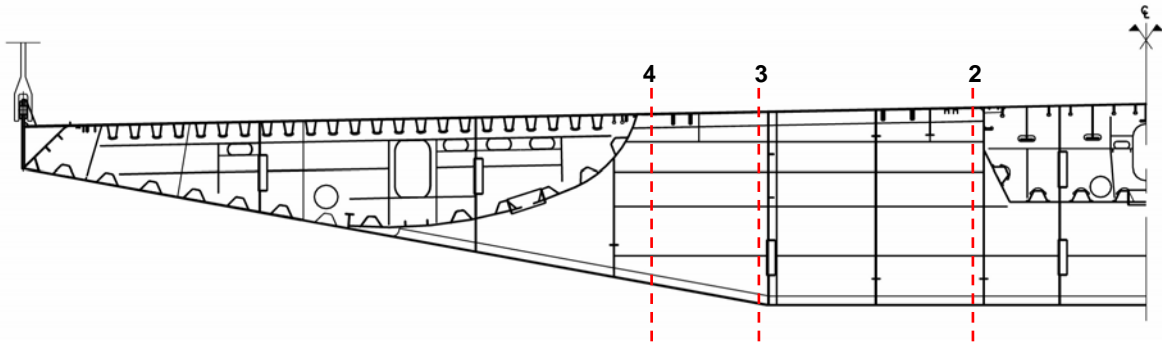


Figure 8-22 Cross girder - sections of verification

ULS Combination with dynamic wind is governing for the ULS design. The load cases are defined in the IBDAS report "Global IBDAS Model Description". Sectional forces for load combination LC6570 used in the verification of the cross girders are shown in Figure 8-23 to Figure 8-25 for section at  $y=4.15\text{m}$ .

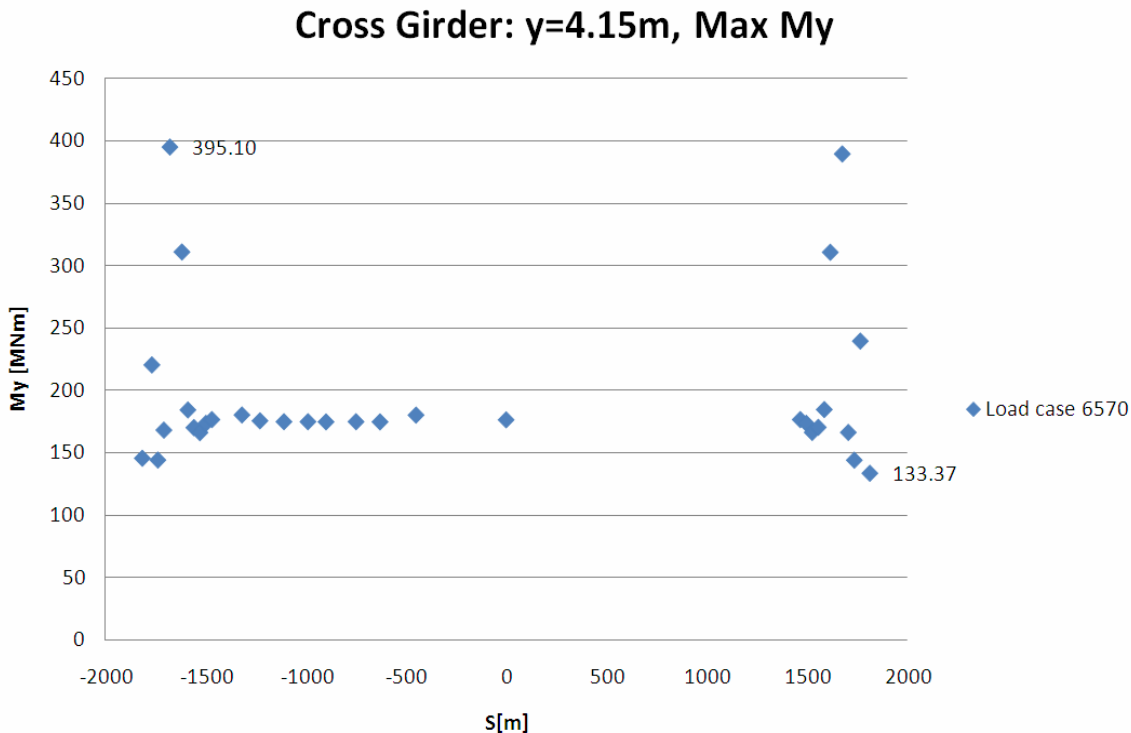


Figure 8-23 Bending moment  $M_y$  in cross girders for ULS dynamic wind

		<b>Ponte sullo Stretto di Messina</b> <b>PROGETTO DEFINITIVO</b>	
Specialist Technical Design Report, Annex		Codice documento PS0075_F0-ok.doc	Rev F0 Data 20/06/2011

**Cross Girder: y=4.15m, Max Vz**

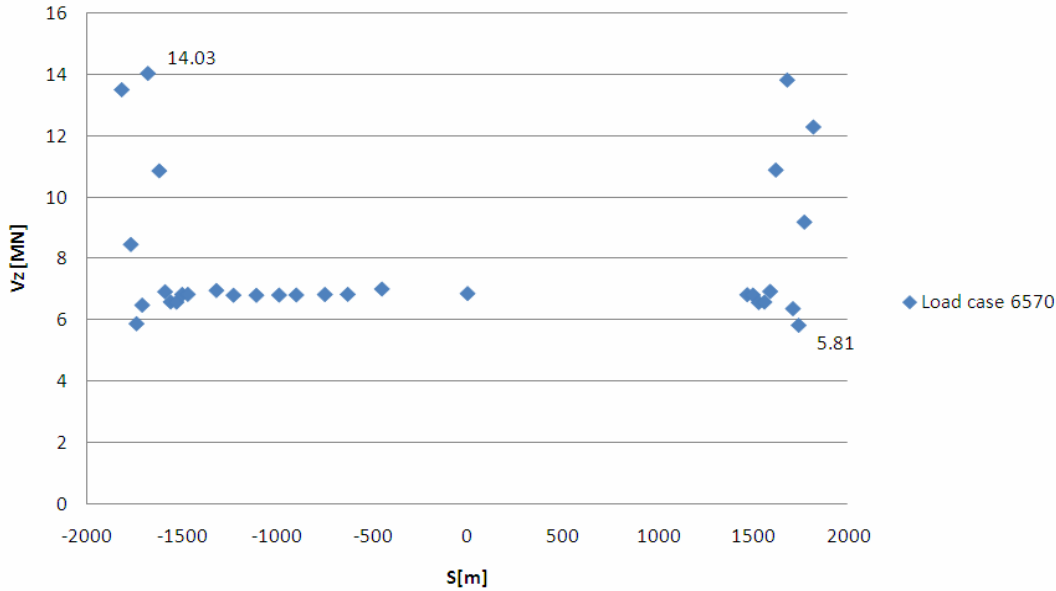


Figure 8-24 Shear force Vz in cross girders for ULS dynamic wind

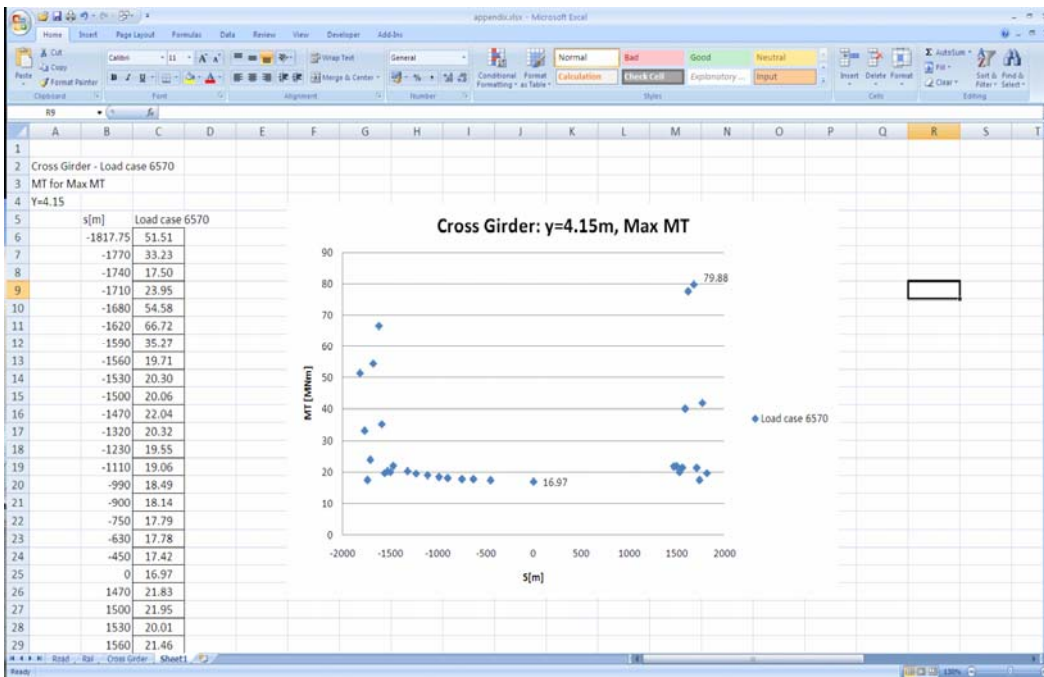


Figure 8-25 Torsional moment Mt in cross girders for ULS dynamic wind

		<b>Ponte sullo Stretto di Messina</b> PROGETTO DEFINITIVO		
Specialist Technical Design Report, Annex		<i>Codice documento</i> PS0075_F0-ok.doc	<i>Rev</i> F0	<i>Data</i> 20/06/2011

The governing ULS load combination has been found to be the dynamic wind and section number 2 of the cross girder T1 turned out to be the most critical one. Results of this section can be found in Figure 8-26 and Figure 8-27, respectively, concerning the dynamic wind load case and the seismic time history analysis, respectively. For the full set of results of all section in all cross girders reference is made to the document "Design Report - Roadway, Railway and Cross Girders".

		<b>Ponte sullo Stretto di Messina</b> <b>PROGETTO DEFINITIVO</b>		
Specialist Technical Design Report, Annex		Codice documento PS0075_F0-ok.doc	Rev F0	Data 20/06/2011

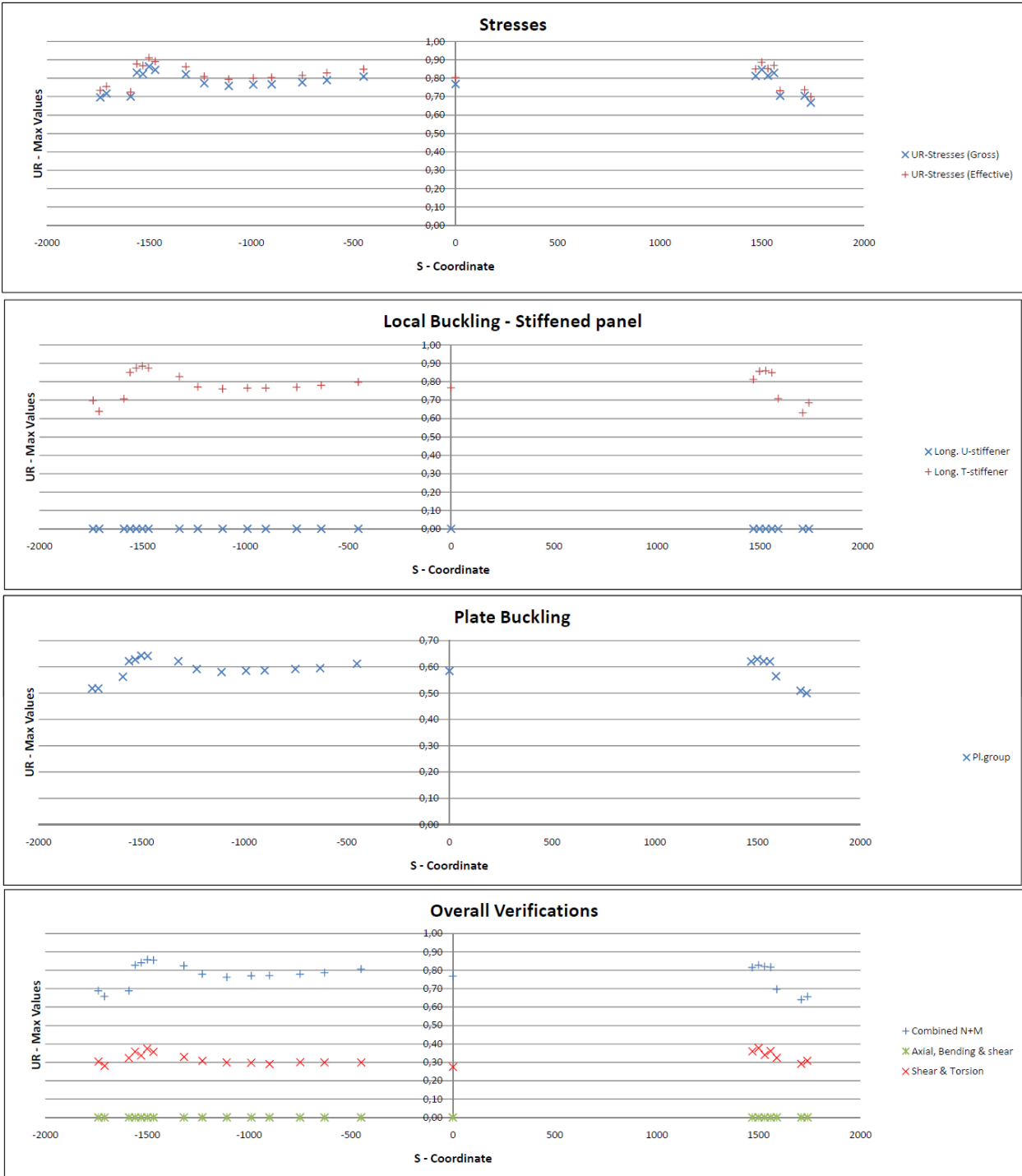


Figure 8-26 Cross girders - utilisation ratios T1 and T3 - section 2 – ULS dynamic wind load combination

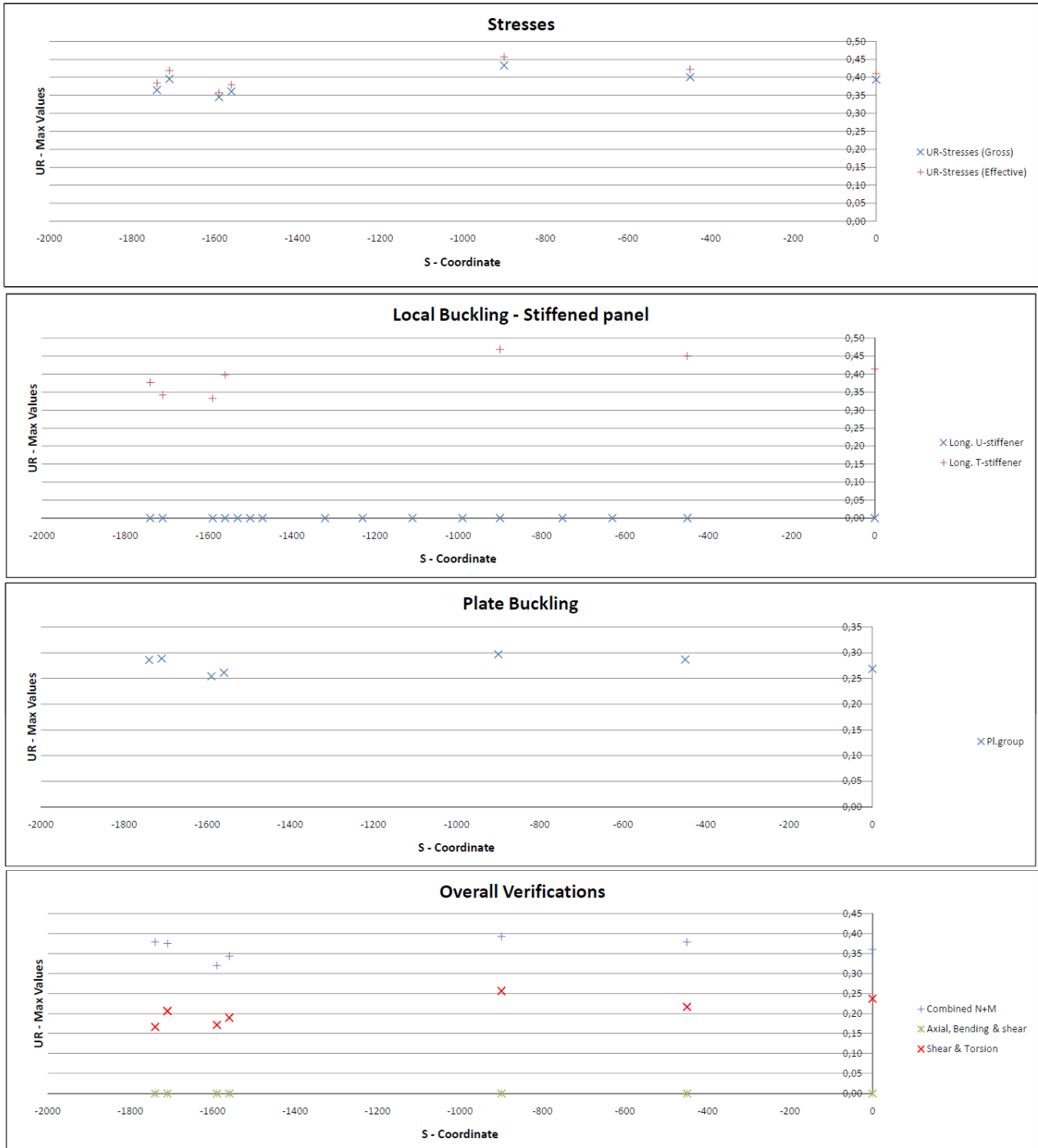


Figure 8-27 Cross girders - utilisation ratios for T1 and T3 - section 2 – ULS seismic (time history) load combination

		<b>Ponte sullo Stretto di Messina</b> <b>PROGETTO DEFINITIVO</b>		
Specialist Technical Design Report, Annex		<i>Codice documento</i> PS0075_F0-ok.doc	<i>Rev</i> F0	<i>Data</i> 20/06/2011

## 8.4 Verification - Transverse Stresses

At the intersection between the cross girder and the roadway- and railway girders the top plate is subjected to compression stresses in two directions. At these intersections a spreadsheet and a calculation program for elastic buckling of plates have been used to investigate the stability of the different plate panels. Compressive stresses have been calculated in ADVERS and in a local bridge FE-model at the location outside the plates of consideration. These stresses have been compared, and the stresses from the local model has been used for the plate stability verification, see Table 8-2.

*Table 8-2 Governing compressive stresses at intersection plates - main span, plate 1*

Intersection	Roadway		Railway	
Stress location	Roadway	Cross Girder	Railway	Cross Girder
$\sigma_{1,comp.}$ [MPa]	190	276	200	298

The stresses calculated in ADVERS are compared to those of a local FE-model for the same loading as applied in IBDAS, and only a minor difference was found. The stresses used from ADVERS are on the conservative side.

The plate panels considered are modelled in an elastic buckling program, see Figure 8-29. For the roadway girder the top plate is divided into three plate panels separated by the cross girder diaphragms. The plate towards the railway girder is denoted "Plate 1", see Figure 8-28. For the railway girder only one plate is considered.

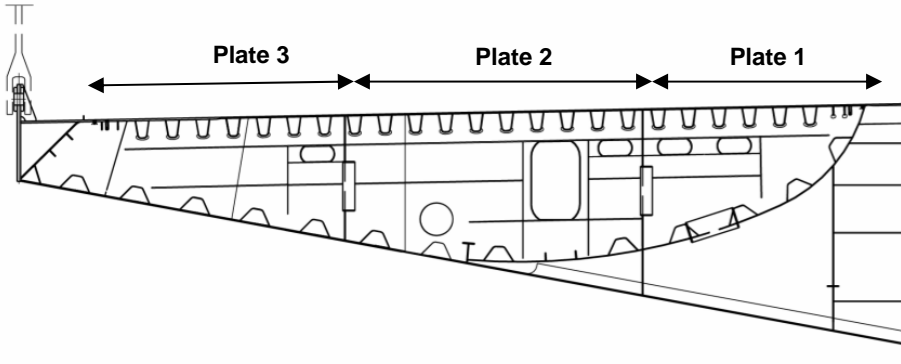


Figure 8-28 Plate fields in roadway girder

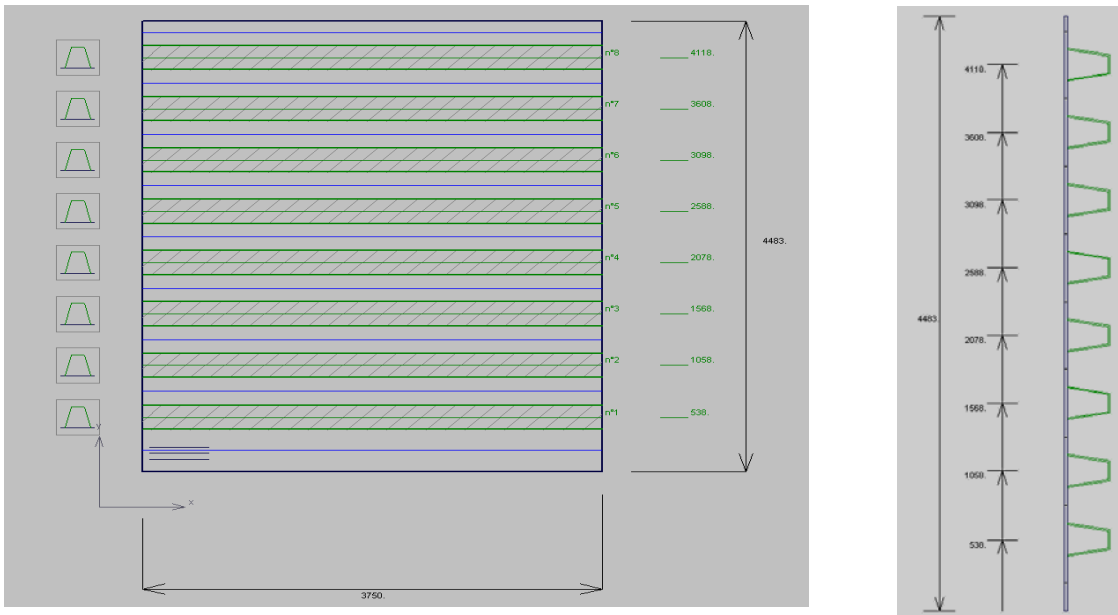


Figure 8-29 Illustration of a plate panel of the roadway girder including dimensions

The critical buckling modes have also been calculated, and the governing for the illustrated plate is given in Figure 8-30.

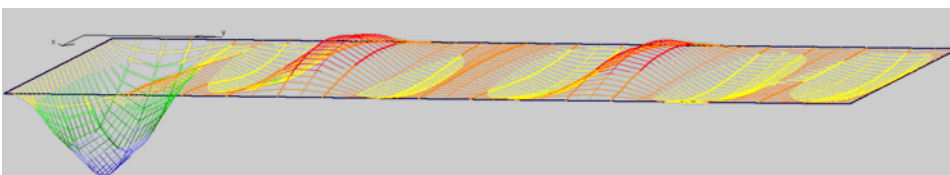


Figure 8-30 Illustration of critical buckling mode for determining critical stresses

		<b>Ponte sullo Stretto di Messina</b> <b>PROGETTO DEFINITIVO</b>	
Specialist Technical Design Report, Annex	<i>Codice documento</i> PS0075_F0-ok.doc	<i>Rev</i> F0	<i>Data</i> 20/06/2011

From the elastic buckling program critical stresses are calculated considering the plate as an orthotropic plate. The critical stresses that have been calculated are corresponding to the stress limits used in the "reduced stress method" of EN 1993-1-5:2005 section 10. This method has been used to determine the utilisation ratios of the considered plates, see Table 8-3.

*Table 8-3 Utilisation ratios for governing plates, main span of roadway deck plate*

UR	Roadway	Railway
Plate 1	1.89*	0.97
Plate 2	0.66	-
Plate 3	0.50	-

It shall be noted that Plate 1 has a  $UR > 1.0$  based on the calculations made as described above. This is due to the arrangement with two flat stiffeners at the edge of this plate panel, thus making it less rigid to transverse stresses when considering buckling. However these flat stiffeners are supported per 1250 mm by transverse plates used for support of the crash barriers providing a large rigidity of the sub-panel, see Figure 8-31. In the elastic buckling program it is not possible to model these local intermediate supports, but substituting the flat stiffeners with a normal trough-stiffener a utilisation ratio  $UR < 1.0$  has been obtained. Thus it is concluded that no global plate buckling problems due to transverse stresses exists at this location.

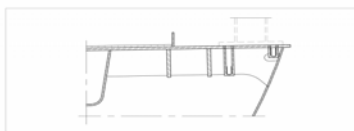


*Figure 8-31 Supports for crash barriers*

		<b>Ponte sullo Stretto di Messina</b> <b>PROGETTO DEFINITIVO</b>		
Specialist Technical Design Report, Annex		<i>Codice documento</i> PS0075_F0-ok.doc	<i>Rev</i> F0	<i>Data</i> 20/06/2011

## 9 Verification - Transverse Steel

### 9.1 Method

The longitudinal steel of the roadway-, railway- and cross girders are in general verified using ADVERS. The spreadsheet does however not consider the transverse diaphragms. The verification of the diaphragm is carried out in two steps. First by using the local FE-models performed in ROBOT of the different bridge section, see Chapter 10. These models give the different stress concentrations in the diaphragm, and investigate the behaviour around utility openings. Secondly a spreadsheet based on EN 1993-1-5:2006 section 10, and a calculation program for elastic buckling of plates are used to investigate the stability of the different sub-panels of the diaphragms.

The diaphragm is divided into sub-panels by distributed vertical stiffeners. It is verified that these stiffeners have capacity to support the diaphragm panels sufficiently. The capacities of these stiffeners have been verified according to EN 1993-1-1:2005 section 6.3. Each sub-panel of the diaphragm is subjected to the stress distribution from both global and local traffic loading at its specific location, as illustrated in Figure 9-1. From this stress distribution it is possible to calculate a critical stress factor  $\phi_{cr}$  indicating the increase in stresses allowed before the panel will buckle. The method used also accounts for stabilising effects such as restraints at edges if any.

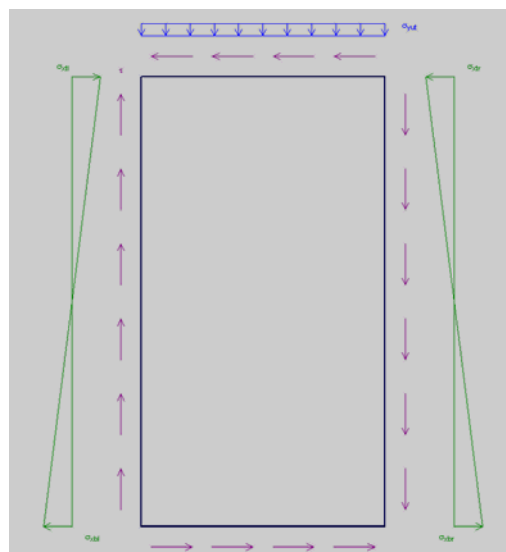
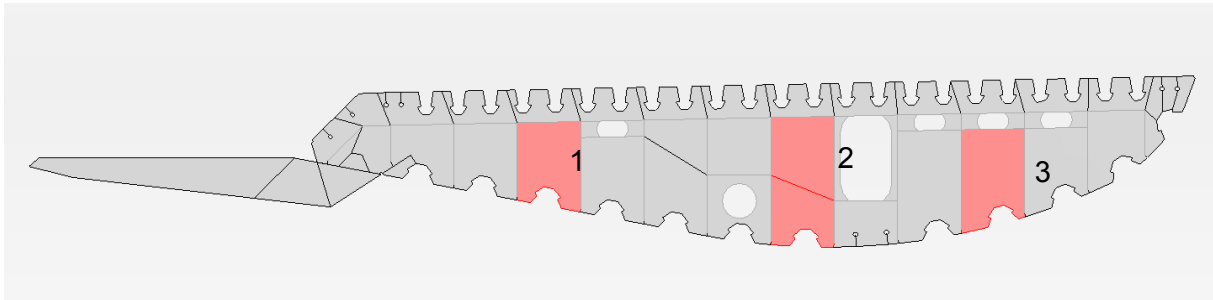


Figure 9-1 Stress distribution at diaphragm panel for buckling investigation

		<b>Ponte sullo Stretto di Messina</b> <b>PROGETTO DEFINITIVO</b>		
Specialist Technical Design Report, Annex		<i>Codice documento</i> PS0075_F0-ok.doc	<i>Rev</i> F0	<i>Data</i> 20/06/2011

Since it is known that the bending stresses (e.g. tension stress) will have a stabilising effect on the panel, a variation of load situations have been investigated to determine the most critical load situation for the panels.



*Figure 9-2 Critical panels chosen for stability verification, roadway girder diaphragm*

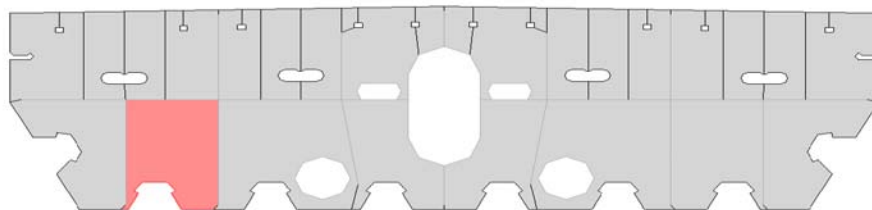


*Figure 9-3 Critical panel chosen for verification, railway girder diaphragm*

The selected panel types investigated are shown in Figure 9-2 and Figure 9-3. For these panels, the stress distribution has been calculated in the local FE-models followed by calculating the critical stress factor  $\phi_{cr}$  using the program for elastic buckling of plates, see Table 9-1. From the applied stress condition a critical stress ratio,  $\phi_{cr}$ , have been calculated indicating the ratio to which the stresses can be increased before elastic buckling instability of the panel occurs. This critical factor have been calculated using an elastic buckling program, and is similar to the value,  $\alpha_{cr}$ , used in the reduced stress method of EN 1993-1-5:2006 section 10. Stability, when considering both plate-buckling and column-buckling behaviour, has been verified. The governing panels have been chosen in respect to bending and shear in combination with the maximum height of the panel.

		<b>Ponte sullo Stretto di Messina</b> <b>PROGETTO DEFINITIVO</b>		
Specialist Technical Design Report, Annex		<i>Codice documento</i> PS0075_F0-ok.doc	<i>Rev</i> F0	<i>Data</i> 20/06/2011

Table 9-1 Critical shear stresses for selected panels, values shown for CS1 & CF1 diaphragm

Location / Panel no.	Critical factor $\phi_{cr}$	Utilisation UR
Type 1, Roadway	1.01	0.14
Type 2, Roadway	1.03	0.19
Type 3, Roadway	3.00	0.02
Type 3, Railway	1.35	0.17

## 10 Verification using Local FE-Models

### 10.1 Introduction

The local FE-models for suspended deck are performed in the computer program Robot Millennium 2010 an integrated graphic program used for modelling, analysing and designing various types of structures. A detailed description of the local FE-models can be found in the report “General Design Principles for Suspended Deck” including the boundary conditions, global- local coordinate systems, geometry, supports, loads and load combinations. The boundary conditions applied on the local FE-models are taken from the global IBDAS model. The most critical load cases used in the local ROBOT FE-models are determined based on influence line plots from IBDAS global model.

In total four different models have been developed for the verification of the suspended deck:

- **Bridge deck local FE-model:** Describing the cross girder and the longitudinal railway and roadway girders determining the stress level in the plate elements with special regards to stresses in the cross girder outer plates, diaphragms and at the intersection between girders. A plot of the bridge deck local FE-model is shown in Figure 10-1.

		<b>Ponte sullo Stretto di Messina</b> PROGETTO DEFINITIVO		
Specialist Technical Design Report, Annex	<i>Codice documento</i> PS0075_F0-ok.doc	<i>Rev</i> F0	<i>Data</i> 20/06/2011	



Figure 10-1 Overall geometry of bridge deck FE-model

- **Roadway local FE-model:** Describing the stress level in the diaphragm of the roadway girder with regards to the stress concentration at the troughs, cope holes, diaphragm stiffeners and openings and further more to determine von Mises stresses in skin plates including local loading effect from local wheel loads. The local longitudinal stresses are a result of the roadway troughs spanning between transverse diaphragms. Since the troughs are continuous, both hogging and sagging moments must be considered in determining local stresses. Therefore, in calculating stresses in the top plate and top plate stiffeners, both minimum and maximum stresses are considered. A plot of the bridge deck local FE-model is shown in Figure 10-2.

		<b>Ponte sullo Stretto di Messina</b> <b>PROGETTO DEFINITIVO</b>		
Specialist Technical Design Report, Annex		<i>Codice documento</i> PS0075_F0-ok.doc	<i>Rev</i> F0	<i>Data</i> 20/06/2011

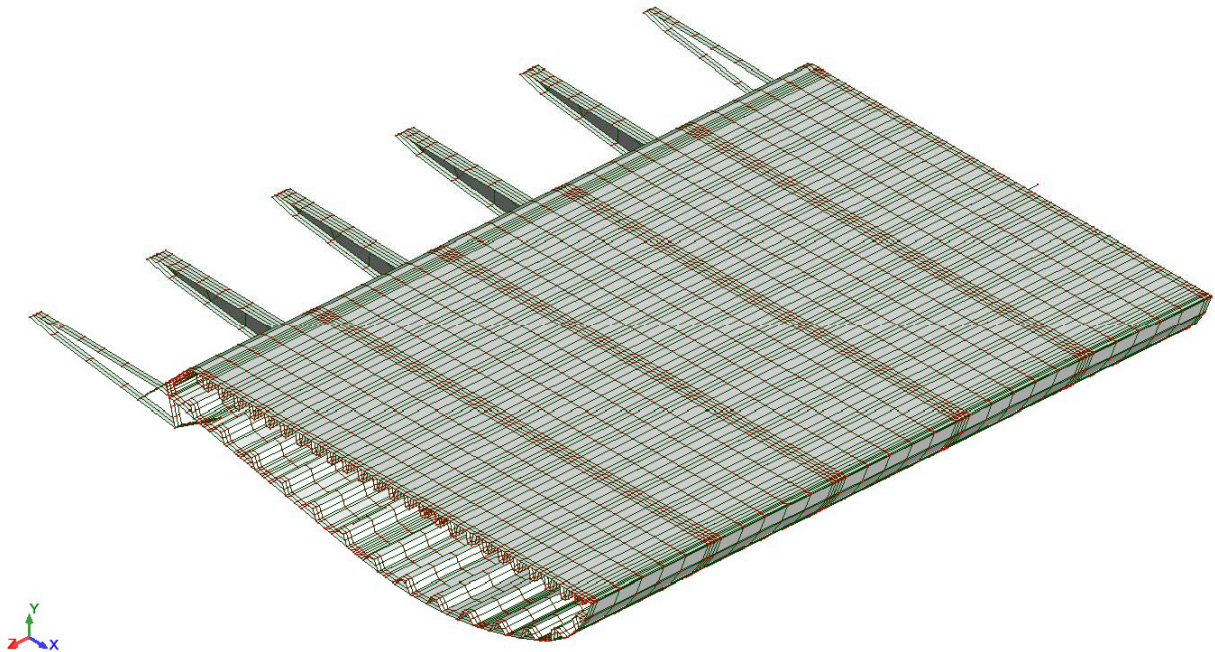


Figure 10-2 Overall geometry of roadway girder FE-model

- Railway local FE-model:** Describing the stress level in the diaphragm of the railway girder with regards to the stress concentration at the troughs, diaphragm stiffeners and openings and further more to determine von Mises stresses in skin plates and top plate stiffeners including local loading effect from local wheel loads. In calculating stresses in the top plate and top plate stiffeners, both minimum and maximum stresses are considered. A plot of the bridge deck local FE-model is shown in Figure 10-3.

		<b>Ponte sullo Stretto di Messina</b> <b>PROGETTO DEFINITIVO</b>					
Specialist Technical Design Report, Annex		<i>Codice documento</i> PS0075_F0-ok.doc	<table border="1" style="width: 100%; border-collapse: collapse;"> <tr> <td style="width: 50%;"><i>Rev</i></td> <td style="width: 50%;"><i>Data</i></td> </tr> <tr> <td>F0</td> <td>20/06/2011</td> </tr> </table>	<i>Rev</i>	<i>Data</i>	F0	20/06/2011
<i>Rev</i>	<i>Data</i>						
F0	20/06/2011						

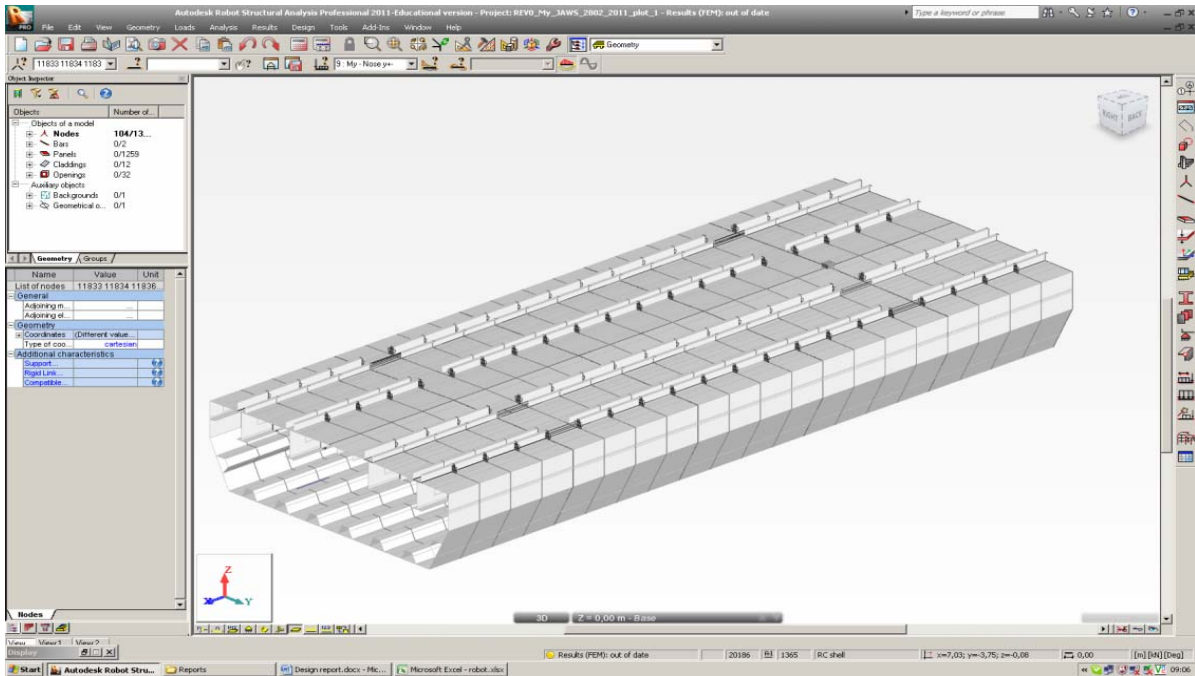


Figure 10-3 Overall geometry of railway girder FE-model

- **Hanger anchorage local FE-model:** Describing the stress level in the plates related to the hanger anchorages. A plot of the bridge deck local FE-model is shown on Figure 10-4.

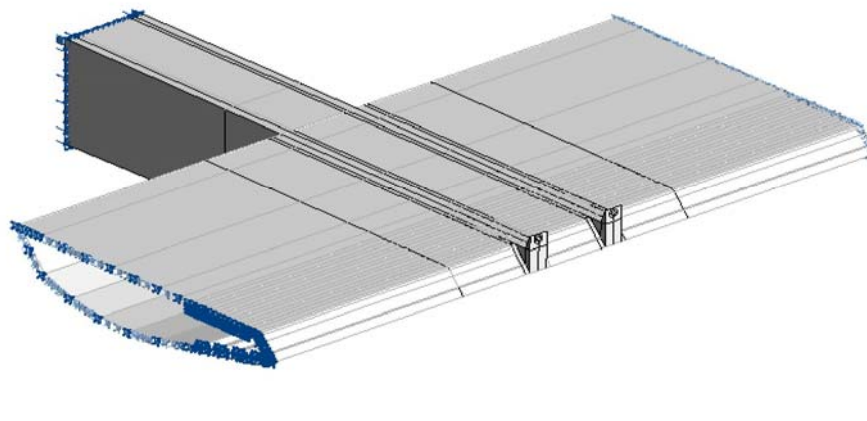


Figure 10-4 Overall geometry of hanger anchorage local FE-model

		<b>Ponte sullo Stretto di Messina</b> <b>PROGETTO DEFINITIVO</b>		
Specialist Technical Design Report, Annex		<i>Codice documento</i> PS0075_F0-ok.doc	<i>Rev</i> F0	<i>Data</i> 20/06/2011

The purpose of the local FE-models is to verify the local design and verify that the stress level is acceptable for applied ULS load combinations. As shown in the following chapters this criteria is fulfilled with some local areas where stresses are within an acceptable yielding range. In these cases it has been verified that yielding areas and peak stresses are acceptable.

Furthermore a semi-local IBDAS FE-model has been developed within the global analysis model enabling a more detailed modeling with shell elements and diaphragms to be used for selected parts. Only a local part of the main span is modeled with shell elements whereas the rest of the suspended deck is modeled with beam elements.

A detailed description of the model can be found in the report “Semi-local IBDAS Model, Suspended Deck”.

As a verification of the local FE-models, axial stress values in the stress plots from the local FE-models is compared with the results from the semi-local IBDAS model.

## 10.2 Local FE-model of Suspended Deck

A local FE-model of the cross girder and adjoining roadway and railway girders has been carried out to determine the stress regime and stress concentrations in the plate elements by means of the finite elements computer program ROBOT. The overall dimensions of the model covers the full width of the bridge deck and extends by 5 modules, 3.75 m each plus two beam elements a side for an overall plan dimension of approximately 24.5 m x 52 m as shown in Figure 10-5. It includes both the roadway and the railway girder enabling the determination of stress concentrations of the latter elements at the intersection with the cross girder as well as a detailed assessment of the stress regime in the outer plates and diaphragms of the cross girder.

		<b>Ponte sullo Stretto di Messina</b> <b>PROGETTO DEFINITIVO</b>	
Specialist Technical Design Report, Annex		Codice documento PS0075_F0-ok.doc	Rev F0 Data 20/06/2011

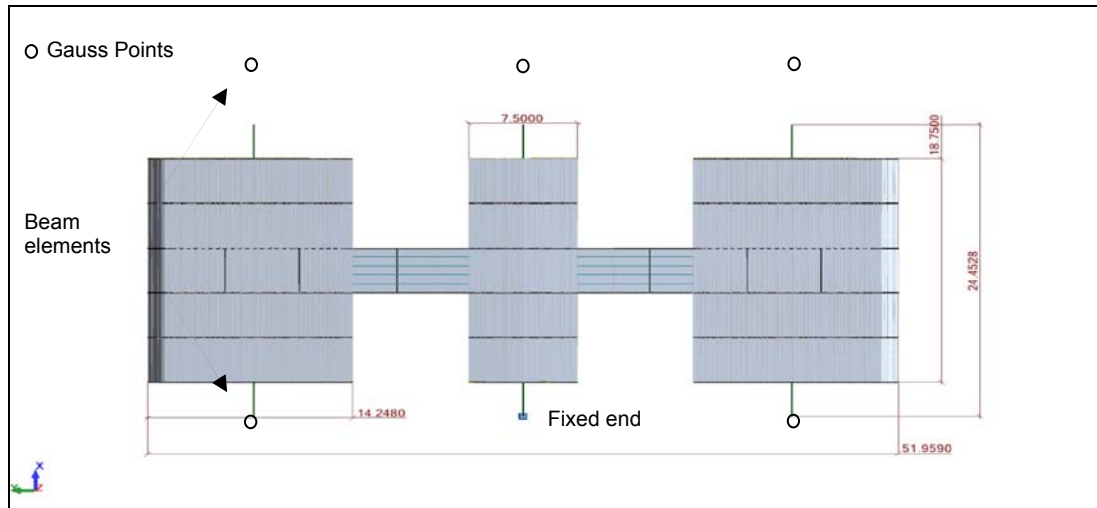


Figure 10-5 Overall geometry of the local suspended deck FE-model

The model is composed by shell elements for the whole longitudinal girders whereas the stiffeners as well as the transverse stiffeners in the cross girders are modelled by beam elements linked to the plates; this assumption have the goal of reducing significantly the complexity and the calculation time without affecting the accuracy of the analysis.

To carry out the analysis for specific load combinations, the loads listed in Table 10-1 have been implemented in the model.

Table 10-1 List of loads implemented into the FE-model

Case	Case name	Nature	Analysis type
1	PP ALL	dead	Static - Linear
7	40mm pavement	dead	Static - Linear
8	PN service lanes	dead	Static - Linear
9	PN rail	dead	Static - Linear
10	PN road	dead	Static - Linear
11	IBDAS Reaction	dead	Static - Linear
13	PN Beam elements	dead	Static - Linear
14	Compensation load	dead	Static - Linear

		<b>Ponte sullo Stretto di Messina</b> <b>PROGETTO DEFINITIVO</b>		
Specialist Technical Design Report, Annex		<i>Codice documento</i> PS0075_F0-ok.doc	<i>Rev</i> F0	<i>Data</i> 20/06/2011

Case	Case name	Nature	Analysis type
15	Water	dead	Static - Linear
22	For Load Cases PP + PN + Compensation	dead	Linear Combination
31	Road LM1 - TS 6542	live	Static - Linear
32	Road LM1 - UDL 6542	live	Static - Linear
33	L71 - Axles 6542	live	Static - Linear
34	LM 71 - UDL 6542	live	Static - Linear
35	LM71 - Braking/acceleration 6542/6532	live	Static - Linear
36	Nosing Force 6542/6532	live	Static - Linear
39	IBDAS Reactions Case 6542	dead	Static - Linear
41	Road LM1 - TS 6532	live	Static - Linear
42	Road LM1 - UDL 6532	live	Static - Linear
43	L71 - Axles 6532	live	Static - Linear
44	LM 71 - UDL 6532	live	Static - Linear
45	SW2 - 6532	live	Static - Linear
48	Wind 6532	dead	Static - Linear
49	IBDAS Reactions Case 6532	dead	Static - Linear
51	Road LM1 – TS 6532	dead	Static - Linear
52	Road LM1 - UDL 6542	dead	Static - Linear
53	L71 - Axles 6542	dead	Static - Linear
54	LM 71 - UDL 6532	dead	Static - Linear
55	SW2 - 6532	dead	Static - Linear
56	LM71 - Braking/acceleration 6542/6532	dead	Static - Linear
57	Nosing Force 6542/6532	dead	Static - Linear
58	Wind 6532	dead	Static - Linear
59	IBDAS Reactions Case 6532	dead	Static - Linear

The three load combinations analysed are described in Table 10-2 and the partial coefficients of the loads are in accordance with the document “Design Basis, Structural”. In addition also the case

		<b>Ponte sullo Stretto di Messina</b> <b>PROGETTO DEFINITIVO</b>		
Specialist Technical Design Report, Annex		<i>Codice documento</i> PS0075_F0-ok.doc	<i>Rev</i> F0	<i>Data</i> 20/06/2011

with dead loads corresponding to the reference condition of the bridge has been determined being essential for the calibration of the model.

*Table 10-2 Table of load combinations considered in the FE-model*

Combi- nation	Name (IBDAS case number)	Description	Nature
21 (C)	Calibration PP + PN	Calibration of structural self weights (PP) and superimposed dead loads (PN). It correspond to the reference condition	SLS
105 (C)	Case 6542	Max reaction of hanger in y+	ULS
106 (C)	Case 6532	Max sagging moment in the cross girder mid-span	ULS
107 (C)	Case 6524	Max torsional moment in the railway girder in the section next to the cross girder	ULS

In the following a short documentation of the von Mises stresses is given. The stress limit has been limited to the design yielding stress of  $f_{yk}/\gamma_{m0}$  which corresponds to  $460/1.05=438$  MPa (the steel grade of all steel elements at the location of the FE-model corresponds to S460). For simplicity rounding in the top plates at the intersection between the longitudinal girder and the cross girder have not been modelled with the consequence of high stress concentration around the corners as can be seen in Figure 10-6 and Figure 10-7. Areas where the stress limit is exceeded are shown as transparent.

		<b>Ponte sullo Stretto di Messina</b> <b>PROGETTO DEFINITIVO</b>		
Specialist Technical Design Report, Annex		<i>Codice documento</i> PS0075_F0-ok.doc	<i>Rev</i> F0	<i>Data</i> 20/06/2011

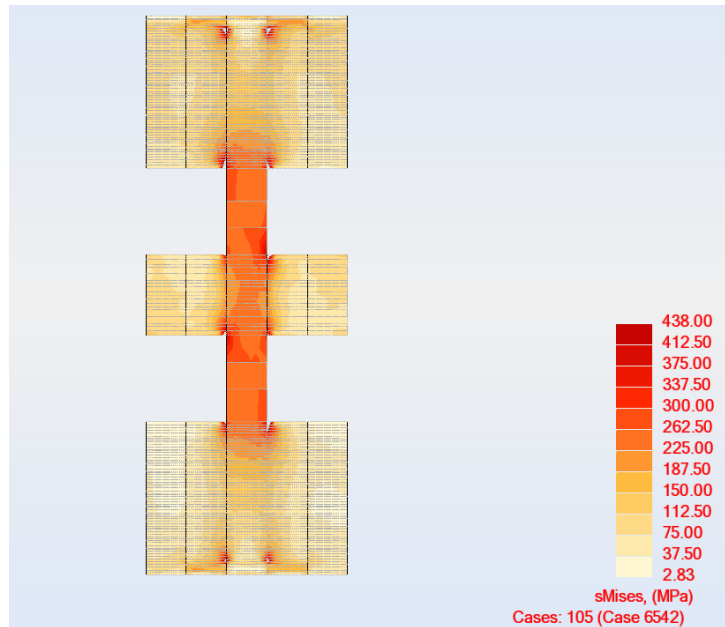


Figure 10-6 von Mises stresses, top plates, combination 106 (Max sagging moment cross girder)

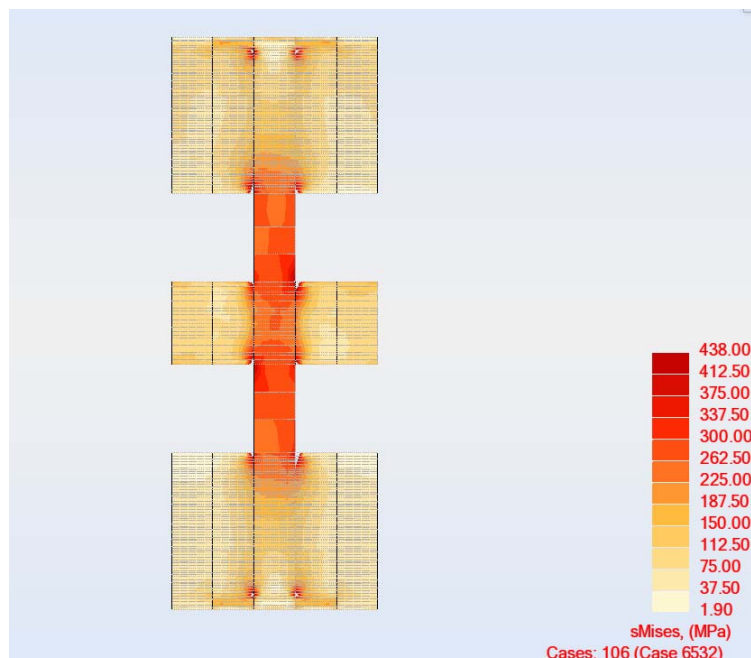


Figure 10-7 von Mises stresses, top plates, combination 105 (Max tension in hanger)

		<b>Ponte sullo Stretto di Messina</b> <b>PROGETTO DEFINITIVO</b>		
Specialist Technical Design Report, Annex		Codice documento PS0075_F0-ok.doc	Rev F0	Data 20/06/2011

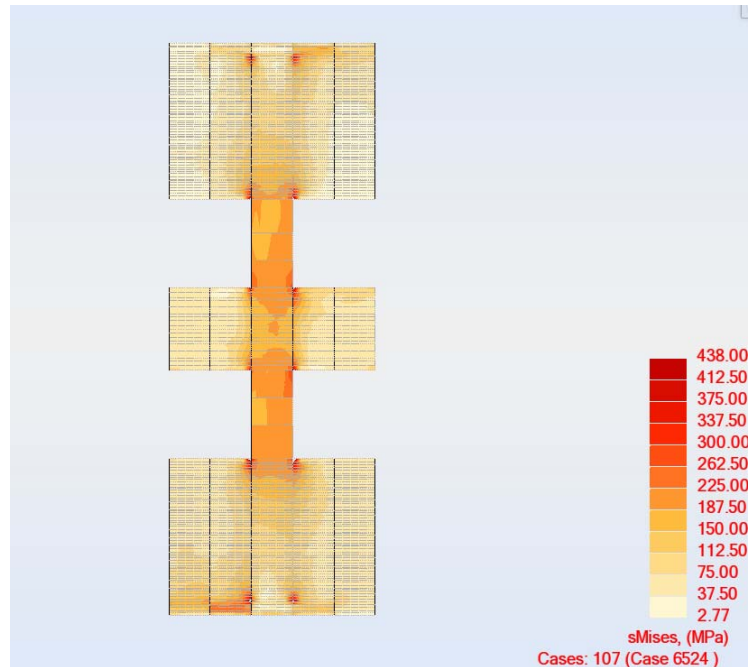


Figure 10-8 von Mises stresses, top plates, combination 107 (Max torsion in the railway girder)

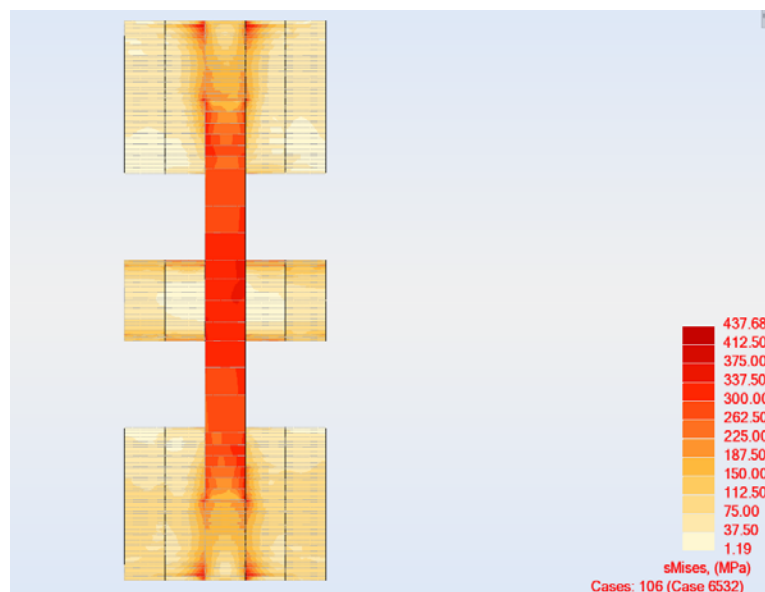


Figure 10-9 von Mises stresses, bottom plates, combination 105 (Max sagging moment cross girder)

		<b>Ponte sullo Stretto di Messina</b> <b>PROGETTO DEFINITIVO</b>		
Specialist Technical Design Report, Annex		<i>Codice documento</i> PS0075_F0-ok.doc	<i>Rev</i> F0	<i>Data</i> 20/06/2011

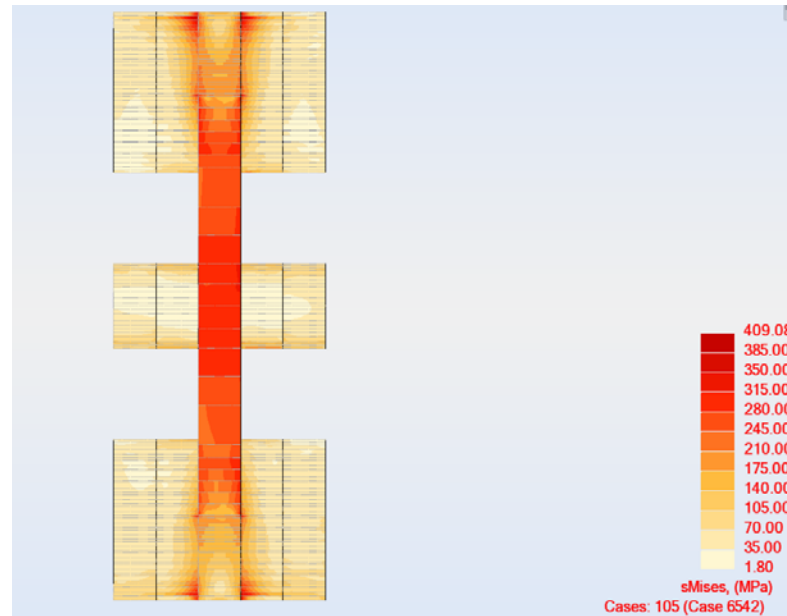


Figure 10-10 von Mises stresses, bottom plates combination 105 (Max tension in hanger)

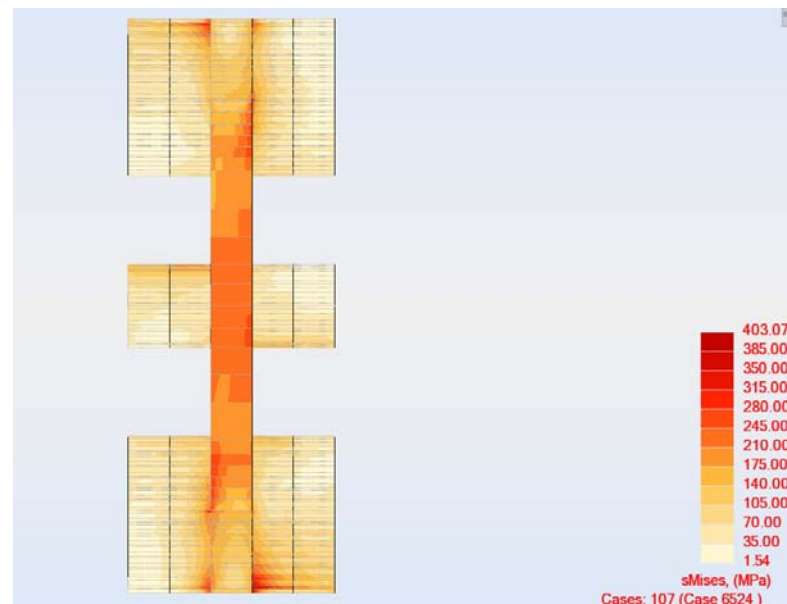


Figure 10-11 von Mises stresses, bottom plates, combination 107 (Max torsion in the railway girder)

The above mentioned stress concentrations are merely a result of the detail level of the model at these locations and will not be real; they don't represent an issue for the general design.

		<b>Ponte sullo Stretto di Messina</b> PROGETTO DEFINITIVO		
Specialist Technical Design Report, Annex		Codice documento <i>PS0075_F0-ok.doc</i>	Rev <i>F0</i>	Data <i>20/06/2011</i>

Stress concentrations can also be seen around the cross girder manhole at the railway location. In Figure 10-12 to Figure 10-14 it can be noticed that this detail is below yielding stress as the correct geometry of the ring stiffeners has been implemented by means of beam elements around the manhole.

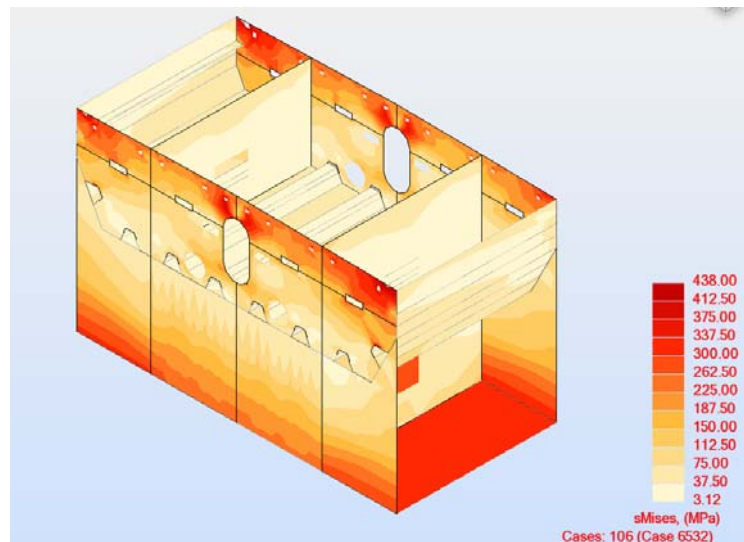
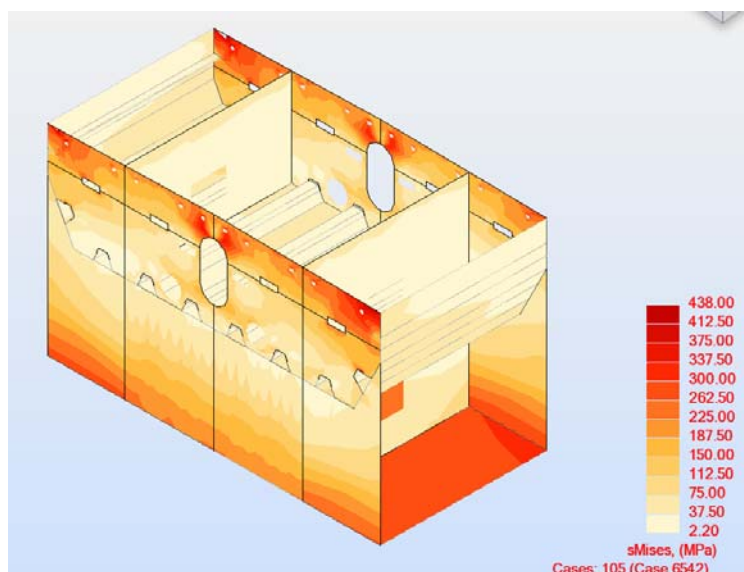


Figure 10-12 von Mises stresses, cross girder web at railway intersection, combination 106 (Max sagging moment cross girder)



		<b>Ponte sullo Stretto di Messina</b> <b>PROGETTO DEFINITIVO</b>		
Specialist Technical Design Report, Annex		<i>Codice documento</i> PS0075_F0-ok.doc	<i>Rev</i> F0	<i>Data</i> 20/06/2011

Figure 10-13 von Mises stresses, cross girder web at railway intersection, combination 105 (Max tension in hanger)

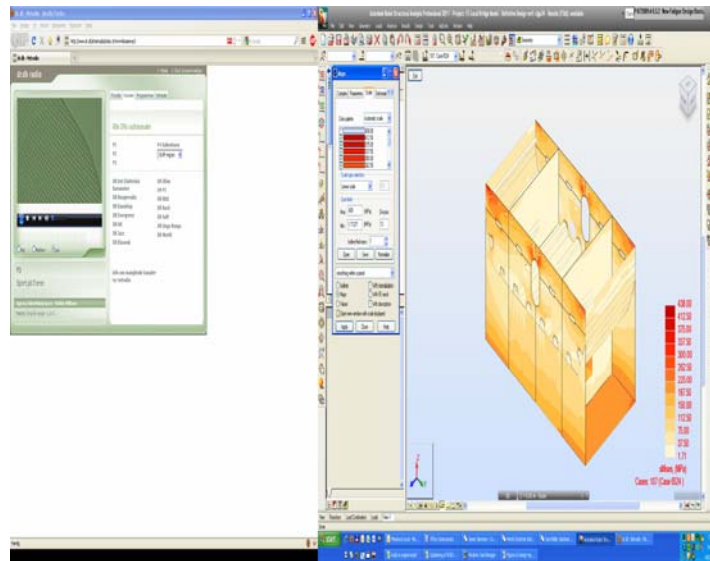


Figure 10-14 von Mises stresses, cross girder web at railway intersection, combination 107 (Max torsion in the railway girder)

Areas where the design yielding stress is exceeded occur typically at the hanger anchorage where the actual hanger force have been directly applied to the web edge as point loads, see Figure 10-15 to Figure 10-17. This excess is a result of the detail level at this location and therefore disregarded in the verification. A more detailed local model of the hanger anchorage can be seen in section 10.4.

		<b>Ponte sullo Stretto di Messina</b> <b>PROGETTO DEFINITIVO</b>	
Specialist Technical Design Report, Annex		Codice documento PS0075_F0-ok.doc	Rev    Data F0    20/06/2011

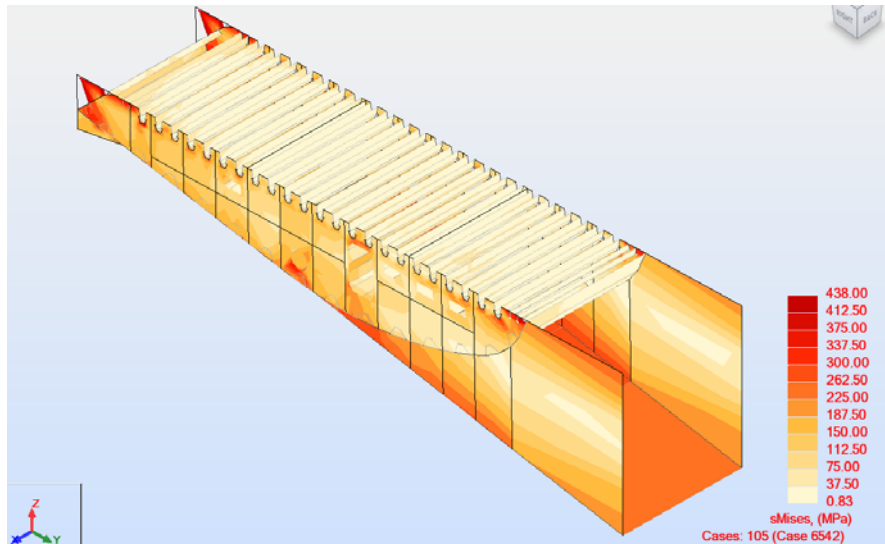


Figure 10-15 von Mises stresses, cross girder web at roadway intersection, combination 105 (Max sagging moment cross girder)

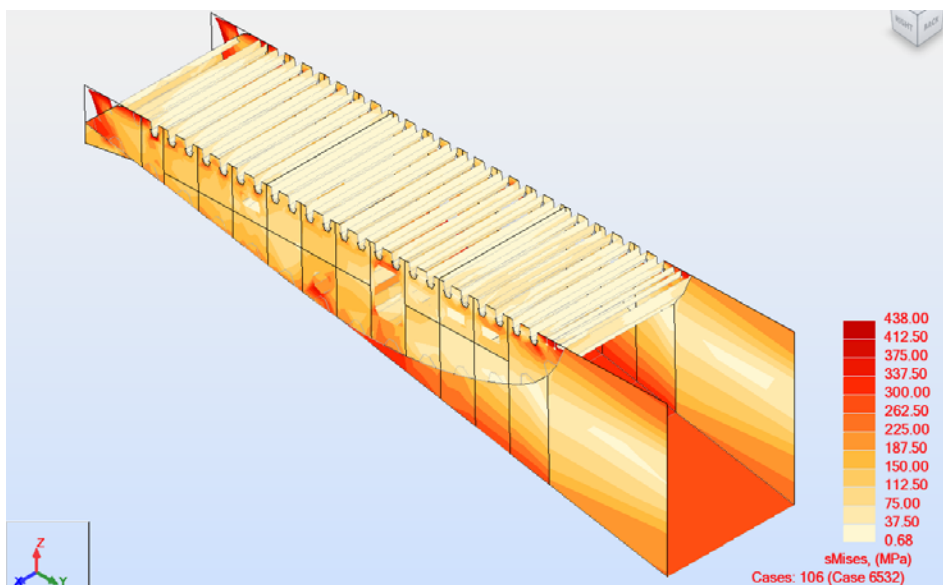


Figure 10-16 von Mises stresses, cross girder web at roadway intersection, combination 106 (Max tension in hanger)

		<b>Ponte sullo Stretto di Messina</b> <b>PROGETTO DEFINITIVO</b>		
Specialist Technical Design Report, Annex		<i>Codice documento</i> PS0075_F0-ok.doc	<i>Rev</i> F0	<i>Data</i> 20/06/2011

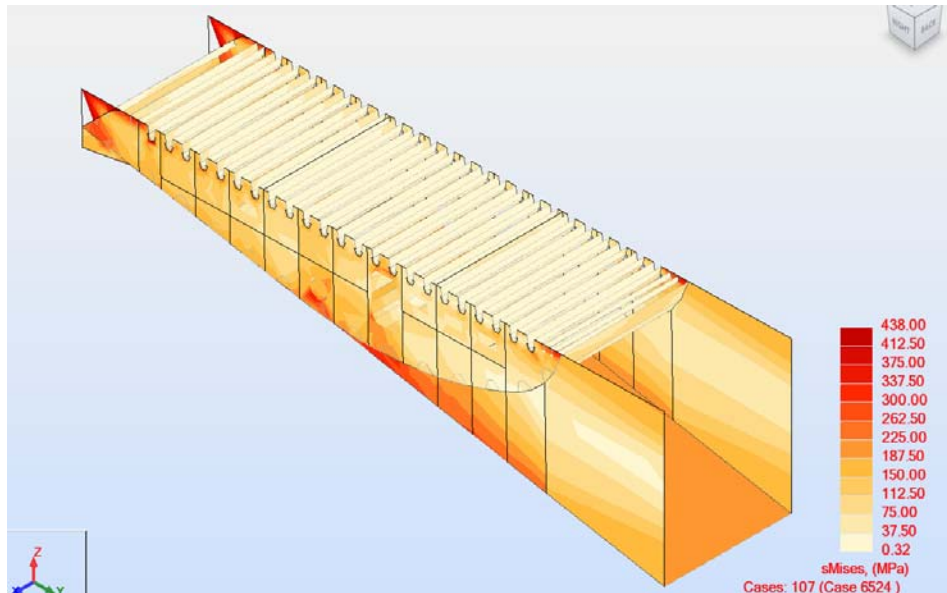


Figure 10-17 von Mises stresses, cross girder web at roadway intersection, combination 107 (Max torsion in the railway girder)

### 10.3 Local FE-Models of Roadway and Railway Girder

Two separate local linear shell FE-models of the roadway and railway box girders are created to determine the stress regime and stress concentrations in the longitudinal steel as well as the local stress distribution of the diaphragms. Each model has a total length of 20.7 m located between two cross girders. The relatively large extension of the model will ensure correct boundary conditions and stress distribution for the plates. Figure 10-18 shows a sketch of the local models consisting of five 3.75 m sections including four diaphragms and a beam element in each end of the model.

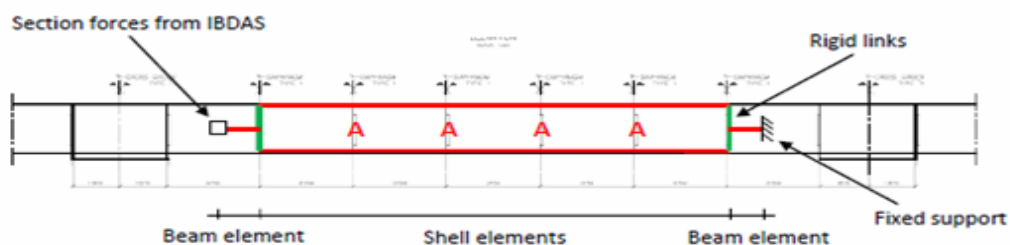


Figure 10-18 Elevation of the model for the roadway and railway diaphragm

		<b>Ponte sullo Stretto di Messina</b> <b>PROGETTO DEFINITIVO</b>		
Specialist Technical Design Report, Annex		<i>Codice documento</i> PS0075_F0-ok.doc	<i>Rev</i> F0	<i>Data</i> 20/06/2011

Both models are placed in the span between cross girder 27 and 28 with a fixed support and IBDAS sectional forces corresponding to s-coordinate -964.65 and -985.35, respectively. The traffic load is fixated for maximising the My and Mz sectional forces in the centre of the span for the roadway and My, Mt and Vz in the centre of the span for the railway girder. The loads have been applied on the models according to IBDAS influence line plots of the governing load cases of traffic loads.

To carry out the analysis for specific load combinations, the loads listed in Table 10-3 to Table 10-6 have been implemented in the models.

*Table 10-3 List of loads implemented in the roadway FE-model*

Case	Case name	Nature	Analysis type
1	PP ALL	dead	Static - Linear
5	PN Parapets, windscreens, lighting, traffic signs	dead	Static - Linear
6	PN Cables	dead	Static - Linear
7	PN Service lane	dead	Static - Linear
8	PN Walkways, interior	dead	Static - Linear
9	PN drainage	dead	Static - Linear
10	PN TOTAL	dead	Linear Combinations
20	IBDAS reactions (PP+PN)	dead	Static - Linear
30	UDL Traffic load case 6561	live	Static - Linear
40	UDL Traffic load case 6566	live	Static - Linear

*Table 10-4 List of load combinations considered in the roadway FE-model*

Combination	Name (IBDAS case number)	Description	Nature	Definition
100 (C)	Calibration PP + PN	Calibration of structural self-weights (PP) and superimposed dead loads (PN)	SLS	$(1+10+20)*1.00$

		<b>Ponte sullo Stretto di Messina</b> <b>PROGETTO DEFINITIVO</b>		
Specialist Technical Design Report, Annex		<i>Codice documento</i> PS0075_F0-ok.doc	<i>Rev</i> F0	<i>Data</i> 20/06/2011

Combination	Name (IBDAS case number)	Description	Nature	Definition
200 (C)	Case 6561	Max moment +My	ULS	1*1,35+10*1,5+20*1,0+30*1,35
210 (C)	Case 6566	Max shear +Vz	ULS	1*1,35+10*1,5+20*1,0+40*1,35

*Table 10-5 List of loads implemented in the railway FE-model*

Case	Case name	Nature	Analysis type
1	PP ALL	dead	Static - Linear
2	PN rail girder	dead	Static - Linear
3	IBDAS reactions (PP+PN)	dead	Static - Linear
4	PN Beam elements	dead	Static - Linear
5	LM 71 - case 6571	live	Static - Linear
6	LM71 - Braking/acceleration 6571	live	Static - Linear
7	Nosing Force case 6571	live	Static - Linear
8	IBDAS Reactions case 6571	dead	Static - Linear
9	SW2 - case 6571	live	Static - Linear
10	SW2 - Braking/acceleration 6571	live	Static - Linear
11	LM 71 - case 6575	live	Static - Linear
12	LM71 - Braking/acceleration 6575	live	Static - Linear
13	Nosing Force case 6575	live	Static - Linear
14	IBDAS Reactions case 6575	dead	Static - Linear
15	SW2 - case 6575	live	Static - Linear
16	SW2 - Braking/acceleration 6575	live	Static - Linear
17	LM 71 - case 6577	live	Static - Linear
18	LM71 - Braking/acceleration 6577	live	Static - Linear
19	Nosing Force case 6577	live	Static - Linear
20	IBDAS Reactions case 6577	dead	Static - Linear

		<b>Ponte sullo Stretto di Messina</b> <b>PROGETTO DEFINITIVO</b>		
Specialist Technical Design Report, Annex		<i>Codice documento</i> PS0075_F0-ok.doc	<i>Rev</i> F0	<i>Data</i> 20/06/2011

Case	Case name	Nature	Analysis type
21	SW2 - case 6577	live	Static - Linear
22	SW2 - Braking/acceleration 6577	live	Static - Linear

The load combinations analysed are described in Table 10-4 and Table 10-6 and the partial coefficients of the loads are in accordance with the Design Basis. In addition a load case with dead loads has been reference for the calibration of the model.

*Table 10-6 List of load combinations considered in the railway FE-model*

Combi-nation	Name (IBDAS case number)	Description	Nature	Definition
4 (C)	Calibration PP + PN	Calibration of structural self-weights (PP) and superimposed dead loads (PN)	SLS	$(1+2+3+4)*1.00$
12 (C)	Case 6571	Max moment +My	ULS	$(1+4)*1.35+2*1.5+(5+6+9+10)*1.45+8*1.0+7*0.73$
15 (C)	Case 6575	Max torsion +Mt	ULS	$(1+4)*1.35+2*1.5+(11+12+15+16)*1.45+14*1.0+13*0.73$

In the following figures the von Mises stresses are presented for the roadway girder for maximum bending moment  $M_y$ . For the longitudinal steel, the yielding stress,  $f_{yk}/\gamma_{m0}$ , corresponds to  $460/1.05=438\text{MPa}$  and for the diaphragms the yielding stress corresponds to  $355/1.05=338\text{MPa}$ .

 <b>Stretto di Messina</b>	 Eurolink	<b>Ponte sullo Stretto di Messina</b> PROGETTO DEFINITIVO		
Specialist Technical Design Report, Annex		<i>Codice documento</i> PS0075_F0-ok.doc	<i>Rev</i> F0	<i>Data</i> 20/06/2011

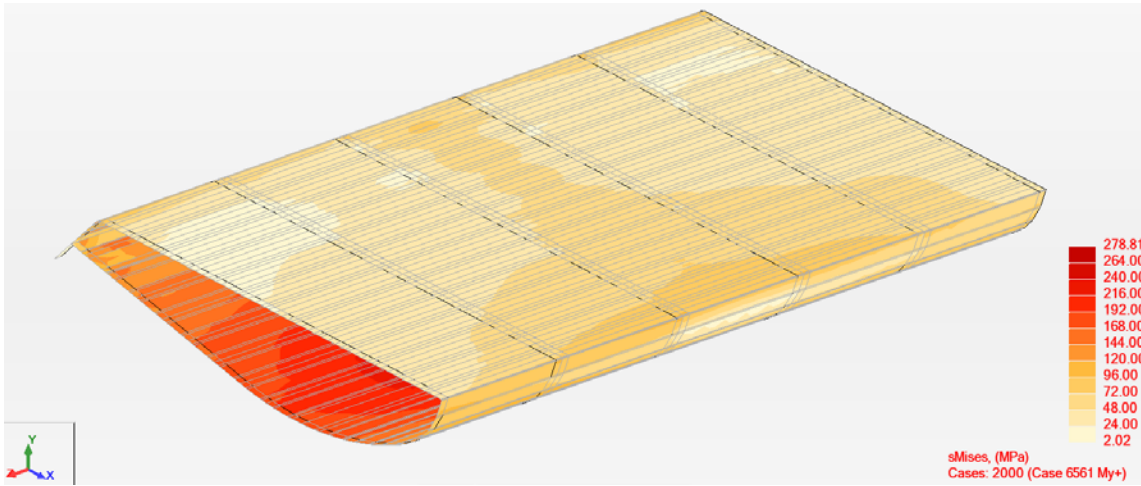


Figure 10-19 von Mises stresses, roadway girder deck plate and inclined web plate, case 2000 (My+)

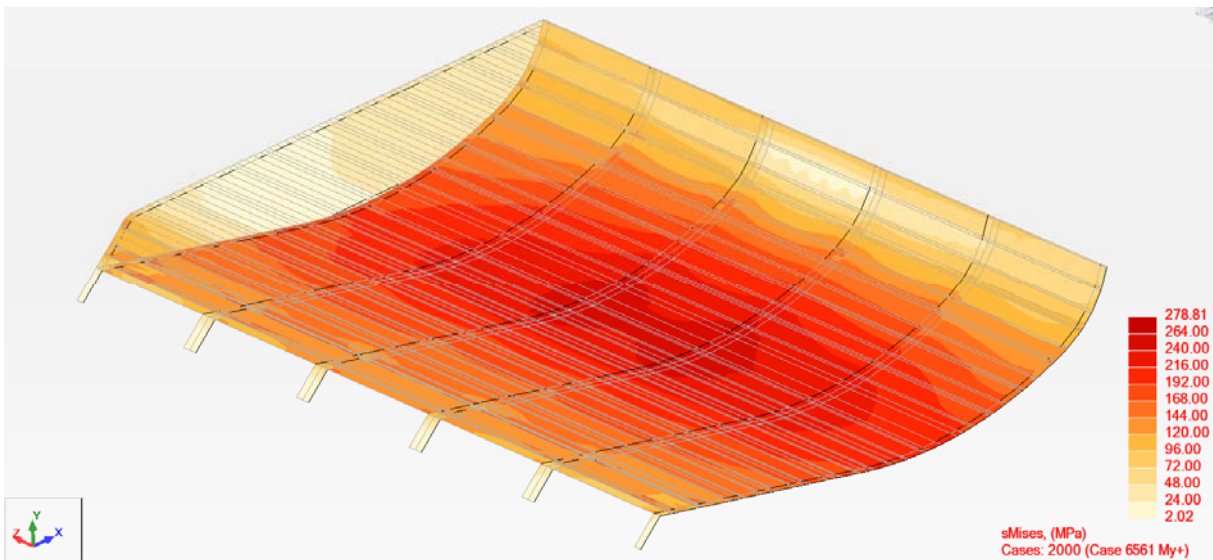


Figure 10-20 von Mises stresses, roadway girder bottom plate and inclined web plate, case 2000 (My+)

		<b>Ponte sullo Stretto di Messina</b> <b>PROGETTO DEFINITIVO</b>		
Specialist Technical Design Report, Annex		Codice documento PS0075_F0-ok.doc	Rev F0	Data 20/06/2011

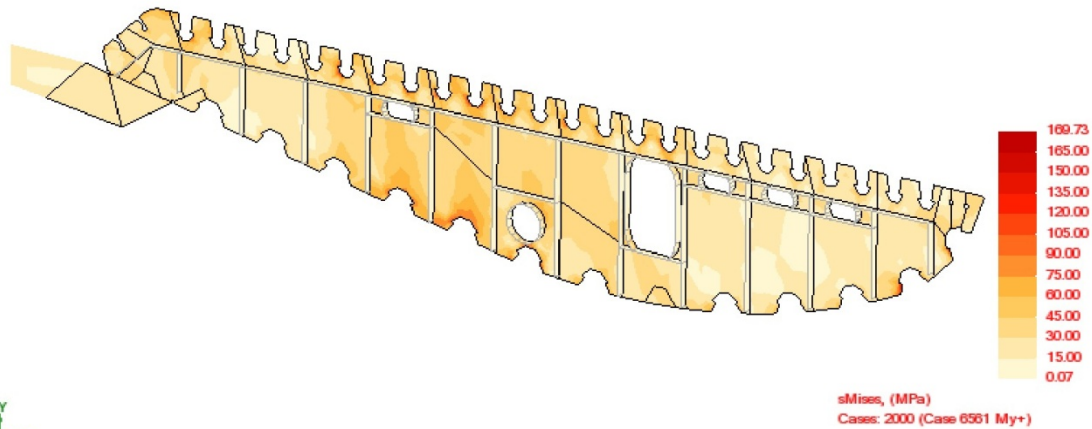


Figure 10-21 von Mises stresses, roadway girder diaphragm, case 2000 (My+)

From the figures it can be seen that the von Mises stress level is acceptable using steel S460 for longitudinal steel and S355 for diaphragms.

In the following a short documentation of the von Mises stresses is given for the railway girder. The steel grade of all steel elements at the location of the FE-model corresponds to S355.

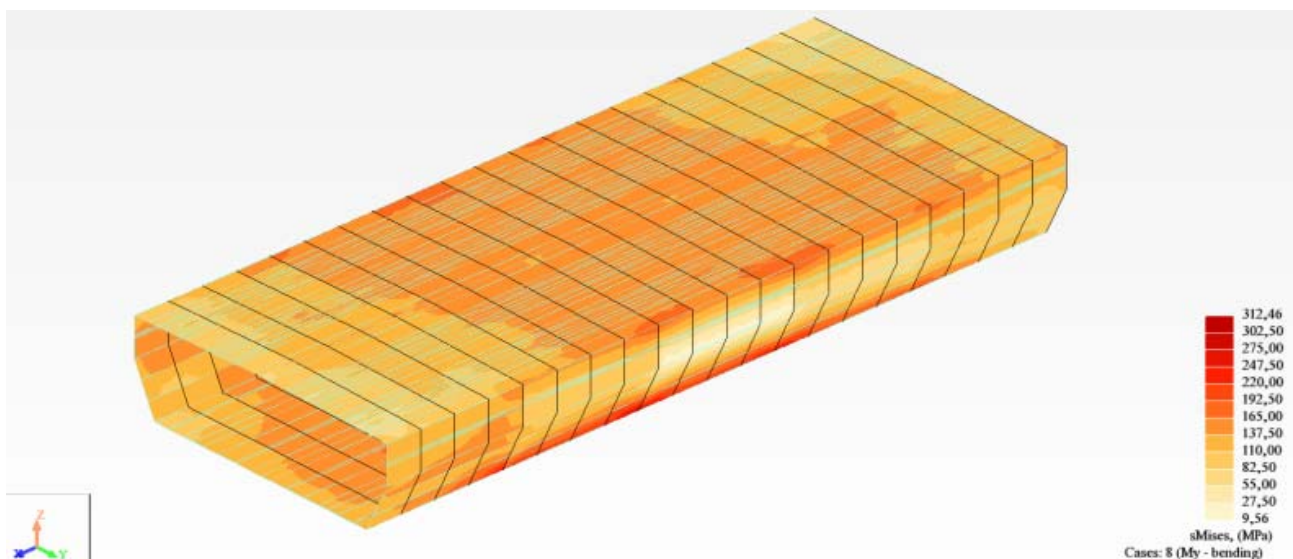


Figure 10-22 von Mises stresses, railway girder deck plate, case 12 (My+)

		<b>Ponte sullo Stretto di Messina</b> <b>PROGETTO DEFINITIVO</b>		
Specialist Technical Design Report, Annex		<i>Codice documento</i> PS0075_F0-ok.doc	<i>Rev</i> F0	<i>Data</i> 20/06/2011

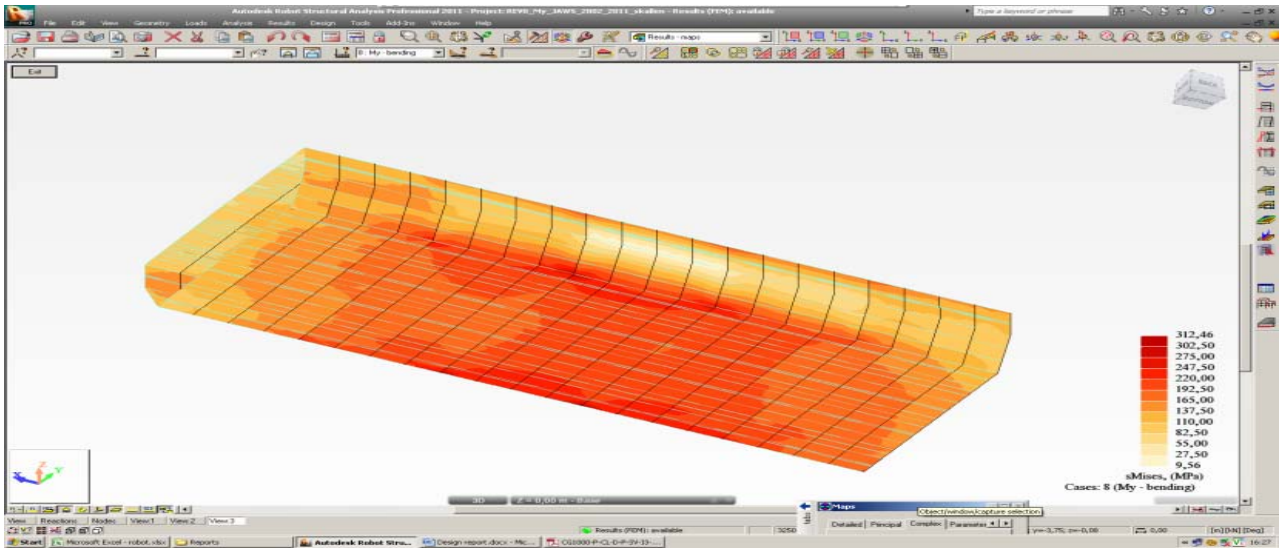


Figure 10-23 von Mises stresses, roadway girder bottom plate and inclined web, case 12 (MY+)

In Figure 10-23 the average von Mises stresses are in the range of 165MPa to 250MPa over the main part of the plate area and the maximum stress in the bottom plate is 313MPa which is acceptable using steel S355. In Figure 10-24 the von Mises stress plots are shown for the diaphragm closest to the mid span of the FE-model for maximum My load case.



Figure 10-24 von Mises stresses, roadway girder diaphragm, case 12 (My+)

From Figure 10-24 it is seen that the overall stress level is acceptable for steel S355. The stress limit is exceeded in very small areas along the edge of the cut out for troughs at the inclined web plate where the stresses reach a maximum value of 280 MPa. However this excess does not

		<b>Ponte sullo Stretto di Messina</b> <b>PROGETTO DEFINITIVO</b>		
Specialist Technical Design Report, Annex		<i>Codice documento</i> PS0075_F0-ok.doc	<i>Rev</i> F0	<i>Data</i> 20/06/2011

reflect a real issue and considering the size of the area the excess of the stress limit is considered acceptable.

#### 10.4 Local FE-Model of Hanger Anchorage

A local shell FE-model of the hanger anchorage has been created to verify the local stress distribution for the hanger anchorage. The overall length of the model is 30 m between mid-spans of the longitudinal roadway girder and a width of 26 m comprising half a cross girder. The relatively large extension of the model will ensure correct boundary conditions and stress distribution for the plates related to the hanger anchorage.

This independent model has been created using the FE-software ROBOT and the applied global hanger forces have been determined in the global IBDAS model. The global hanger forces are acting in the centre of the pinhole and are applied as an approximation of hertz stress distribution by means of three point loads. The model is supported in each end of the 30 meter roadway in the longitudinal direction and the cross girder is supported in the centreline of the bridge deck. To comply for the vertical shear distribution in the longitudinal direction an external force has been applied.

The following hanger anchorage models have been modelled; AP1 with spherical bearings, AP1 without spherical bearings, AP2 and AP3, which in total represents the hanger anchorages from cross girder number 9 to 111.

The hanger load has been applied under an ULS rotation of maximum 13.9 degrees for rotation around the y-axis and 11.2 degrees for the ULS rotation around the s-axis. The sign convention for the rotations is shown in Figure 10-25. The maximum rotations are both represented in cross girder 60, which is in the centre of main span.

		<b>Ponte sullo Stretto di Messina</b> PROGETTO DEFINITIVO		
Specialist Technical Design Report, Annex		<i>Codice documento</i> PS0075_F0-ok.doc	<i>Rev</i> F0	<i>Data</i> 20/06/2011

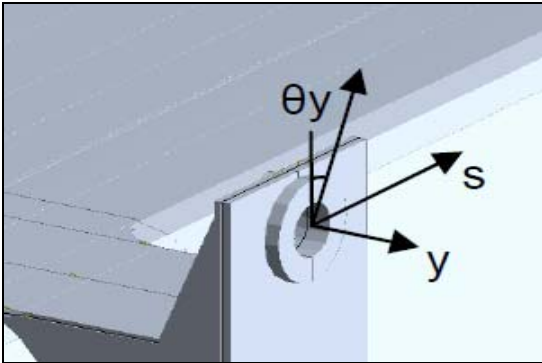


Figure 10-25 Sign convention for the hanger anchorage

Plot of von Mises stresses is used for verification of the stresses as shown in Figure 10-26.

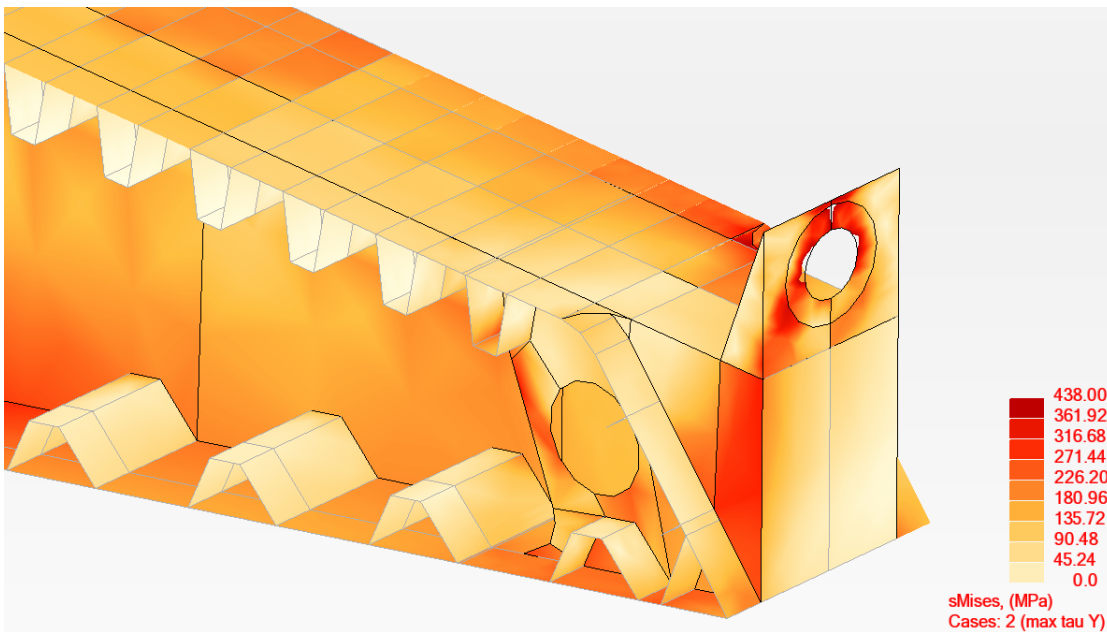


Figure 10-26 von Mises stress plot of AP1 on cross girder 60 with maximum  $\theta_y$  rotation

As shown in Figure 10-26 for the hanger anchorages at cross girder number 52 to 68, it has been necessary to add an extra stiffener due to the relatively large hanger rotation in this area.

		<b>Ponte sullo Stretto di Messina</b> <b>PROGETTO DEFINITIVO</b>		
Specialist Technical Design Report, Annex		<i>Codice documento</i> PS0075_F0-ok.doc	<i>Rev</i> F0	<i>Data</i> 20/06/2011

## 11 Verification - Fatigue Assessments

According to the Design Basis a number of transits of 67 trains per day per track and  $2.0 \times 10^6$   $N_{obs}$  per year of heavy vehicles for each direction have been assumed for the fatigue verification. During the 200 years design life of the bridge the total number of transits on the railway girder becomes  $4.89 \times 10^6$  for each track and on the roadway girder  $4.0 \times 10^8$  in each slow lane.

The unlimited life and the damage accumulation method (Palmgren-Miners summation of damage) have both been used to check the fatigue capacity of the main structural components subject to direct man generated loads.

For the cross girders, railway and roadway girders in general, a safety factor  $\gamma_m=1.35$  has been applied in accordance with the "Safe Life method", whereas for local investigation of the roadway orthotropic deck a safety factor  $\gamma_m=1.15$  has been assumed.

### 11.1 Non man generated loads

The non man generated loads accounted for are temperature, seismic and wind loads. The following have been considered:

- Wind during the design life of 200 years.
- +/- 10°C uniform variation daily during the design life of 200 years.
- SLS1 earthquake 4 times, 5 minutes per event (i.e. total of 20 minutes)

The effect of temperature and seismic loads have been considered isolated and their effects have none or a minor contribution to the fatigue damages, and hence according to the basis of design needs not to be considered for fatigue assessments in combination with man generated loads.

Wind however has a noticeable contribution to the calculated fatigue damage. The response due to wind on the structure can be divided into response due to mean wind (static contribution) and response due to buffeting (dynamic response). Due to a fairly low number of cycles (storm return periods) the contribution from mean wind to the fatigue damage is very limited and can be disregarded in the fatigue calculations. However the dynamic wind response (buffeting) produce a

		<b>Ponte sullo Stretto di Messina</b> <b>PROGETTO DEFINITIVO</b>		
Specialist Technical Design Report, Annex		<i>Codice documento</i> PS0075_F0-ok.doc	<i>Rev</i> F0	<i>Data</i> 20/06/2011

large number of stress cycles of the bridge and will contribute to the fatigue damage in a notable scale.

The accumulated damage is calculated for the following combinations in order to estimate the effect of wind buffeting on the total damage:

**Roadway girder:**

- LM3 vehicle (global and local load effects) + 1 train (EN5) without train meetings
- LM3 vehicle (global and local load effects) + 1 train (EN5) without train meetings + wind

**Railway girder:**

- 1 train (EN5) on both tracks (global and local loads, without train meetings)
- 1 train (EN5) on both tracks (global and local loads, without train meetings) + wind

Wind time series are used in order to assess the effect of wind. A series of different wind speed intervals are considered in the analyses (5, 10, 15, 20, 25, 30, 35 and 39 m/s) weighted by the occurrence and distribution of components perpendicular to the bridge girder to obtain the accumulated damage in combination with man-generated loads.

The additional effect due to wind has been found to be less than 5% and hence the assessment of damage is consequently performed following the formula of Palmgren-Miner, checking that the following result is obtained

$$D = \sum_i \frac{n_i(\text{rail} + \text{road})}{N_i} \leq 1.0 - 0.05 = 0.95$$

**11.2 Fatigue Load Models**

The stress-history plots required for the fatigue verification have been analysed for various elements along the bridge using the global IBDAS model including the main span, the tower location and the side spans. The results have been taken at the centre and at the end of the bottom and top plate for the railway and roadway girders and at the top and bottom plates of the cross girder.

		<b>Ponte sullo Stretto di Messina</b> <b>PROGETTO DEFINITIVO</b>					
Specialist Technical Design Report, Annex		<i>Codice documento</i> PS0075_F0-ok.doc	<table border="1" style="width: 100%; border-collapse: collapse;"> <thead> <tr> <th style="text-align: left;"><i>Rev</i></th> <th style="text-align: left;"><i>Data</i></th> </tr> </thead> <tbody> <tr> <td>F0</td> <td>20/06/2011</td> </tr> </tbody> </table>	<i>Rev</i>	<i>Data</i>	F0	20/06/2011
<i>Rev</i>	<i>Data</i>						
F0	20/06/2011						

### 11.2.1 Fatigue Loads for Rail Traffic

The fatigue loads for the rail traffic includes in total 8 different fatigue trains according to standard train mix in Annex D of Eurocode 1991-2:2003.

Examples of the fatigue train (EN5) passing the bridge are shown in Figure 11-1 , Figure 11-2 and Figure 11-3.

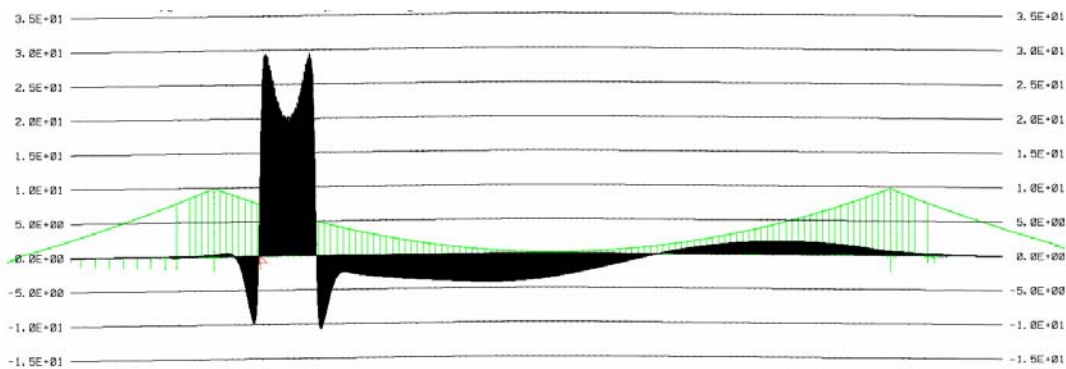


Figure 11-1 Stress-history plot of the bottom plate of the railway girder for EN5 train passing on the bridge

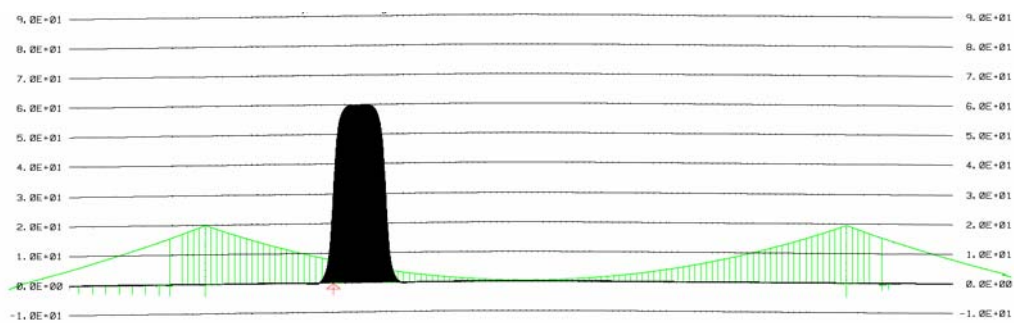


Figure 11-2 Stress-history plot of the bottom plate of the cross girder for EN5 train passing on the bridge

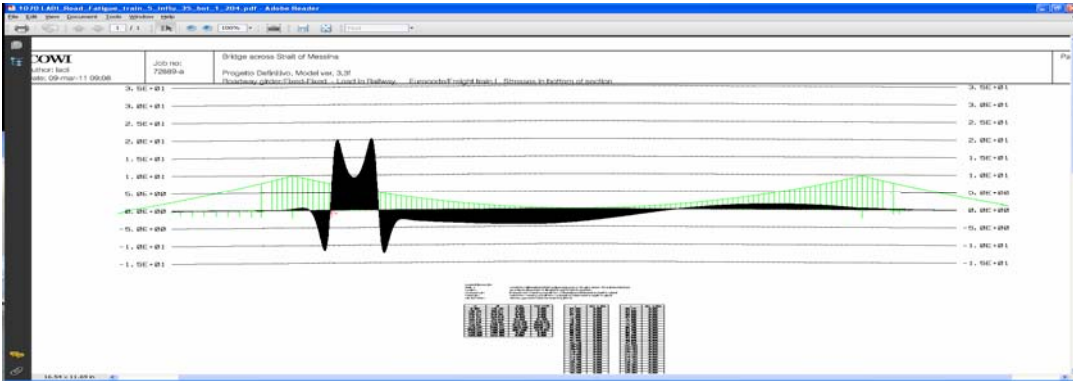


Figure 11-3 Stress-history plot of the bottom plate of the roadway girder for EN5 train passing on the bridge

The number of trains per track per day number of train meetings and the dynamic factors shown in Table 11-1 are in accordance with the Eurocode.

Table 11-1 Dynamic factors for real trains

		speed	local effects	global effects
Fatigue trains EN 1991-2: 2003	EN 1	200	1.300	1.165
	EN 2	160	1.230	1.125
	EN 3	250	1.400	1.224
	EN 4	250	1.400	1.224
	EN 5	80	1.181	1.056
	EN 6	100	1.190	1.071
	EN 7	120	1.200	1.088
	EN 8	100	1.190	1.071

### 11.2.2 Fatigue Loads for Road Traffic

Roadway fatigue Load Model 2 has been utilised for the unlimited life method, whereas Load Model 3 has been used for the damage accumulation method (Palmgren-Miners summation of damage).

		<b>Ponte sullo Stretto di Messina</b> PROGETTO DEFINITIVO		
Specialist Technical Design Report, Annex		<i>Codice documento</i> PS0075_F0-ok.doc	<i>Rev</i> F0	<i>Data</i> 20/06/2011

An example of the roadway fatigue load model 3 passing the bridge is shown in Figure 11-4.

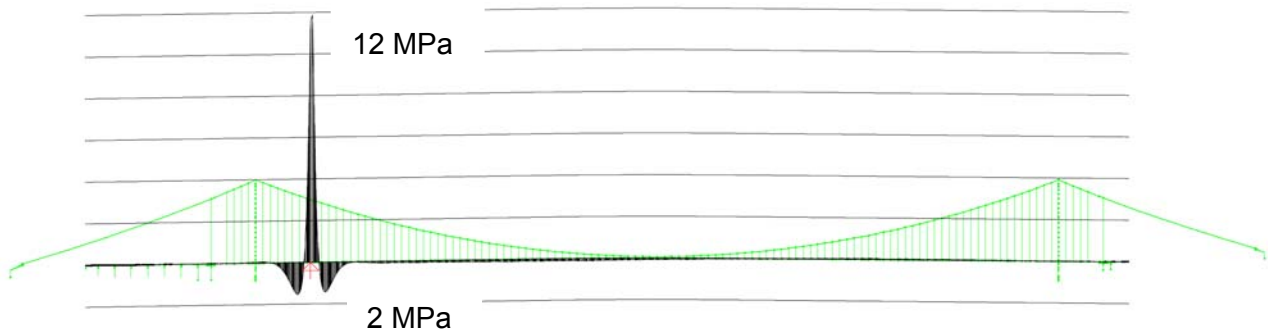


Figure 11-4 Stress-history plot of the bottom plate of the roadway girder for EN5 train passing on the bridge

### 11.2.3 Verification of Roadway Girder Deck Plate - Local Effects

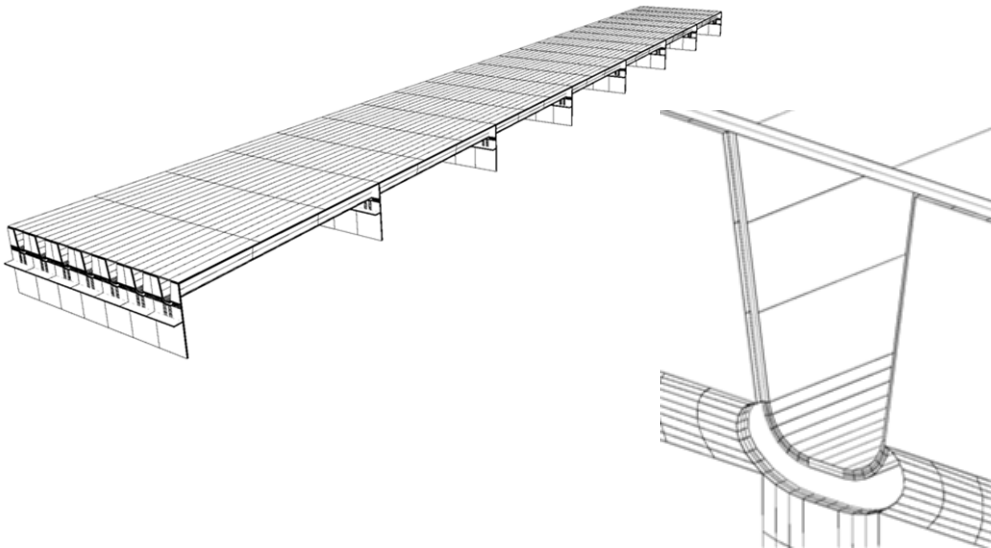
A local IBDAS model has been developed for the orthotropic roadway deck plate in order to investigate the effects from wheel the loads of fatigue load models LM2 and LM3 in EN 1991-2:2003 (E).

Table 11-2 states the key geometrical parameters used in the local model and visualises the geometry of the model which has been generated as a full shell model.

Table 11-2 Local FE-model geometrical dimensions

Outer dimensions	Width	0.51 m x 7 = 3.57 m
	Length	3.75 m x 7 = 26.25 m
Other dimensions	Deck thickness	0.017 m
	Trough thickness	0.009 m
	Trough height (bottom steel deck to bottom trough)	0.309 m
	Trough width at steel deck (centre-centre)	0.239 m
	Trough width at bottom (centre-centre)	0.139 m
	Roadway surfacing thickness	0.012 m
	Diaphragm thickness	0.015 m

		<b>Ponte sullo Stretto di Messina</b> <b>PROGETTO DEFINITIVO</b>		
Specialist Technical Design Report, Annex		<i>Codice documento</i> PS0075_F0-ok.doc	<i>Rev</i> F0	<i>Data</i> 20/06/2011



*Figure 11-5 Geometry of local IBDAS model of the steel deck*

As the boundary conditions in a local model are questionable by nature, only the middle trough with the corresponding deck plate area in the middle section longitudinally has been used as basis for analysis results.

The diaphragms have been modelled directly in the FE-model with a fully detailed inclusion of the cut-outs around the lower part of the troughs. The diaphragms are modelled to 1 m beneath the steel deck in order not to introduce boundary effects in the vicinity of the regions of interest.

All the specified vehicles in LM2 and LM3 are automatically placed in the most adverse positions on the model by utilisation of influence surfaces. In the longitudinal direction IBDAS can move the vehicles completely continuous for determination of worst case loads whereas the transversal position is investigated in seven intervals of 10 cm starting from a placement symmetrically above the middle trough.

Six stress points (A to F) have been defined for fatigue verification as shown below.

		<b>Ponte sullo Stretto di Messina</b> PROGETTO DEFINITIVO		
Specialist Technical Design Report, Annex		<i>Codice documento</i> PS0075_F0-ok.doc	<i>Rev</i> F0	<i>Data</i> 20/06/2011

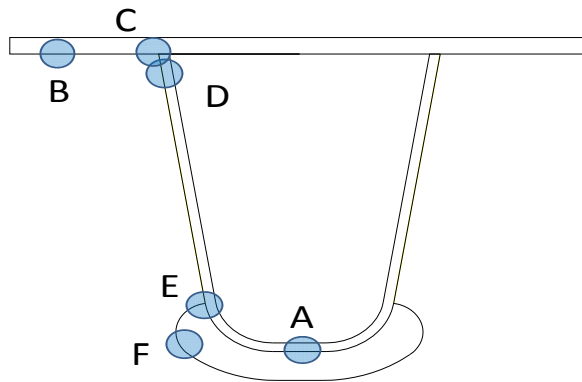


Figure 11-6 Orthotropic deck details

In the following a series of influence line plots for the longitudinal and transverse stresses is presented for stress point A, B and D at the diaphragm. The loads applied comprise:

Table 11-3 Loads applied for generation of influence lines

Load model	Vehicle	Transverse position
LM2	Most severe among the five trucks specified	Most severe among seven "tracks" from symmetrically above trough to 60 cm eccentricity from trough centre
LM3	Only one vehicle	

In Figure 11-7 is the longitudinal stress shown for LM2 truck 3 at bottom of the trough (point A) for 0 cm eccentricity. Figure 11-8 shows small transverse stresses at point A for a 20 cm offset of the load from centre trough. Stress point A is also important in respect to the position of the trough splice in longitudinal direction.

		<b>Ponte sullo Stretto di Messina</b> <b>PROGETTO DEFINITIVO</b>		
Specialist Technical Design Report, Annex		<i>Codice documento</i> PS0075_F0-ok.doc	<i>Rev</i> F0	<i>Data</i> 20/06/2011

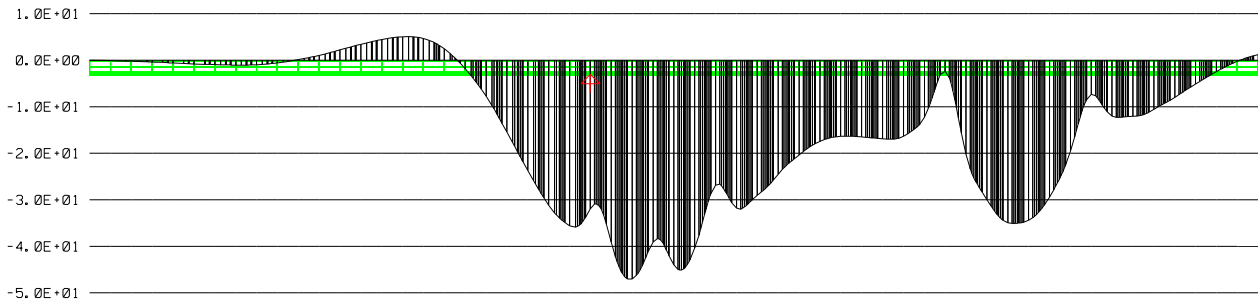


Figure 11-7 Stress point A at diaphragm, longitudinal stress, Truck3 in LM2, 0 cm eccentricity

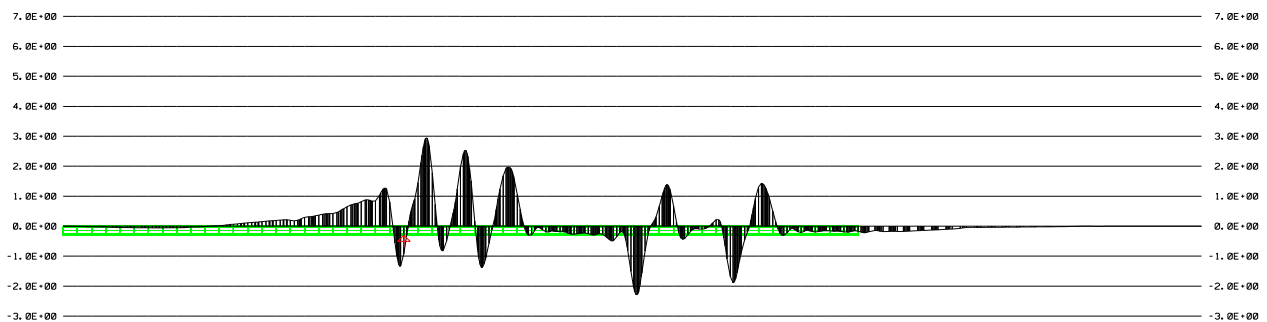


Figure 11-8 Stress point A at diaphragm, transverse stress, Truck3 in LM2, 20 cm eccentricity

The above mentioned trough stress points A to F have been verified for local fatigue traffic load using load model 2 (LM2) in combination with the "Unlimited life method". In the verification, the troughs splices have been positioned 200 mm and 600 mm from the diaphragm.

## 11.3 Stress Concentration Factor (SCF)

### 11.3.1 Points investigated

The calculation of stress ranges used for the fatigue verification is based on the global IBDAS beam model. Further a semi local shell model has been developed in IBDAS in order to verify the stress flow over the span and therefore to evaluate the stress concentration occurring in the plate edges in correspondence of the diaphragms and the shear lag effects at the web of the cross girder. In this section the difference in stress ranges between using the semi-local shell model and the IBDAS global beam model is shown and stress concentration factor to be added to the fatigue stress are presented. The investigation involves span 12 which has been chosen to be

		<b>Ponte sullo Stretto di Messina</b> <b>PROGETTO DEFINITIVO</b>	
Specialist Technical Design Report, Annex	Codice documento <i>PS0075_F0-ok.doc</i>	Rev F0	Data 20/06/2011

representative of all main spans. Its results have been also been adopted for all the side spans where the global effects (given by the train located far away from the section investigated) may lead to lower stress concentrations.

Stress ranges are considered in the following locations of the two models, see Figure 11-9. Two points respectively at 165 mm from the plate edge in the loaded side and at 165 mm from the axis of the plate are distributed over the bottom plate at the following locations along the railway span 12: at mid span ( $s=-1425.0$  m), at the third diaphragm from cross girder 13 ( $s=-1423.13$  m) at the second diaphragm from cross girder 13 ( $s=-1419.38$  m), at 1 m from the cross girder web ( $s=-1412.88$  m), at 0.4 m from the cross girder web ( $s=-1412.28$  m), at 0.2 m from the cross girder web ( $s=-1412.08$  m) and right in correspondence of the cross girder web ( $s=-1411.88$  m). The point at 0.2 m has been also investigated at the transversal location of the trough splice approximately at 0.4 m from the bottom plate edge.

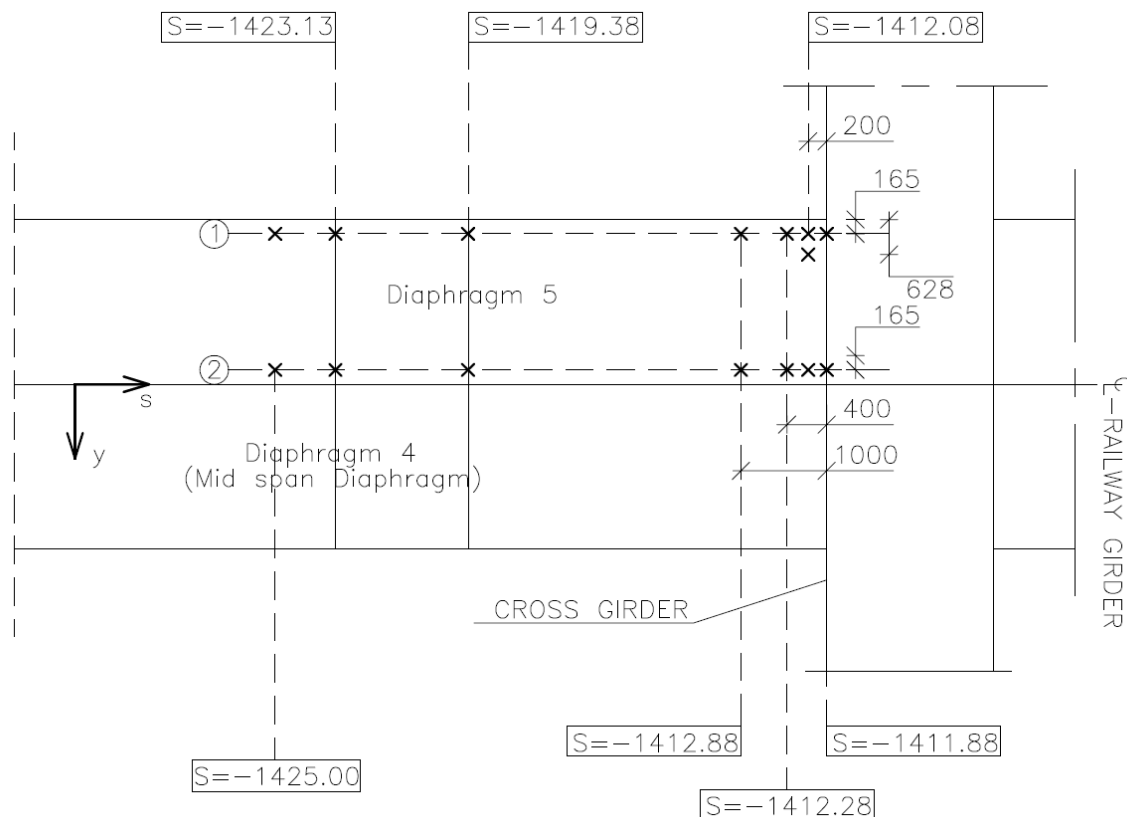


Figure 11-9 Span 12 bottom plate - Location of points selected for verification

		<b>Ponte sullo Stretto di Messina</b> <b>PROGETTO DEFINITIVO</b>		
Specialist Technical Design Report, Annex		<i>Codice documento</i> PS0075_F0-ok.doc	<i>Rev</i> F0	<i>Data</i> 20/06/2011

In Figure 11-10 the Gauss point positions and the dimensions of a typical shell element are shown. The values in flush to the diaphragm have been extrapolated along the gauss points and therefore at 165 mm from the plate edge. The type of the shell elements are parabolic and further information can be found in the document “Semi-local IBDAS Model, Suspended Deck”.

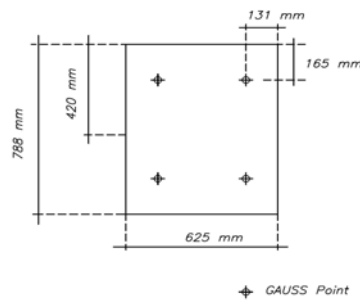


Figure 11-10 Mesh element geometry

### 11.3.2 Stress range determination and SCF results

The stress ranges are calculated for the EN5 train passing in the track located in the negative part of the y axis namely along line 1 of Figure 11-9. Additionally the effects of LM2 vehicle 3 transiting in the roadway girder located in y negative has been investigated and added.

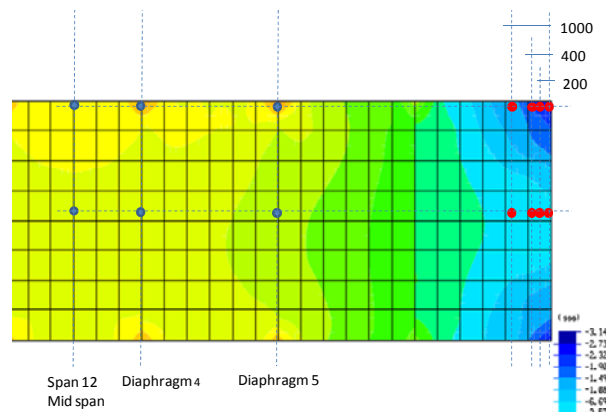
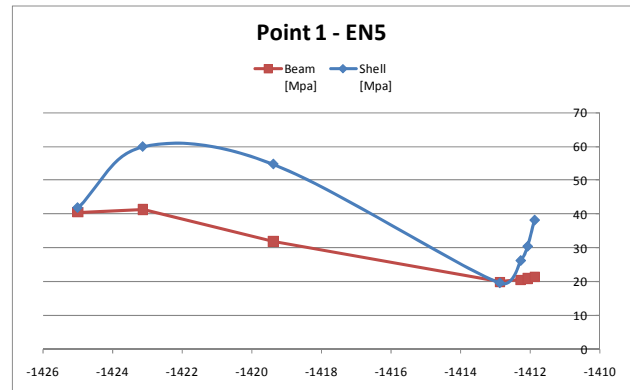
The stress ranges obtained running the EN5 train over the bridge using the IBDAS global beam model and the semi local shell model is presented in Table 11-4. The stress ranges are calculated for each of the considered points in both models. In the table the comparison between the results of the two models are compared, and the difference in stress range is calculated. It can be seen that for the mid span the stress ranges are comparable whereas at the diaphragm locations large variation in stress ranges occurs due a combination of detailing shear lag and torsion due to the unsymmetrical load condition. Since no stress concentrations are experienced using the beam model, a stress concentration factor has been applied for each location.

		<b>Ponte sullo Stretto di Messina</b> <b>PROGETTO DEFINITIVO</b>	
Specialist Technical Design Report, Annex		Codice documento PS0075_F0-ok.doc	Rev    Data F0     20/06/2011

**Table 11-4 Stress ranges calculated for EN5 train, IBDAS global beam model and shell local model**

Type	EN5		
	Shell [Mpa]	Beam [Mpa]	Deviation [%]
Location	s=-1425		
Point 1	41.9	40.5	<b>3.44%</b>
Point 2	39.4	40.4	<b>-2.55%</b>
Location	s=-1423.13		
Point 1	59.9	41.3	<b>45.05%</b>
Point 2	38.4	41.2	<b>-6.79%</b>
Location	s=-1419.38		
Point 1	54.7	31.9	<b>71.52%</b>
Point 2	33.8	31.8	<b>6.27%</b>
Location	s=-1412.88		
Point 1	19.7	20.0	<b>-1.43%</b>
Point 2	18.0	19.9	<b>-9.26%</b>
Location	s=-1412.28		
Point 1	26.3	20.6	<b>27.50%</b>
Point 2	16.8	20.5	<b>-18.05%</b>
Location	s=-1412.08		
Point 1	30.5	21.0	<b>45.37%</b>
Point 2	16.5	20.9	<b>-20.98%</b>
Location	s=-1411.88		
Point 1	38.2	21.3	<b>78.92%</b>
Point 2	16.3	21.2	<b>-23.45%</b>

Location	s=-1412.08		
Extra point	25.9	21.0	<b>23.38%</b>



As an example the stress history plot of the point along line one in correspondence of diaphragm 4 in the shell local model is given in Figure 11-11 and a stress range of approximately 60 MPa is shown.

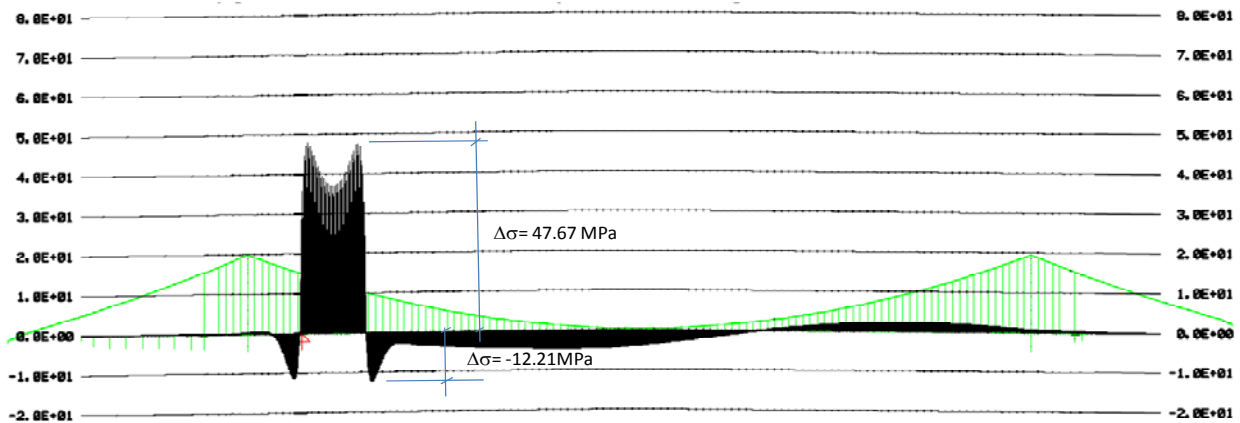
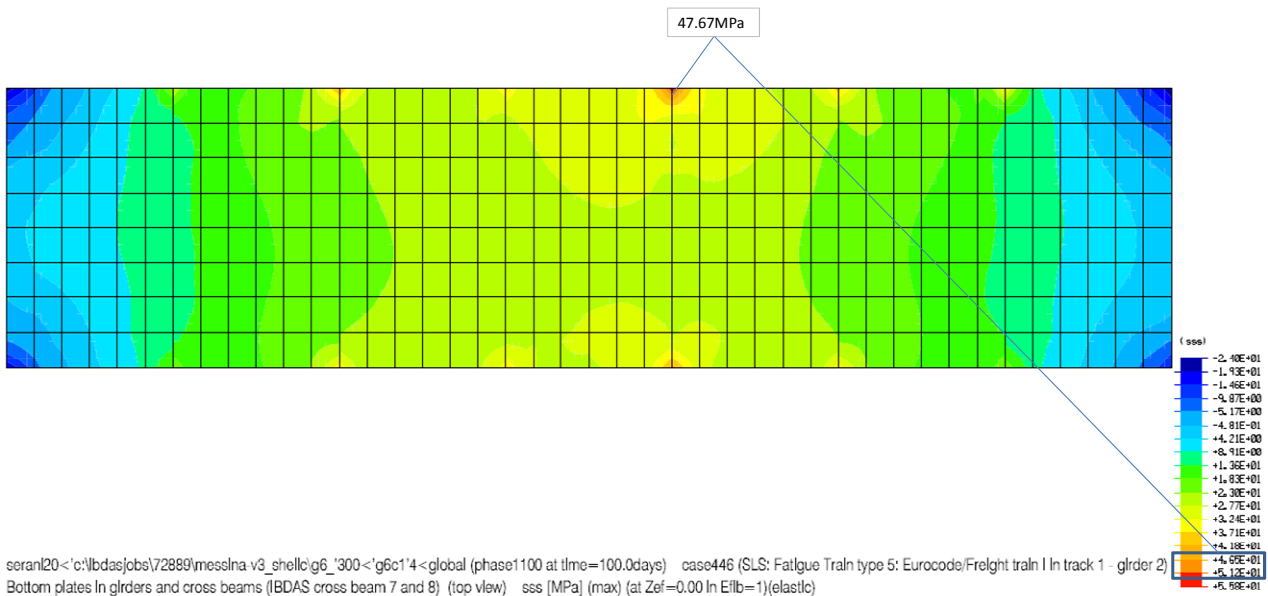


Figure 11-11 Stress time history plot for the point along line 1 on diaphragm 4 – EN5 train

As an example of the stress flow, the bottom plate of shell model for the load configuration maximizing the positive stress in correspondence of diaphragm 4 can be seen in Figure 11-12.



IBDAS V1.10-4 pc34001 c:\ibdas\jobs\72889\messina-v3\_shell\shelloutput\_girder

Figure 11-12 Stress flow (sss) in the bottom plates of the semi-local IBDAS model

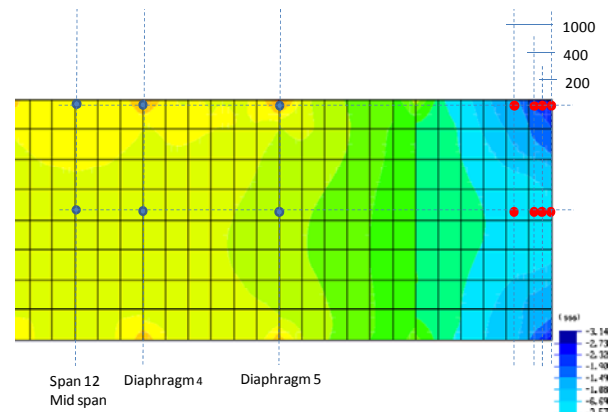
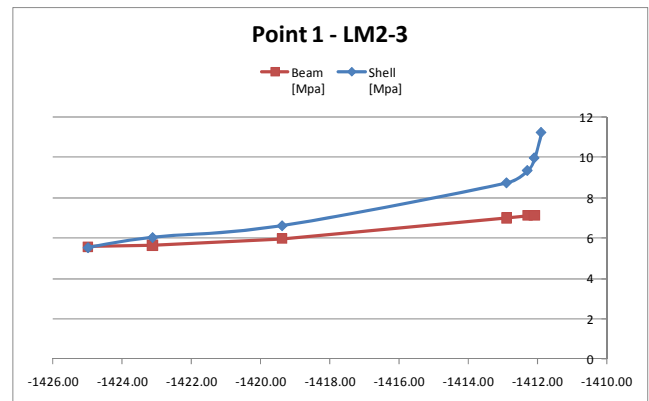
		<b>Ponte sullo Stretto di Messina</b> <b>PROGETTO DEFINITIVO</b>		
Specialist Technical Design Report, Annex		Codice documento PS0075_F0-ok.doc	Rev F0	Data 20/06/2011

In the same manner the results from the two models are compared considering LM2 vehicle 3, and the difference in stress range is calculated, see Table 11-5.

Table 11-5 Comparison of stress ranges between the beam and the shell model running LM2 vehicle 3. Railway girder bottom plate considered

Type	LM2		
	Shell [Mpa]	Beam [Mpa]	Deviation [%]
Location	s=-1425		
Point 1	5.5	5.6	<b>-0.87%</b>
Point 2	5.7	5.4	<b>6.29%</b>
Location	s=-1423.13		
Point 1	6.0	5.6	<b>6.87%</b>
Point 2	5.8	5.4	<b>5.72%</b>
Location	s=-1419.38		
Point 1	6.6	6.0	<b>10.65%</b>
Point 2	6.3	5.8	<b>9.19%</b>
Location	s=-1412.88		
Point 1	8.7	7.0	<b>24.68%</b>
Point 2	7.0	6.9	<b>1.37%</b>
Location	s=-1412.28		
Point 1	9.3	7.1	<b>31.11%</b>
Point 2	6.8	7.0	<b>-2.86%</b>
Location	s=-1412.08		
Point 1	10.0	7.2	<b>39.01%</b>
Point 2	6.8	7.1	<b>-4.08%</b>
Location	s=-1411.88		
Point 1	11.2	7.2	<b>55.72%</b>
Point 2	6.8	7.1	<b>-4.23%</b>

Location	s=-1412.08		
Point 1	9.2	7.2	<b>27.89%</b>

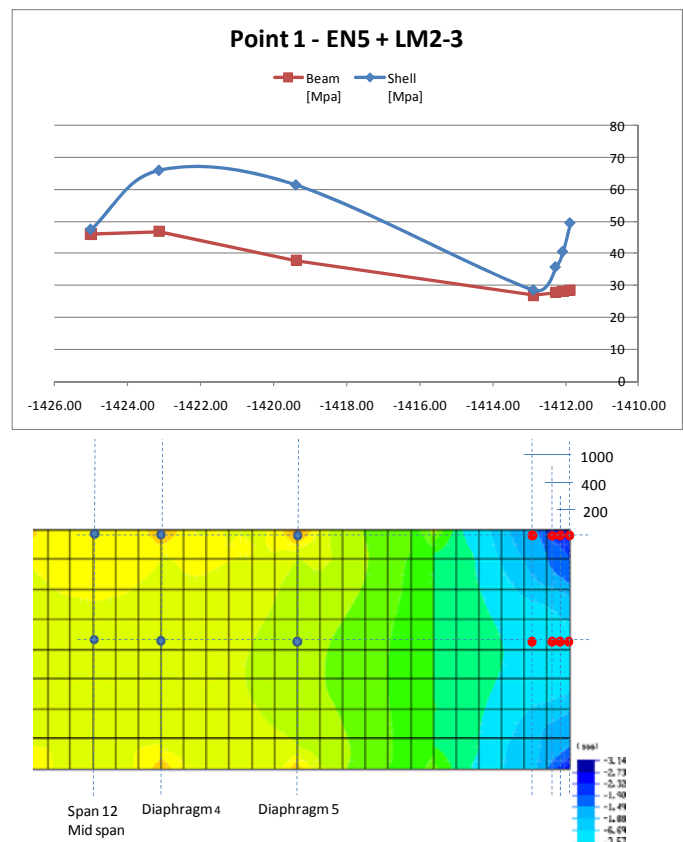


The stress ranges for the two load situations have been then summed up and the following total deviation is found, see Table 11-6.

**Table 11-6 Comparison of stress ranges between the beam and the shell model considering LM2 vehicle 3 and EN5 train. Railway girder bottom plate considered**

Type	EN5 + LM2		
	Shell [Mpa]	Beam [Mpa]	Deviation [%]
Location	s=-1425		
Point 1	47.4	46.1	<b>2.92%</b>
Point 2	45.1	45.8	<b>-1.51%</b>
Location	s=-1423.13		
Point 1	65.9	46.9	<b>40.47%</b>
Point 2	44.1	46.6	<b>-5.33%</b>
Location	s=-1419.38		
Point 1	61.3	37.9	<b>61.93%</b>
Point 2	40.1	37.6	<b>6.72%</b>
Location	s=-1412.88		
Point 1	28.4	27.0	<b>5.35%</b>
Point 2	25.0	26.8	<b>-6.52%</b>
Location	s=-1412.28		
Point 1	35.6	27.7	<b>28.43%</b>
Point 2	23.6	27.5	<b>-14.16%</b>
Location	s=-1412.08		
Point 1	40.4	28.1	<b>43.75%</b>
Point 2	23.3	27.9	<b>-16.69%</b>
Location	s=-1411.88		
Point 1	49.4	28.6	<b>73.06%</b>
Point 2	23.0	28.3	<b>-18.65%</b>

Location	s=-1412.08		
Point 1	35.0	28.1	<b>24.53%</b>



		<b>Ponte sullo Stretto di Messina</b> <b>PROGETTO DEFINITIVO</b>	
Specialist Technical Design Report, Annex		Codice documento PS0075_F0-ok.doc	Rev F0 Data 20/06/2011

Based on the results shown the charts representing the actual stress concentration factors at the various locations investigated are shown in Figure 11-13 where the detail next to the web and those next to the mid span are shown.

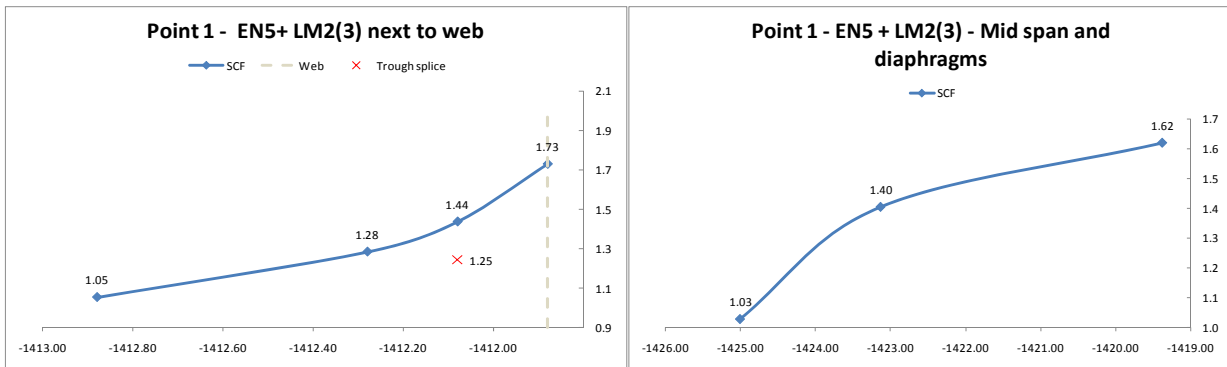


Figure 11-13 Stress concentration factors (SCF)

In the charts above it can be noticed that the trough splice detail has a SCF=1,25. This has been worked out as an average between the results in the upper gauss point and the lower one in order to match the trough splice location. The detail of the location of the trough splice in relation to the mesh element as well as the mesh dimension can be seen in the figure below.

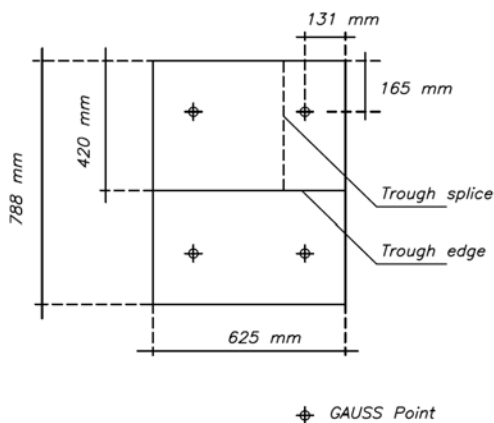


Figure 11-14 Shell elements, Gauss points location and their position relative to the trough splice

Further adjustments to the SCF have been performed in order to account for the position where the fatigue stresses are extrapolated in the global beam model. The fatigue verification of the various spans has been carried out using the stresses in the mid span and at 0.4 m from the cross girder web. This implies that the shell model stresses must be scaled against the beam stress at the said

		<b>Ponte sullo Stretto di Messina</b> <b>PROGETTO DEFINITIVO</b>		
Specialist Technical Design Report, Annex		<i>Codice documento</i> PS0075_F0-ok.doc	<i>Rev</i> F0	<i>Data</i> 20/06/2011

locations. Moreover the details where the stress concentration occurs are the ones in correspondence of the diaphragms next to the mid span and at the cross girder web. The structural details where the stress concentration factor has been taken into account are listed below:

- Bottom plate to diaphragm weld at the section in correspondence of the diaphragm next to the girder mid span
- Bottom plate to diaphragm weld at the section at the cross girder web
- Trough splice next to the plate edge at the shop joint

In Figure 11-15 the SCF scaled against the global beam stresses used in the fatigue verification (at the relevant location) are shown.

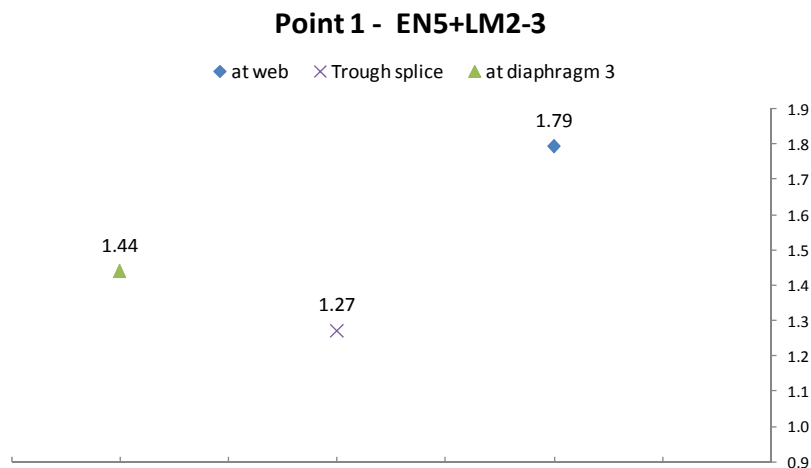


*Figure 11-15 Stress concentration factors (SCF) at the location of the fatigue verification*

Furthermore the SCF shown above will be lowered by the introduction of a local strengthening at the kink between the bottom plate and the inclined web.

For those girders where the strengthening at the cross girder is not necessary the trough splice detail presents utilization ratios which are always lower than the web to bottom plate detail throughout the bridge as the latter detail has been kept without weld improvement and therefore as class 80 MPa. Furthermore as it can be seen in Figure 11-21 and Figure 11-23 in section 11.3.3 where the strengthening is required the SCF at the trough splice is lower than one. Therefore in the chapter relative to the railway verification the trough splice details are omitted. The spans where local strengthening is not necessary have been found out to be spans 4 to 6, all the spans between 12 and 107 included, 113, 114 and 115. For these spans fatigue verification has been performed

		<b>Ponte sullo Stretto di Messina</b> <b>PROGETTO DEFINITIVO</b>		
Specialist Technical Design Report, Annex		<i>Codice documento</i> PS0075_F0-ok.doc	<i>Rev</i> F0	<i>Data</i> 20/06/2011

increasing the stress values by 1.79 at the cross girder web and 1.27 at the trough splice. In Appendix D the stress history plots and the bottom plate contour plots of longitudinal stresses for the load condition maximizing and minimizing the stress in the considered point are presented. Results are presented for those locations which affect the railway girder fatigue verification as shown in Figure 11-16.

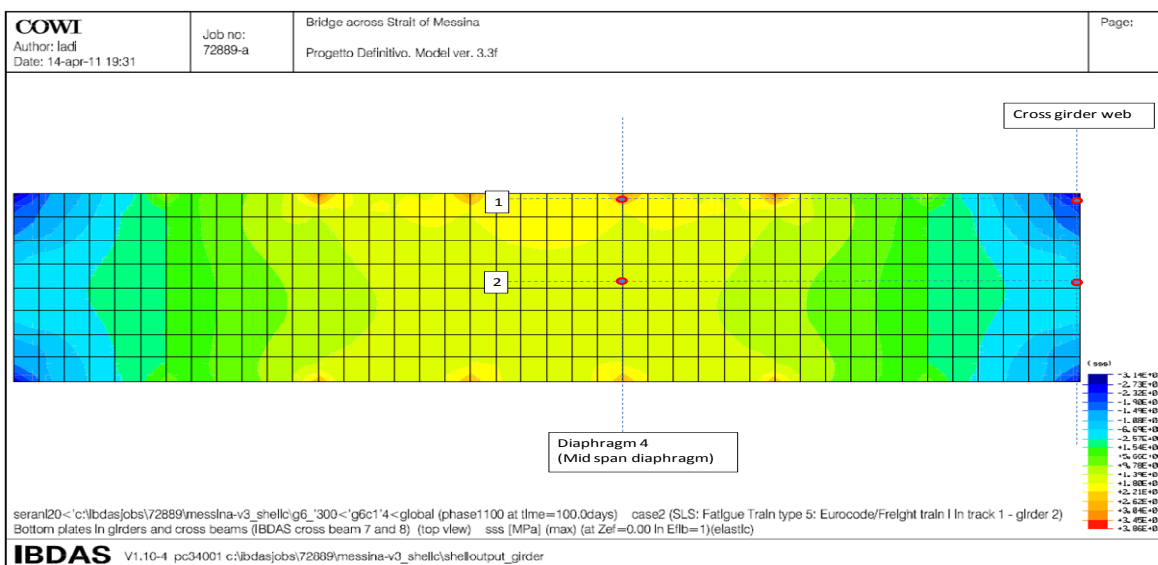


Figure 11-16 Locations where stress history plots and stress contour are presented in Appendix D

### 11.3.3 Determination of the strengthening thickness – ROBOT model

In order to fulfil the fatigue verification including the stress concentration a local strengthening has been implemented in the girder geometry. This comprises of a local thickening of a portion of bottom plate and inclined web for a width in longitudinal direction of 80 mm on each side of the diaphragm. The strengthening occurs in correspondence of the mid span diaphragms as well as at the cross girder web. The thickening considered varies between the main span girders and the side span and in general terms a thickening of 5 mm for bottom plates of 10 mm (which include the girder types CF1 and CF2) and 6 mm for bottom plates of 20 mm has been applied. The influence in the stress level due to the introduction of the local strengthening has been accounted for by a detail factor which has been determined by means of a ROBOT model that can be seen in Figure 11-17. The model comprises of 4 diaphragms and it takes account of global effects with boundary conditions applied to beam elements placed at the sides of the shell elements and connected to them by rigid links. The model is representative of span 12 and has been developed to compare

		<b>Ponte sullo Stretto di Messina</b> <b>PROGETTO DEFINITIVO</b>		
Specialist Technical Design Report, Annex		<i>Codice documento</i> PS0075_F0-ok.doc	<i>Rev</i> F0	<i>Data</i> 20/06/2011

the stress concentrations for a load situation where the EN5 train locomotive is positioned at  $s=1300$ . The aim of the model is to determine the stress variation from the unreinforced cross section to the strengthened one by means of a detailed model with fine meshing. As for the IBDAS semi local shell model also for the ROBOT model the stress points have been located right on the diaphragm/web and 165 mm away from the plate edge in the loaded side.

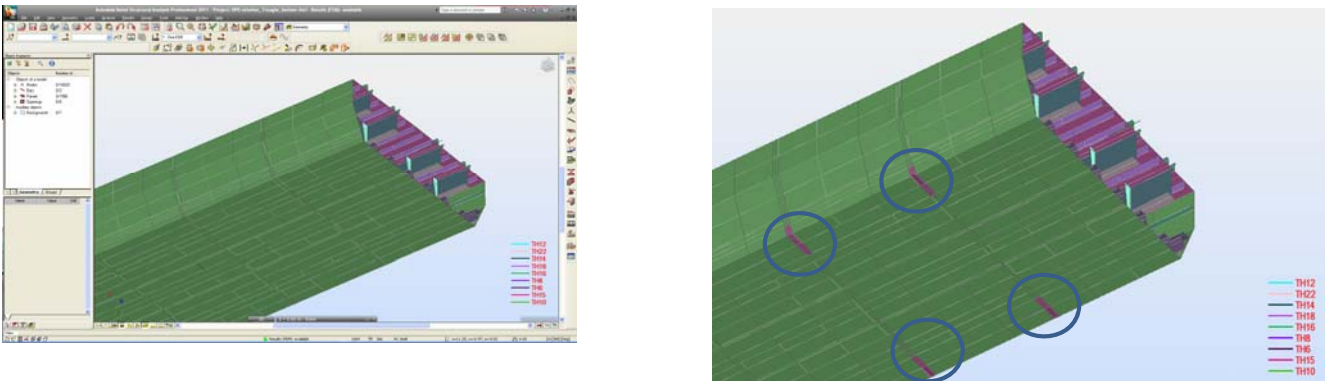


Figure 11-17 Robot model of span 12 – The figure to the right shows the locations of the strengthening

The longitudinal stress distribution used to determine the stress concentration with the reinforcement has been obtained by panel cuts as shown in Figure 11-18.

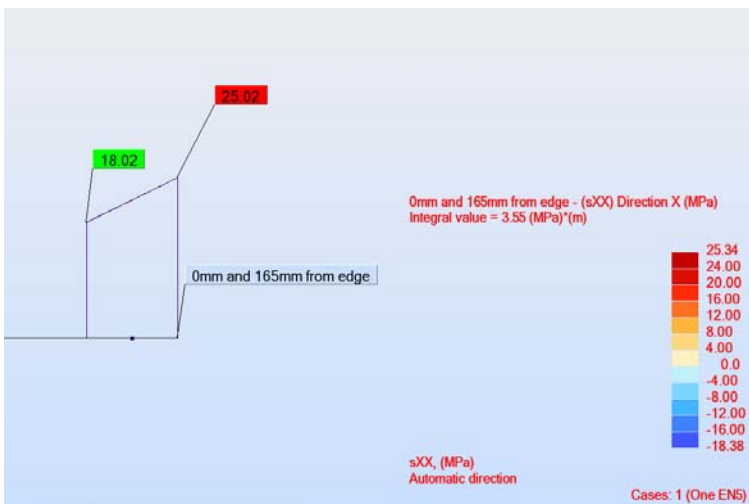


Figure 11-18 Stress distribution within the strengthening in the bottom plate – strengthened geometry

As seen in figure above the stress at 165mm from the edge is  $\sigma_{\text{reinf}} = 18.02\text{MPa}$ . Stresses are shown for the middle element layer and are presented as smoothed within the panel. To determine

		<b>Ponte sullo Stretto di Messina</b> <b>PROGETTO DEFINITIVO</b>	
Specialist Technical Design Report, Annex		Codice documento PS0075_F0-ok.doc	Rev    Data F0    20/06/2011

the detail factor for this reinforcement, the stress at the same locations is found for the unreinforced geometry. The longitudinal stresses distribution used to determine the stress concentration in the reference condition is shown in the figure below.

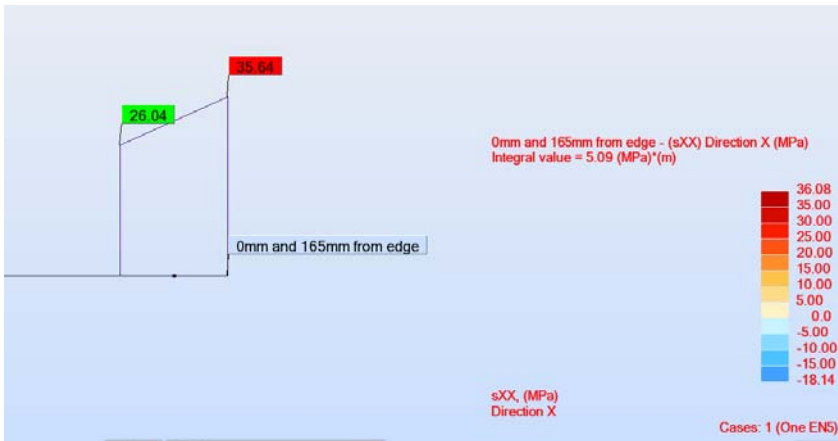


Figure 11-19 Stress distribution within the strengthening in the bottom plate – reference geometry

As seen in the figure above the stress 165mm from the edge is  $\sigma_{ref} = 26.04\text{MPa}$ . The detail factor is hereby determined to:

$$DF = \frac{\sigma_{ref}}{\sigma_{refinf}} = \frac{26.04}{18.02} = 1.45$$

In the same manner the assessment has been performed also for other thickening namely for 2 and 8 mm. The results can be seen in Figure 11-20.

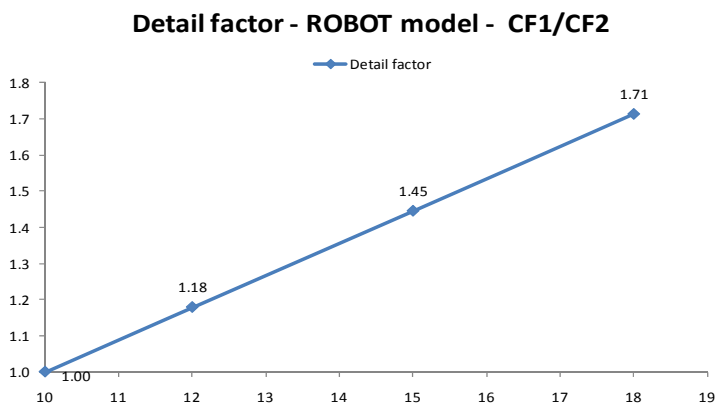


Figure 11-20 Detail factor to thickness relation. The reference condition is a 10 mm bottom plate as for CF1/CF2

		<b>Ponte sullo Stretto di Messina</b> <b>PROGETTO DEFINITIVO</b>		
Specialist Technical Design Report, Annex		<i>Codice documento</i> PS0075_F0-ok.doc	<i>Rev</i> F0	<i>Data</i> 20/06/2011

Adopting 5 mm thickening of a 10 mm bottom plate the following SCF have been derived taking the SCF values from Figure 11-15 divided by the detail factor shown in Figure 11-20.

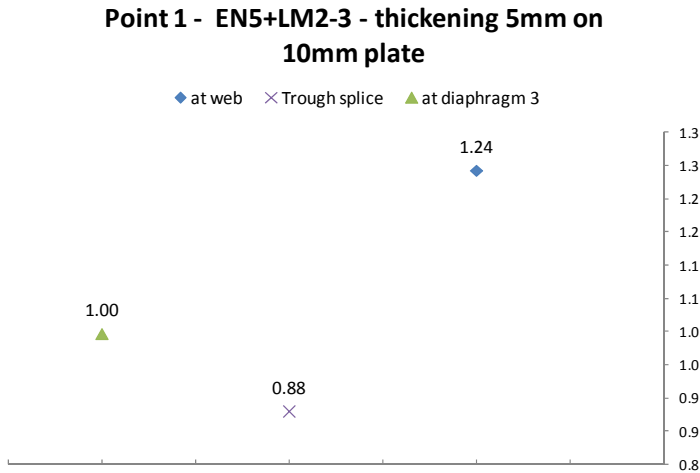


Figure 11-21 Stress concentration factor SCF used for the CF1 and CF2 girders

Similarly the same evaluation has been done for the bottom plate of 20 mm representative of the railway girder type CF6 whose utilisation ratio was the highest in the side span. The relation between the thickening and the detail factor can be found in the figure below.

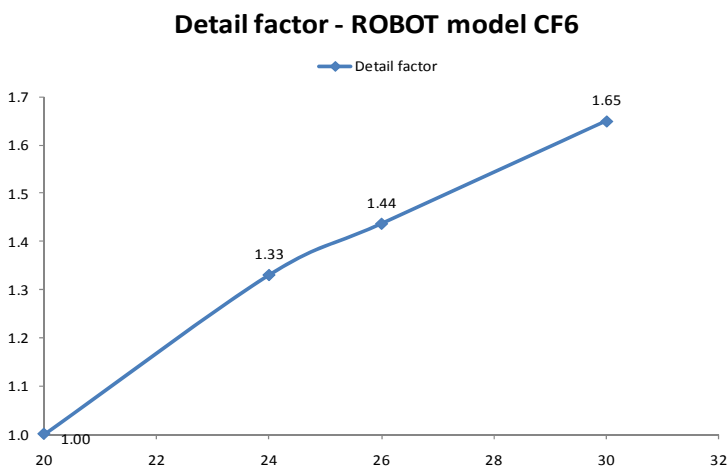


Figure 11-22 Detail factor to thickness relation The reference condition is a 10 mm bottom plate as for CF6

		<b>Ponte sullo Stretto di Messina</b> <b>PROGETTO DEFINITIVO</b>					
Specialist Technical Design Report, Annex		<i>Codice documento</i> PS0075_F0-ok.doc	<table border="1" style="width: 100%; border-collapse: collapse;"> <thead> <tr> <th style="text-align: left;"><i>Rev</i></th> <th style="text-align: left;"><i>Data</i></th> </tr> </thead> <tbody> <tr> <td>F0</td> <td>20/06/2011</td> </tr> </tbody> </table>	<i>Rev</i>	<i>Data</i>	F0	20/06/2011
<i>Rev</i>	<i>Data</i>						
F0	20/06/2011						

Adopting 6 mm thickening of a 20 mm bottom plate the following SCF have been derived taking the SCF values from Figure 11-15 divided by the detail factor shown in Figure 11-22.

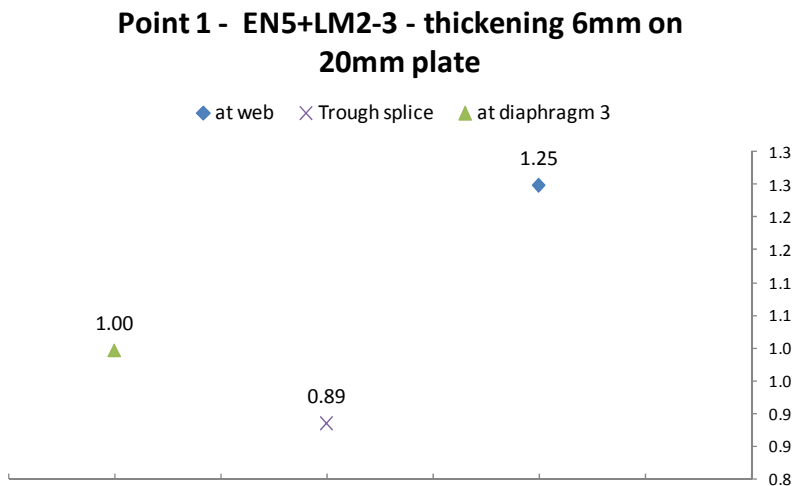


Figure 11-23 Stress concentration factor SCF used for the CF6 girder

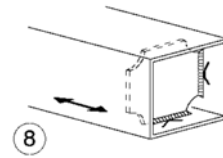
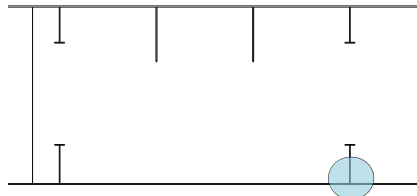
The spans where local strengthening is necessary the fatigue verification has been performed increasing the stress values by 1.25 only at the cross girder web to bottom plate connection as the other details presents SCF's lower or equal to one. No factor has been applied to the 60 m spans as the SCF decreases with the increase of the plate thickness as well as the safety is guaranteed by the high margin of the utilisation ratios: at the shop joint it is equal to 0.61 with class improved to 100 MPa giving allowance for a  $SCF=1/0.61=1.63$  and similarly at the mid span diaphragm the allowance becomes  $1/0.67=1.49$  yet considering the improvement of the weld.

#### 11.3.4 Conclusions

Through the FE analysis of the railway box girder it has been found which stress concentration factors are to be applied to the stresses for the fatigue verification, which is based of the IBDAS beam model. In the following a description of the details affected by the SCF is presented.

#### **BOTTOM PLATE TO DIAPHRAGM WELD – LOCATION 2**

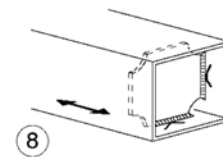
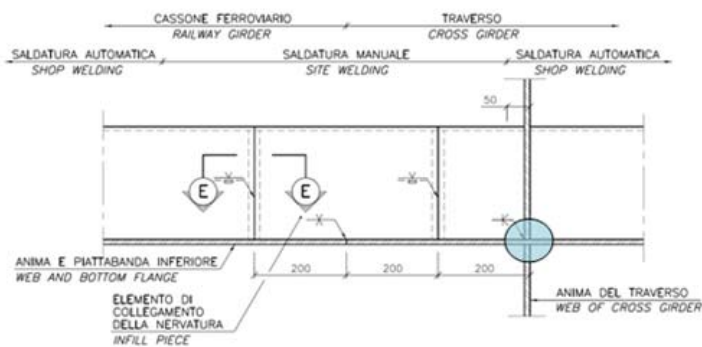
		<b>Ponte sullo Stretto di Messina</b> <b>PROGETTO DEFINITIVO</b>		
Specialist Technical Design Report, Annex		<i>Codice documento</i> PS0075_F0-ok.doc	<i>Rev</i> F0	<i>Data</i> 20/06/2011



$\Delta\sigma_c$	$\Delta\sigma_D$	$\Delta\sigma_L$
80.0	58.9	32.4

$\Delta\sigma_{cWI}$	$\Delta\sigma_{DWI}$	$\Delta\sigma_{LWI}$
100.0	73.7	40.5

### SHOP JOINT – CROSS GIRDER WEB TO BOTTOM PLATE WELD - LOCATION 3



$\Delta\sigma_c$	$\Delta\sigma_D$	$\Delta\sigma_L$
80.0	58.9	32.4

$\Delta\sigma_{cWI}$	$\Delta\sigma_{DWI}$	$\Delta\sigma_{LWI}$
100.0	73.7	40.5

The SCF of first detail “Bottom plate to diaphragm weld – location 2” equal to 1.44 has led to a local thickening of 5-6 mm along the whole bridge at exception of the 60 m spans. As a consequence the SCF of the same detail has lowered to 1.00.

The second and the third details, with a SCF of 1.27 and 1.79 respectively, do not require any improvement in the main span (12 to 107 included) as well as in the tower area (spans 4, 5, 6, 113, 114 and 115).

For all the other spans a local improvement has been developed leading to a reduction of the SCF to 0.89 - 1.00 for the trough splice detail and 1.24-1.25 for the cross girder web to bottom plate weld.

		<b>Ponte sullo Stretto di Messina</b> <b>PROGETTO DEFINITIVO</b>		
Specialist Technical Design Report, Annex		<i>Codice documento</i> PS0075_F0-ok.doc	<i>Rev</i> F0	<i>Data</i> 20/06/2011

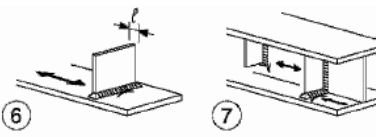
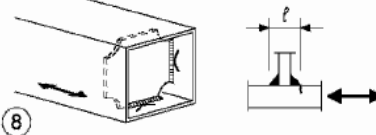
## 11.4 Fatigue Detail Categories

Each welded detail has been classified in accordance to the EN 1993-1-9:2005 and EN 1993-2:2006.

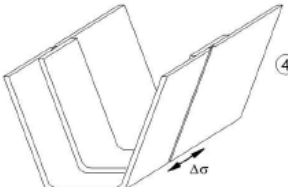
### 11.4.1 Roadway and railway bottom plate details

In the calculations only the most onerous for the fatigue verification have been considered, namely:

1. The connection of the diaphragm to bottom plate. The weld corresponds to detail category 80 (EN1993-1-9 Table 8.4, detail no.8)

80	$t \leq 50\text{mm}$	
71	$50 < t \leq 80\text{mm}$	

2. The bottom plate trough splices in correspondence of the erection joint and the shop joint (EN1993-1-9 Table 8.8, detail no.4).

71	
----	--------------------------------------------------------------------------------------

### 11.4.2 Roadway deck details

The fatigue analyses of the local actions in points A, B, C, D, E, F has been performed using a local IBIDAS model of the orthotropic steel deck, refer to General Design Principles for Suspended Deck section 10.9.2 for more information.

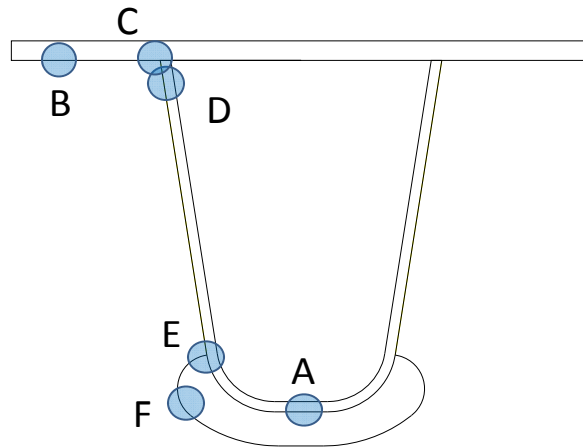
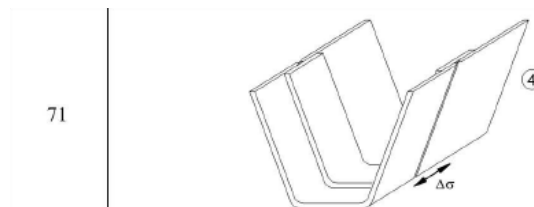


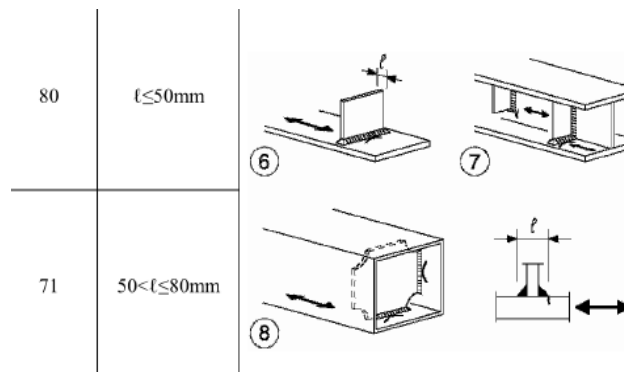
Figure 11-24 Roadway orthotropic deck details

The fatigue assessment concerns the following details:

- Point A represents the full penetration butt weld in trough with steel backing plate. The weld corresponds to detail category 71, see EN1993-1-9 Table 8.8, detail no.4.

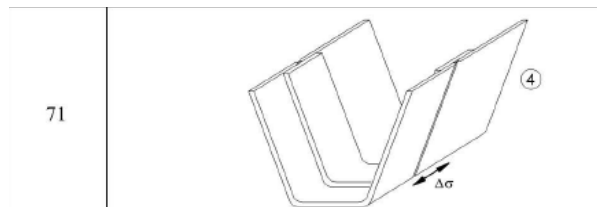


- Point B represents the deck connected to the diaphragm. The weld corresponds to detail category 80, see EN1993-1-9 Table 8.4, detail no.8.

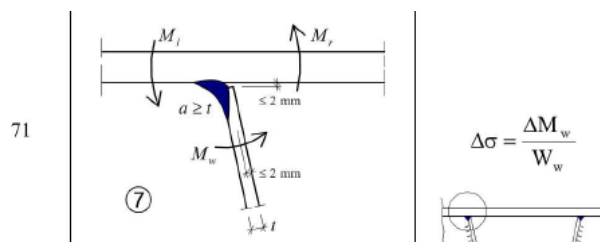


		<b>Ponte sullo Stretto di Messina</b> <b>PROGETTO DEFINITIVO</b>					
Specialist Technical Design Report, Annex		<i>Codice documento</i> PS0075_F0-ok.doc	<table border="1" style="width: 100%;"> <tr> <td style="width: 50%;"><i>Rev</i></td> <td style="width: 50%;"><i>Data</i></td> </tr> <tr> <td>F0</td> <td>20/06/2011</td> </tr> </table>	<i>Rev</i>	<i>Data</i>	F0	20/06/2011
<i>Rev</i>	<i>Data</i>						
F0	20/06/2011						

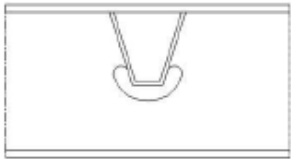
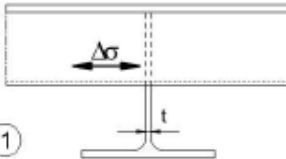
3. Point C represents the continuation in the plate of the limitation due to the trough splice; this is thus taking place only at the structural joints (erection and shop). The detail category must then fulfil the same limitation as for point A. External to the structural joints it represents also the sections where the longitudinal fillet weld of the trough intersects a transverse full penetration butt weld splice of the deck plate and a fatigue detail 80 is prescribed, see EN1993-1-9 Table 8.3, detail no.9. In the latest configuration being a shop weld the category might be increased to 112 MPa thus becoming less critical than detail B and therefore it has never been considered.



4. Point D represents the weld connecting deck plate to trough web. Being a partial penetration weld, an additional parasite bending moment becomes present due to the compression in the web of the trough and the eccentricity of the weld. This detail is only subjected to local effects. The weld corresponds to a detail category 71, see EN1993-1-9 Table 8.8, detail no.7.



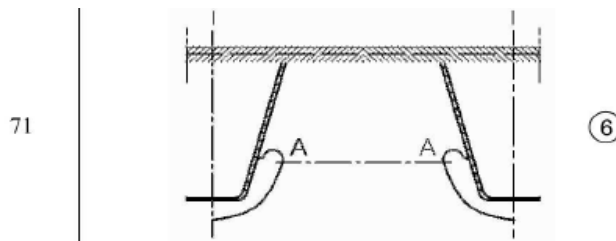
5. Point E represents the connection between the trough and the cut out in the diaphragm. As the diaphragm thickness is 15mm the weld corresponds to detail category 71, see EN1993-1-9 Table 8.8, detail no.1.

80	$t \leq 12\text{mm}$		
71	$t > 12\text{mm}$		

Point F represents one end of the critical section in the diaphragm due to cut outs. The tooth plate at the diaphragm is only subject to stresses due to local roadway loads and being not

		<b>Ponte sullo Stretto di Messina</b> <b>PROGETTO DEFINITIVO</b>		
Specialist Technical Design Report, Annex		<i>Codice documento</i> PS0075_F0-ok.doc	<i>Rev</i> F0	<i>Data</i> 20/06/2011

affected by other global effects such as the railway girder load. Thus it is only verified according to the unlimited life method. The same detail has been also verified at the cross girder web and the verification has also included the combined effects of the local wheel load and the global railway load.



Points A and D have been checked at specific points between two diaphragms as the results at point A have been used to optimise the trough splice location whereas point D must be fulfilled at any location between diaphragms; for more information see the local roadway FE-model in the document General Design Principles for Suspended Deck, section 10.9.2. Points B, E and F have been checked only at the location of the diaphragms.

### 11.4.3 Railway deck details

The fatigue analyses of the local actions of points WA and WB has been performed using a local IBDAS model of the T stiffener including the effective top plate, refer to General Design Principles for Suspended Deck 10.9.4.

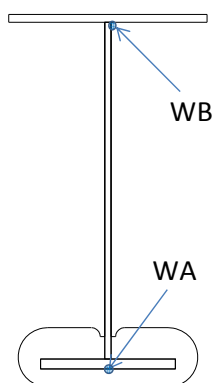


Figure 11-25 Railway orthotropic deck details

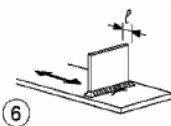
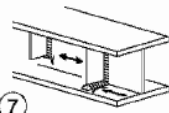
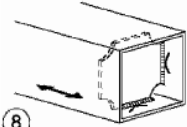
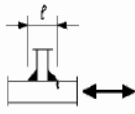
The fatigue assessment concerns the following details in proximity of the structural joints:

		<b>Ponte sullo Stretto di Messina</b> <b>PROGETTO DEFINITIVO</b>					
Specialist Technical Design Report, Annex		<i>Codice documento</i> PS0075_F0-ok.doc	<table border="1" style="width: 100%; border-collapse: collapse;"> <tr> <td style="width: 50%;"><i>Rev</i></td> <td style="width: 50%;"><i>Data</i></td> </tr> <tr> <td>F0</td> <td>20/06/2011</td> </tr> </table>	<i>Rev</i>	<i>Data</i>	F0	20/06/2011
<i>Rev</i>	<i>Data</i>						
F0	20/06/2011						

- Point WA represents the longitudinal fillet weld with a cope hole height not greater than 60 mm. The weld corresponds to detail category 71, see EN1993-1-9 Table 8.2, detail no.9.



- Point WB represents the top of the stiffener web connected to the either the main diaphragms or the intermediate diaphragms. Detail category 80, see EN1993-1-9 Table 8.4, detail no.8.

80	$t \leq 50\text{mm}$	 
71	$50 < t \leq 80\text{mm}$	 

#### LOCAL FE-MODEL OF SUPPORT OF T-BEAMS

A local FE-model is constructed with the purpose of verifying the fatigue stresses in the support of T-beams in the railway girder. The model consists of one T-beam along with a part of the deck plate and diaphragm. The applied load is a bogie load from train EN5 with a distance of 1.8m between the axles. The bogie load is placed in three different positions investigating the maximum stress level in the 15mm diaphragm. The largest stress level in the diaphragm is obtained by applying one axle directly over the centre diaphragm and two axles symmetrically on each side.

In Figure 11-26 a stress plot is shown of the von Mises stresses for the load case described above.

		<b>Ponte sullo Stretto di Messina</b> <b>PROGETTO DEFINITIVO</b>		
Specialist Technical Design Report, Annex		<i>Codice documento</i> PS0075_F0-ok.doc	<i>Rev</i> F0	<i>Data</i> 20/06/2011

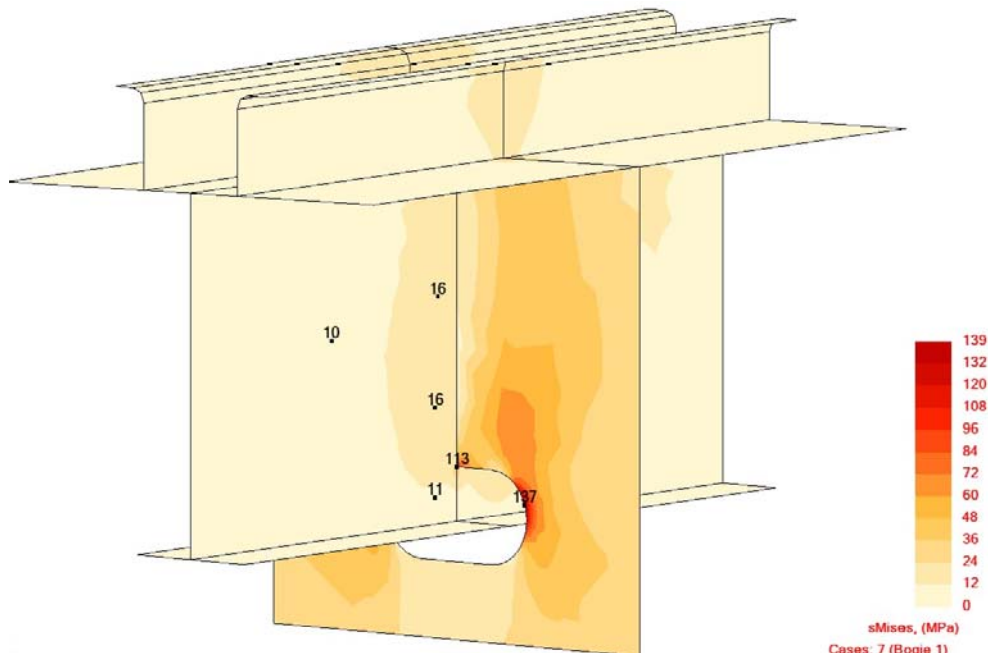


Figure 11-26 Stress plot of von Mises stresses for the diaphragm and T-beam

In the connection between the web of the T-beam and the diaphragm the von Mises stress reaches a peak level of 113MPa. Due to the geometry a very local stress concentration occurs with the peak value for the normal stress in the transverse direction located where the diaphragm is connected to the web of the T-beam. The layout of the detail will be further investigated in Progetto Esecutivo where also fatigue tests will be carried out for the detail.

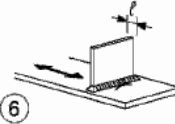
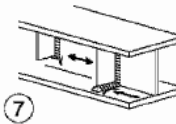
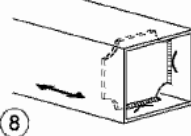
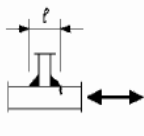
The rounding in the cut out in the diaphragm has a maximum von Mises stress of 137MPa and corresponds to detail category 125. The compression stresses in the point can be reduced for the non-welded detail according to EN 1993-1-9, clause 7.2 and the stress level is acceptable with respect to fatigue.

#### 11.4.4 Cross girder details

In the following calculations only the most onerous for the fatigue verification have been considered, namely:

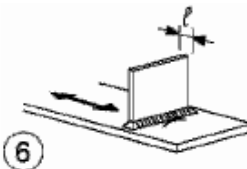
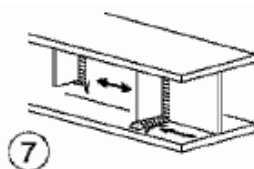
1. Welded connection of the girder diaphragm to the top plate, bottom plate or the web. The weld corresponds to detail category 80, see EN1993-1-9 Table 8.4, detail no.8 .

		<b>Ponte sullo Stretto di Messina</b> <b>PROGETTO DEFINITIVO</b>					
Specialist Technical Design Report, Annex		<i>Codice documento</i> PS0075_F0-ok.doc	<table border="1" style="width: 100%; border-collapse: collapse;"> <tr> <td style="width: 50%;"><i>Rev</i></td> <td><i>Data</i></td> </tr> <tr> <td>F0</td> <td>20/06/2011</td> </tr> </table>	<i>Rev</i>	<i>Data</i>	F0	20/06/2011
<i>Rev</i>	<i>Data</i>						
F0	20/06/2011						

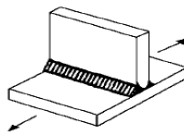
80	$t \leq 50\text{mm}$	 
71	$50 < t \leq 80\text{mm}$	 

### 11.4.5 Weld Improvement

Verification of the road, rail and cross girders requires that some of the weld connections shall be improved by grinding the toe smooth. The connections of the girder diaphragm to the top plate, bottom plate or the web correspond to detail category 80 according to EN1993-1-9 Table 8.4, detail no.8.

80	$t \leq 50\text{mm}$	 
----	----------------------	--------------------------------------------------------------------------------------------------------------------------------------------------------------------------

This weld can however be improved by grinding the toe smooth and thereby get an increased detail category of 100 according to "Recommendations for Fatigue Design of Welded Joints and Components", International Institute of Welding (IIW), doc. XIII-2151-07/XV-1254-07, May 2007.

511		Transverse non-load-carrying attachment, not thicker than main plate K-butt weld, toe ground Two sided fillets, toe ground Fillet weld(s), as welded thicker than main plate	100 100- 80 71
-----	-------------------------------------------------------------------------------------	------------------------------------------------------------------------------------------------------------------------------------------------------------------------------------------	-------------------------

		<b>Ponte sullo Stretto di Messina</b> <b>PROGETTO DEFINITIVO</b>		
Specialist Technical Design Report, Annex		<i>Codice documento</i> PS0075_F0-ok.doc	<i>Rev</i> F0	<i>Data</i> 20/06/2011

#### 11.4.6 Verification of Cross Girder

Table 11-7 shows the highest utilisation ratios in top and bottom plate for each cross girder and the associated damage according to the Miner's sum.

Table 11-7 Summary of fatigue verifications, cross girder

Section	s-coord (IBDAS)	Type	Method	Bottom plate	Top plate
27	-990	T1	U.L.: $\Delta\sigma^*\gamma_{MF}/\Delta\sigma_D$	0.998	0.971
			Miner: $\sum n_i/N_i + 0.05$	0.322	0.258
8	-1560	T1	U.L.: $\Delta\sigma^*\gamma_{MF}/\Delta\sigma_D$	0.990	0.978
			Miner: $\sum n_i/N_i + 0.05$	0.299	0.262
7	-1590	T3	U.L.: $\Delta\sigma^*\gamma_{MF}/\Delta\sigma_D$	0.888	0.852
			Miner: $\sum n_i/N_i + 0.05$	0.188	0.154
6	-1620	T4b	U.L.: $\Delta\sigma^*\gamma_{MF}/\Delta\sigma_D$	0.789	0.708
			Miner: $\sum n_i/N_i + 0.05$	0.119	0.093
5	-1680	T4a	U.L.: $\Delta\sigma^*\gamma_{MF}/\Delta\sigma_D$	0.766	0.610
			Miner: $\sum n_i/N_i + 0.05$	0.113	0.067
4	-1710	T3	U.L.: $\Delta\sigma^*\gamma_{MF}/\Delta\sigma_D$	0.870	0.757
			Miner: $\sum n_i/N_i + 0.05$	0.172	0.110
3	-1740	T1	U.L.: $\Delta\sigma^*\gamma_{MF}/\Delta\sigma_D$	0.860	0.742
			Miner: $\sum n_i/N_i + 0.05$	0.168	0.105
2	-1770	T6	U.L.: $\Delta\sigma^*\gamma_{MF}/\Delta\sigma_D$	0.585	0.694
			Miner: $\sum n_i/N_i + 0.05$	0.066	0.082
1	-1817.75	T7	U.L.: $\Delta\sigma^*\gamma_{MF}/\Delta\sigma_D$	0.995	0.962
			Miner: $\sum n_i/N_i + 0.05$	0.289	0.252

#### 11.4.7 Verification of Railway Girder

The summary of the most onerous results of each element is listed in Table 11-9. It summarizes all the analysed spans at the main span, the tower location and at the side spans and consider the construction details with the highest utilization ratio based on the unlimited life method.

		<b>Ponte sullo Stretto di Messina</b> <b>PROGETTO DEFINITIVO</b>		
		Specialist Technical Design Report, Annex	Codice documento PS0075_F0-ok.doc	Rev F0

**Table 11-8 Summary of fatigue verifications, railway girder**

	detail	Bottom plate			Top Plate		
		Erection joint	At diaphragm	Shop joint	At diaphragm	Between diaphragm	Bottom of T beam
Main - spans 39, 28, 19, 12, 11, 10, 9, 8, 7 and 6	location	1	2	3	1 or 2	1 & 2	1
	span / ref	09/8.7.1.1	19/8.3.1.2	09/8.7.1.3	06/8.10.2.1	06/8.10.2.2	06/8.10.2.3
	$\Delta\sigma^*\gamma_{MF}/\Delta\sigma_D$	0.991	0.962	0.987	0.980	0.996	0.868
	$\Sigma n_i/N_i + 0.05$	0.579	0.671	0.542	0.370	0.357	0.245
Tower - span 5	location	1	2	3	3	3	1
	ref	05/8.11.1.1	05/8.11.1.2	05/8.11.1.3	05/8.11.2.4	05/8.11.2.5	05/8.11.2.3
	$\Delta\sigma^*\gamma_{MF}/\Delta\sigma_D$	0.761	0.840	0.765	0.838	0.877	0.710
	$\Sigma n_i/N_i + 0.05$	0.150	0.230	0.137	0.167	0.183	0.112
Side - spans 0, 1, 2, 3 and 4	location	1	2	3	1 or 2	3	3
	span / ref	02/8.14.1.1	03/8.13.1.1	02/8.14.1.3	01/8.15.2.1	00/8.16.2.4	00/8.16.2.5
	$\Delta\sigma^*\gamma_{MF}/\Delta\sigma_D$	0.988	0.959	0.880	0.991	0.995	0.909
	$\Sigma n_i/N_i + 0.05$	0.454	0.390	0.277	0.395	0.335	0.261

#### 11.4.8 Verification of Roadway Girder

The summary of the most onerous results of each element is listed in Table 11-9. It summarizes all the analysed spans at the main span, the tower location and at the side spans and consider the construction details with the highest utilization ratio based on the unlimited life method.

**Table 11-9 Summary of fatigue verifications, roadway girder**

	detail	Bottom plate			Top plate		
		Erection joint	At diaphragm	Shop joint	Point C	Point A	Point E
Main - spans 39, 28, 19, 12, 11, 10, 9, 8, 7 and 6	location	1	2	3	1 & 2	3	1 & 2
	span / ref	11/7.5.1.1	12/7.4.1.2	12/7.4.1.3	09/7.7.2.2	09/7.7.2.11	09/7.7.2.6
	$\Delta\sigma^*\gamma_{MF}/\Delta\sigma_D$	0.986	0.970	0.994	0.777	0.772	0.826
	$\Sigma n_i/N_i + 0.05$	0.420	0.417	0.526	0.065	0.188	0.096
tower - span 5	location	NA	2	NA	NA	NA	NA
	ref		7.11				
	$\Delta\sigma^*\gamma_{MF}/\Delta\sigma_D$		0.572				
	$\Sigma n_i/N_i + 0.05$		0.050				
side - spans 1, 2, 3 and 4	location	1	2	3	3	3	3
	span / ref	02/7.14.1.1	04/7.12.1.2	02/7.14.1.3	02/7.14.2.8	01/7.15.2.11	01/7.15.2.12
	$\Delta\sigma^*\gamma_{MF}/\Delta\sigma_D$	0.974	0.959	0.998	0.812	0.792	0.841
	$\Sigma n_i/N_i + 0.05$	0.342	0.317	0.403	0.073	0.194	0.100

		<b>Ponte sullo Stretto di Messina</b> PROGETTO DEFINITIVO		
Specialist Technical Design Report, Annex		<i>Codice documento</i> PS0075_F0-ok.doc	<i>Rev</i> F0	<i>Data</i> 20/06/2011

#### 11.4.9 Verification of Hanger Anchorage

The local FE-model of the hanger anchorage, shown in Figure 11-27 is used to determine the local fatigue stresses in the hanger anchorage. The applied force range from the hanger reaction and rotation range is obtained from the global IBDAS model. The hanger force range is applied to the pinhole in three points, as a simultaneous application of traffic and railway load. The load contribution from the railway is determined as a passage of an EN5 train, in the track closest to the considered hanger anchorage and the contribution from the road traffic taken as load model 2, vehicle 3. Four different points are checked for fatigue stresses, as illustrated in Figure 11-27.

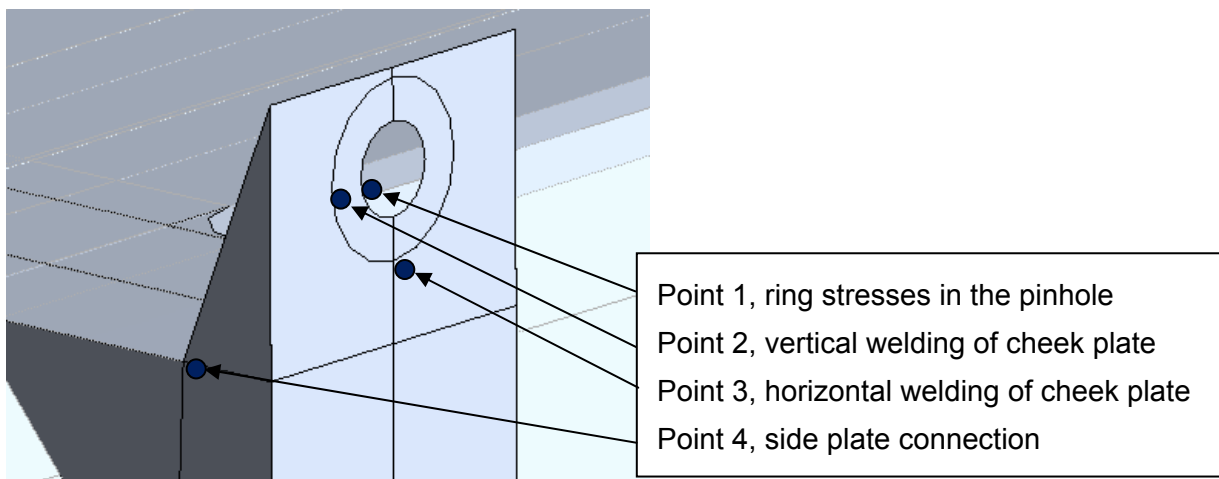


*Figure 11-27 Location of stress points for fatigue evaluation of hanger anchorage*

To evaluate the stresses in point 1 to 3, a plot of von Mises stresses in the anchor plate is shown in Figure 11-28.

		<b>Ponte sullo Stretto di Messina</b> <b>PROGETTO DEFINITIVO</b>	
Specialist Technical Design Report, Annex		Codice documento PS0075_F0-ok.doc	Rev    Data F0     20/06/2011

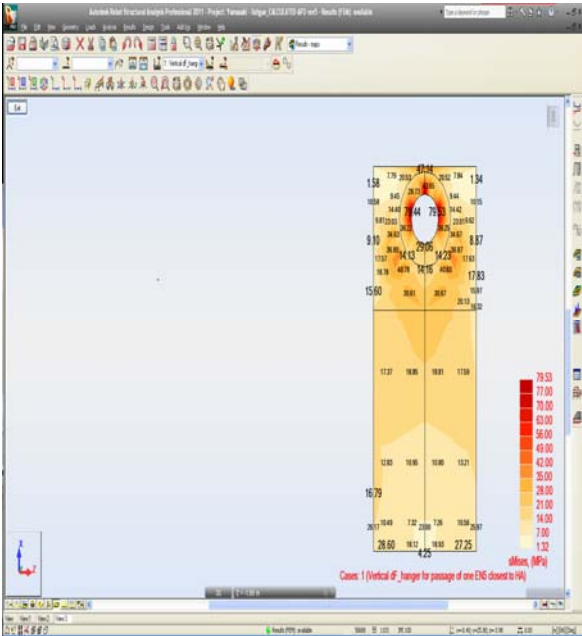


Figure 11-28 von Mises stresses for fatigue in anchor plate

To evaluate the stresses in point 4, a plot of von Mises stresses in the side plate is shown in Figure 11-29.

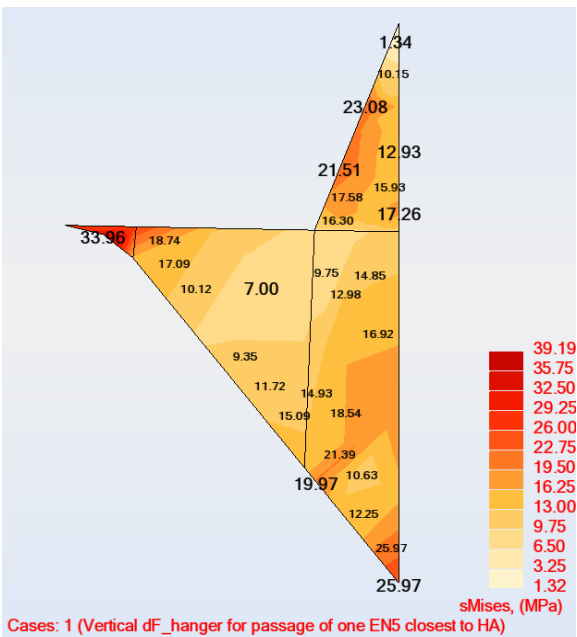


Figure 11-29 von Mises stresses for fatigue in side plate

		<b>Ponte sullo Stretto di Messina</b> <b>PROGETTO DEFINITIVO</b>		
Specialist Technical Design Report, Annex		<i>Codice documento</i> PS0075_F0-ok.doc	<i>Rev</i> F0	<i>Data</i> 20/06/2011

#### 11.4.10 Articulation system: X-Structure

Various sections of the X-structure have been verified: they comprise all the struts/ties forming the support arrangement at tower as shown in the figure below. The main scope of the structure is to limit the large longitudinal and transversal deformation of the bridge mainly due to non-man generated actions.

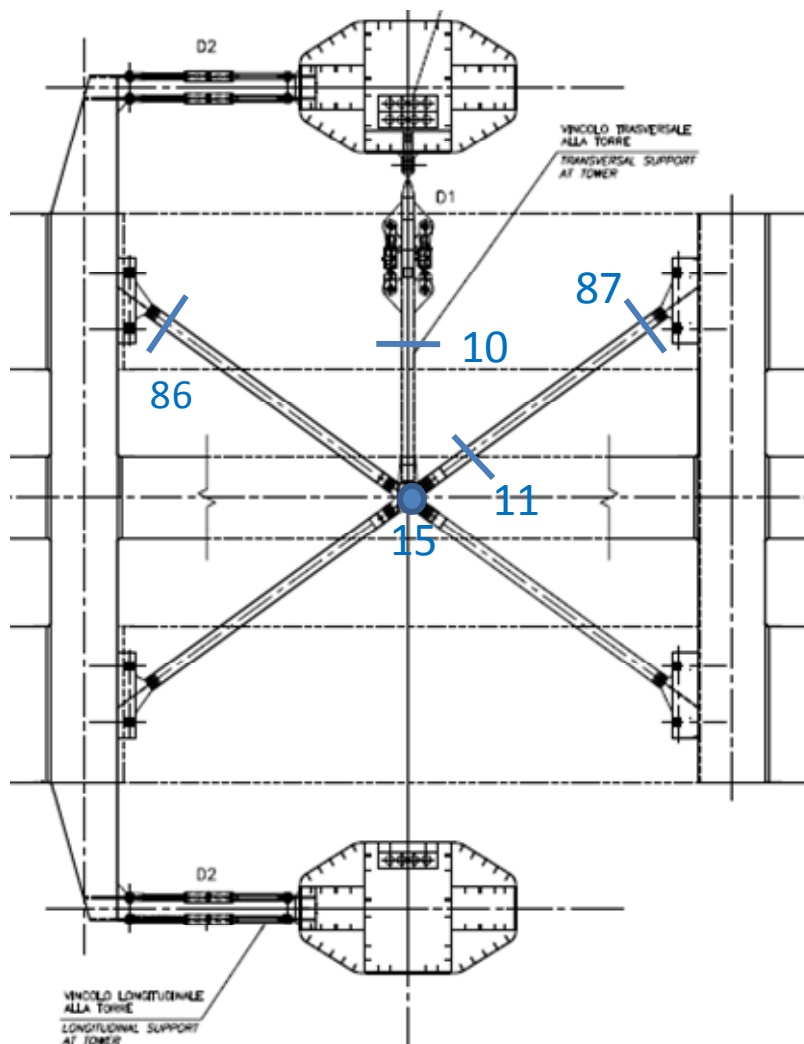


Figure 11-30 Sections to be verified in the X-structure

The Miner summation of damage as well as wind induced effects have been investigated and all points were acceptable and below an utilisation ratio of 1.

		<b>Ponte sullo Stretto di Messina</b> <b>PROGETTO DEFINITIVO</b>		
Specialist Technical Design Report, Annex		<i>Codice documento</i> PS0075_F0-ok.doc	<i>Rev</i> F0	<i>Data</i> 20/06/2011

## 12 Special Design Investigations

The following load situations have been considered as special design investigations in the ultimate limit state (ULS).

- Hanger replacement
- Hanger rupture (ALS in the ULS load combinations)

All results presented in the report are a preliminary investigation made based on the global IBIDAS beam-model version 3.3.

### 12.1 Hanger Replacement

The replacement operation of hangers has been verified using ADVERS in a few locations of the bridge. A replacement operation of hangers without using temporary hangers has shown only to be feasible at locations in the main span without affecting the deck structure and cause structural damage. The result of replacing Hanger 5 at the drop-in span is given in Figure 12-1 showing severe problems in the roadway girder. Since also such a replacement strategy will cause an adverse loading effect in the adjacent hangers a replacement strategy using temporary hangers have been found more feasible and are adopted for the Messina Bridge.

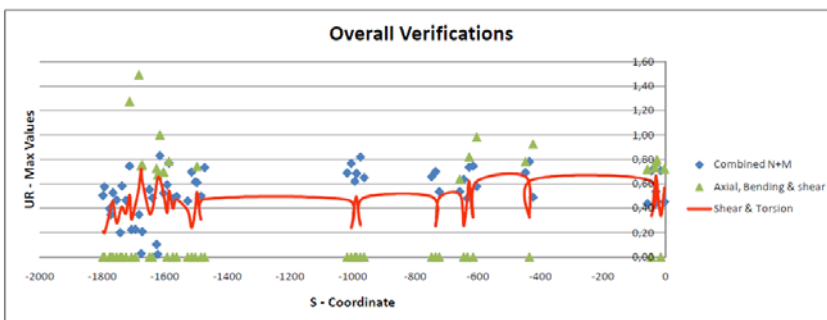
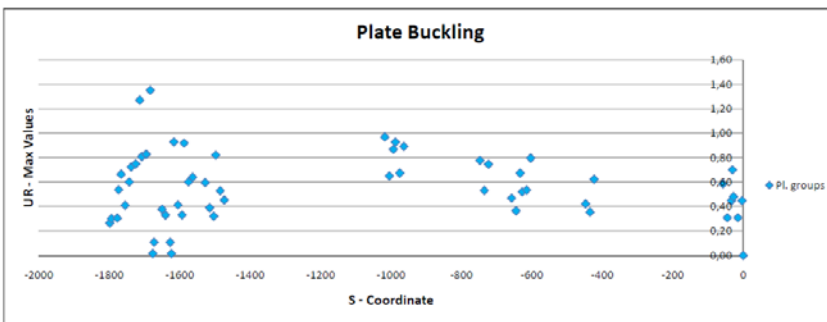
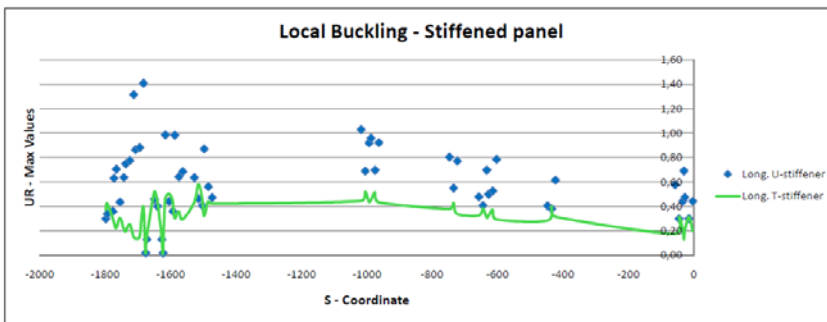
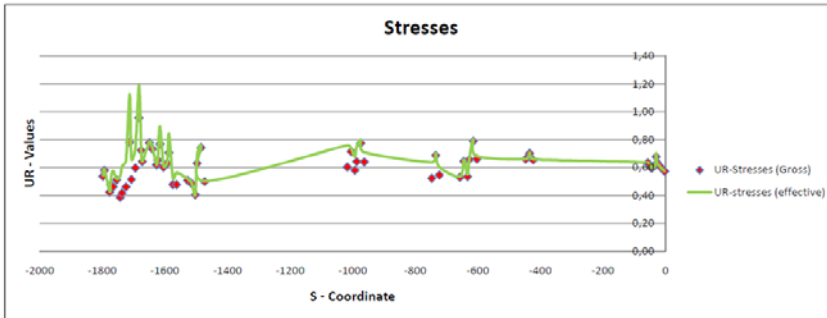


Figure 12-1 ADVERS results for roadway girder - replacement of hanger 5

		<b>Ponte sullo Stretto di Messina</b> PROGETTO DEFINITIVO	
Specialist Technical Design Report, Annex	<i>Codice documento</i> PS0075_F0-ok.doc	<i>Rev</i> F0	<i>Data</i> 20/06/2011

## 12.2 Hanger Rupture

The analysis in IBDAS has been done in the dynamic region assuming instant rupture of both hangers simultaneously. The effect of this for the suspended deck has been verified using the spreadsheet ADVERS and sectional forces calculated in the global IBDAS model.

For the verification of the suspended deck structure during the hanger rupture a few different locations has been selected in the side span and around the towers, see Figure 12-2.

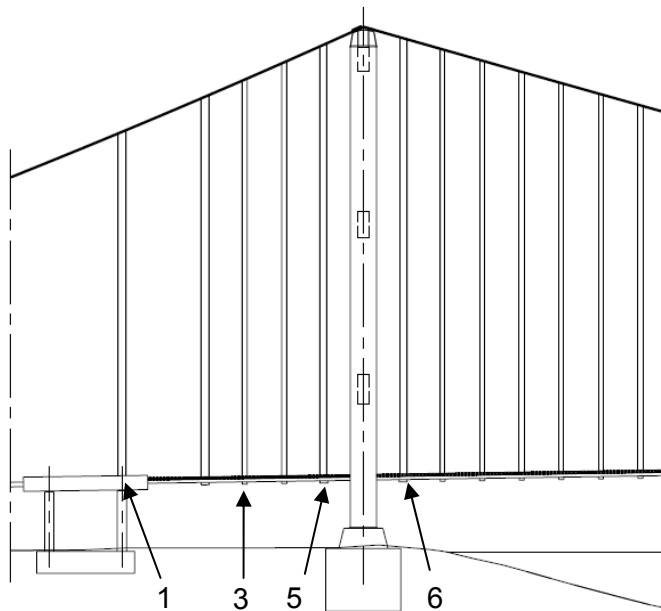


*Figure 12-2 Location of hangers considered for rupture*

This location has been chosen due to that the largest dynamic effects occur at this location. Most critical is the tie-down hanger and the hangers around the 60 m drop-in span, as the girder span will increase significantly after rupture. Hanger rupture is most severe for the roadway girder, and the result for hanger 1 is given in Figure 12-3.

		<b>Ponte sullo Stretto di Messina</b> <b>PROGETTO DEFINITIVO</b>		
Specialist Technical Design Report, Annex		Codice documento PS0075_F0-ok.doc	Rev F0	Data 20/06/2011

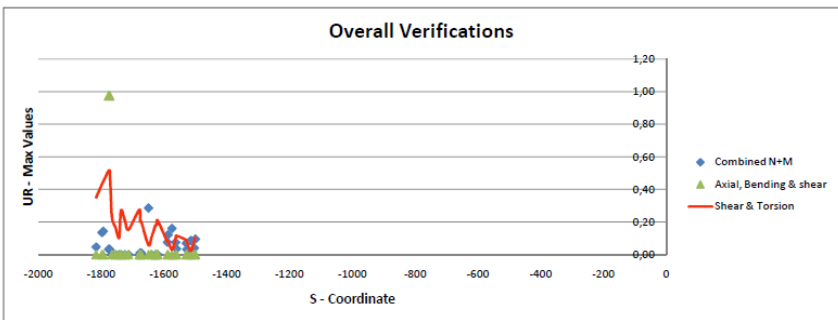
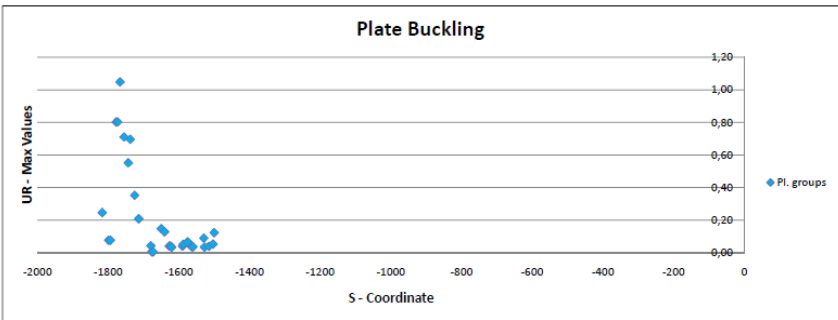
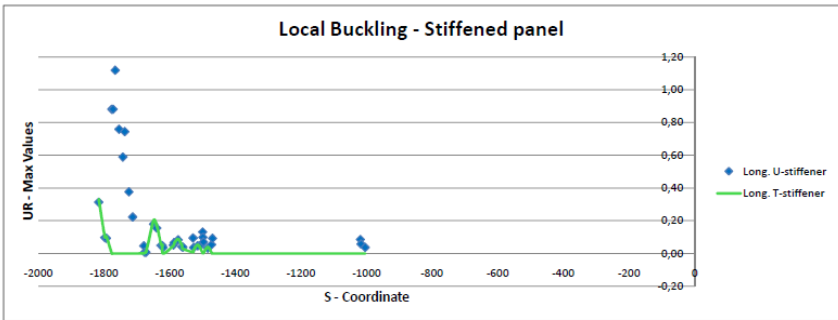
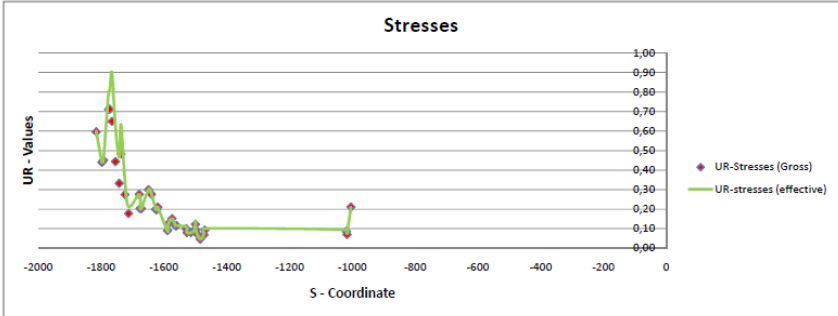


Figure 12-3 ADVERS results for roadway girder - rupture of hanger 1

		<p align="center"><b>Ponte sullo Stretto di Messina</b> PROGETTO DEFINITIVO</p>		
<p align="center">Specialist Technical Design Report, Annex</p>	<p><i>Codice documento</i> PS0075_F0-ok.doc</p>	<p><i>Rev</i> F0</p>	<p><i>Data</i> 20/06/2011</p>	

For rupture of hanger 1 an utilisation factor  $UR > 1.00$  are calculated for local buckling of stiffeners. However, this calculation is for a location close to the web in the cross girder, where buckling shall not be considered, and in the adjacent point no buckling problems occur, thus indicating that no problem exists.